NASA
Technical
Memorandum

NASA TM - 103596

WEAR MECHANISMS FOUND IN ANGULAR CONTACT BALL BEARINGS OF THE SSME'S LOX TURBOPUMP

By T.J. Chase

Propulsion Laboratory
Science and Engineering Directorate

July 1992

National Aeronautics and
Space Administration

George C. Marshall Space Flight Center

REPORT DOCUMENTATION PAGE

Form Approved
OMB No. 0704-0188

1. AGENCY USE ONLY (Leave blank)	2. REPORT DATE	3. REPORT TYPE AND DATES COVERED
	July 1992	Technical Memorandum

4. TITLE AND SUBTITLE
Wear Mechanisms Found in Angular Contact Ball Bearings of the SSME's Lox Turbopumps

5. FUNDING NUMBERS

6. AUTHOR(S)
T.J. Chase

7. PERFORMING ORGANIZATION NAME(S) AND ADDRESS(ES)
George C. Marshall Space Flight Center
Marshall Space Flight Center, Alabama 35812

8. PERFORMING ORGANIZATION REPORT NUMBER

9. SPONSORING/MONITORING AGENCY NAME(S) AND ADDRESS(ES)
National Aeronautics and Space Administration
Washington, DC 20546

10. SPONSORING/MONITORING AGENCY REPORT NUMBER
NASA TM-103596

11. SUPPLEMENTARY NOTES
Prepared by Propulsion Laboratory, Science and Engineering Directorate

12a. DISTRIBUTION/AVAILABILITY STATEMENT
Unclassified—Unlimited
Subject Category: 37

12b. DISTRIBUTION CODE

13. ABSTRACT *(Maximum 200 words)*

Extensive experimental investigation has been carried out on used flight bearings of the phase II high-pressure oxygen turbopump (HPOTP) of the space shuttle main engine (SSME) in order to determine the wear mechanisms, dominant wear modes, and their extent and causes. The report shows methodology, surface analysis techniques used, results, and discussion. The mode largely responsible for heavy bearing wear in lox has been identified as adhesive/shear peeling of the upper layers of bearing balls and rings. The mode relies on the mechanisms of scale formation, breakdown, and removal, all of which are greatly enhanced by the heavy oxidation environment of the HPOTP. Major causes of the high wear in bearings appear to be lubrication and cooling, both inadequate for the imposed conditions of operation. Numerous illustrations and evidence are given.

14. SUBJECT TERMS
cryogenic bearings, turbopumps, wear mechanisms, angular contact ball bearings, wear modes, surface science in tribology

15. NUMBER OF PAGES
113

16. PRICE CODE
NTIS

17. SECURITY CLASSIFICATION OF REPORT	18. SECURITY CLASSIFICATION OF THIS PAGE	19. SECURITY CLASSIFICATION OF ABSTRACT	20. LIMITATION OF ABSTRACT
Unclassified	Unclassified	Unclassified	Unlimited

ACKNOWLEDGMENTS

This work was done while the author held Associateship of the National Research Council. The author wishes to acknowledge Messrs. John P. McCarty and Charles S. Cornelius of Propulsion Laboratory and Dr. Ilmars Dalins of Materials and Processes Laboratory.

TABLE OF CONTENTS

LIST OF ILLUSTRATIONS

LIST OF ILLUSTRATIONS (Continued)

LIST OF ILLUSTRATIONS (Continued)

LIST OF ILLUSTRATIONS (Continued)

LIST OF ILLUSTRATIONS (Continued)

LIST OF ILLUSTRATIONS (Continued)

LIST OF ILLUSTRATIONS (Continued)

LIST OF TABLES

TECHNICAL MEMORANDUM

WEAR MECHANISMS FOUND IN ANGULAR CONTACT BALL BEARINGS OF THE SSME'S LOX TURBOPUMPS

I. PURPOSE OF THE STUDY

This study was aimed at gaining some insight into the physical phenomena occurring in bearings of the liquid oxygen (lox) turbopumps, which could subsequently be used to improve their life expectancy. The overall objective of the project was to acquire detailed factual information on wear of angular contact ball bearings operating in the lox environment of the turbopumps.

Immediate Objective: Determine the wear modes active in ball bearings operating in lox.

Further Objectives:

1. Determine the degree of participation of the known wear modes in the overall wear of the lox turbopump bearings.

2. Evaluate the effect of operational variables on the wear rate of the lox turbopump bearings.

3. Reevaluate design criteria for bearings operating in lox.

Implicit Goal: Extend bearing life.

II. GENERAL APPROACH

1. Study present and past lox turbopump bearing wear.

2. Isolate the wear controlling mechanisms.

3. Devise methodology and design program plan.

4. Implement the plan, keep on updating.

5. Communicate results with the scientific community.

III. GENERAL METHODOLOGY

The general methodology adopted for this primarily experimental study relies upon the strict scientific collecting of unbiased raw evidence on wear of bearing elements, relating it to the known wear

modes pertaining to the similar tribological applications, and drawing conclusions based on this evidence. The methodology involves the following major tasks:

1. Collect evidence and search for clues to prevalent wear modes by studying:

   a. Wear tracks on flight and test turbopump bearings

   b. Wear debris from bearings named above and from bearings currently tested utilizing the bearing and seal materials tester (BSMT).

2. Cross correlate evidence from a and b above, and interpret it in terms of the state-of-the-art on tribology data bases. Draw conclusions regarding wear modes.

3. If a clear wear mode emerges from 2 above,

   a. Determine the critical variables

   b. Evaluate their effect on bearing wear rate by modeling and/or testing

   c. Otherwise, return to item 1 for more evidence and further study.

4. Project the results of item 3 above on design criteria for the lox turbopump bearings.

The research reported on in this report has been performed on engine turbopump bearings, actual space flight hardware, after it has been retrieved, under the strict requirement that only nondestructive testing (NDT) be allowed. This limitation excluded some traditional procedures, such as sectioning, etching, hardness testing, etc. However, availability of modern NDT and surface analytical tools at Marshall Space Flight Center (MSFC) has more than made up for the limitation as far as meeting the objectives of this study, i.e., determination of the major wear modes, is concerned.

In a way, all research presented here has been searching for clues and explanations to what happened to bearings in engine service, based upon the microscopic record of various tribological and mechanical events that had shaped the final morphology of the bearing balls, races, and cages. Thus, it has been a de facto forensic investigation.

IV. DETAILED METHODOLOGY

Nine No. 2 phase II high-pressure oxidizer turbopump (HPOTP) bearings were selected for a detailed study, based on the wear record and availability only. Wear debris from these bearings was carried away with the lox that passed through them in the space shuttle main engine (SSME), but the BSMT wear debris from the ongoing tests designed to simulate operation of the HPOTP bearings has been available for the study, and it provided some very important clues.

The following is an itemized outline of the techniques and instruments used to collect and/or analyze the experimental data. The items quoted below refer to "general methodology."

Ad 1 – Collect evidence and search for clues on flight bearings and wear debris.

1.1 NDT only.

1.2 Scope: study wear in the lox turbopump bearing No. 2.

1.3 Bearing selection criterion: wear record.

1.4 Sampling rate: 9 bearings, population of 180.

1.5 Extent of research:

a. Microgeometry

b. Topography

c. Morphology

d. Structure

e. Composition of the upper layers for the wear tracks of balls and rings.

1.6 Analytical techniques/instruments employed:

a. Optical microscopy (OM)

b. X-ray photoelectron spectroscopy (XPS)

c. Auger electron spectroscopy (AES)

d. Electron microprobe with scanning electron microscopy (SEM) and electron diffraction spectroscopy (EDS)

e. SEM

f. EDS

g. Form Talysurf profilometry (FTP)

h. X-ray fluorescence spectroscopy (XFS)

i. 0.00001-in mechanical micrometer (MM)

j. 0.01-mg digital scale.

1.7 "Clues" include all surface features observed and/or recorded on wear tracks of balls and races using the techniques named in item 1.6, and, in particular, the following:

a. Spalls

b. Pits

c. Indentations

d. Scratches

e. Holes

f. Deposits

g. Debris on the surface

h. Size, shape, location, orientation, etc.

i. Analytical data on surfaces features, e.g., deposit chemistry by means of EDS.

V. WEAR MECHANISM

Traditionally, in describing wear phenomena. authors enjoyed a dose of liberty which often resulted in an ambiguity or confusion in the literature regarding the classification[1] of wear. Wear terminology quite often reflects that situation by not having any well defined boundaries for such commonly used terms as "mode,"[2] "mechanism," and sometimes "process." Herein, the first two terms are being used nearly simultaneously. Thus, a wear mechanism (mode) is a means of removal of wear particles from the surface.

This study has confirmed the existence of the following generic wear modes acting simultaneously in turbopump bearings:

1. Adhesion (smearing, scaling)
2. Abrasion
3. Fatigue:
    a. Spalling (pitting)
    b. Flaking (delamination)
4. Oxidation
5. Gouging (plastic deformation)
6. Corrosion.

VI. FINDINGS AND CONCLUSIONS

After a thorough study of all relevant literature and a careful analysis of all pertinent results, the following findings and/or conclusions have been drawn:

1. There is evidence of several known wear modes.

2. A mode dominating the wear picture is the adhesive/shear peeling of the upper layers. For the phase II HPOTP bearings, this mode relies upon the mechanisms of scale formation and removal.

3. The dominant wear mode discovered in the phase II HPOTP bearings has a universal character. The mode has been confirmed on:

   a. Turbopump bearing balls and rings

   b. BSMT tested balls in lox and liquid nitrogen (LN_2)

   c. Brand new 1/2-in balls

   d. Failed turbine bearings.[22]

4. Oxidation accelerates wear by rapidly rebuilding the upper oxide layer (scale) under the operating conditions (high contact and shear stress, and high temperature at real contact areas).

5. It appears that a major cause of wear in phase II HPOTP bearings is the lubrication which is inadequate for the imposed conditions of operation. Likewise, cooling seems to be inadequate.

VII. DETAILED EXPLANATIONS

A. Background

Preloaded angular contact ball bearings are commonly used in a variety of spacecraft applications,[3] ranging from very light duties of controlling movement of shutters or pointing antennas, to the very heavy duty of supporting turbine rotors. Under the best of circumstances, these bearings can reliably support the combined radial and axial loads and accommodate the unavoidable thermal distortions of the space hardware over a wide range of operational variables in a light duty service, wherein loads and/or speeds are low.

Lubrication in rocket motors, and in outer space in general, is difficult because of the weight limitations which virtually eliminate all heavy auxiliary lubrication equipment like pumps, motors, sumps etc., as well as the limitations imposed by the vacuum environment.[4] With a few exceptions,[5] liquid lubricants cannot be used. The most successful solid lubricants used in outer space[6] are the filled polytetrafluorethylene (PTFE), sputtered molybdenum-disulfide ($Mo-S_2$), and ion-plated soft metals (e.g., Pb). Since solid lubricants cannot prevent the solid-solid interaction of the load bearing surfaces, surface distress and resulting mechanical wear are unavoidable. Successful applications under these circumstances are the ones which result in a manageable wear rate, in addition to satisfying various other

requirements. The current HPOTP bearings are lubricated with the PTFE contained within the glass fiber reinforced cages.

Traditionally, the severity of a bearing application has been judged by the value of its "DN" product, where "D" is the nominal diameter of the bearing in millimeters, and "N" is its speed in revolutions per minute (r/min). Wear may be low in applications characterized by a low DN value and short or infrequent operation. However, a high DN value, heavy use, and corrosive or contaminated environment tend to produce heavy wear. In most space applications, these bearings operate well below 1 million DN (1 MDN) but not in the case under consideration.

Bearings of the HPOTP of the SSME operate at approximately 2 MDN in the lox environment which precludes any effective liquid film lubrication and imposes cryogenic temperatures, high thermal gradients, and heavy transient loads. Under these conditions, bearings fail from excessive wear despite application of the best available materials, best workmanship, and the state-of-the-art installation and maintenance techniques. There is no engineering data base available on life rating for these bearings, except for the general guidelines by NASA,[7] and no reasonable extrapolation to standard rating procedures (compare Anti-Friction Bearing Manufacturers Association (AFBMA)) can be made because of the exoticism and the severity of application.

These separable, angular contact ball bearings are made of 440C stainless steel, have a customized internal geometry, and work in a back-to-back preloaded tandem. They were not reusable in the past due to their high wear and the strict safety and reliability precautions imposed by NASA. Current HPOTP bearings sustain two to three flight cycles, depending on the outcome of the individual inspection carried out after each flight. Scrapped bearings, after dismantling and cleaning, are being deposited as permanent material records and thereby preserved for future reference, such as the one reported herein.

Many technical issues related to the HPOTP bearings have been studied recently, ranging from the performance[8] and materials[9] to a new cage design[10] and testing,[11] and optimization of race curvatures[12] for heat generation and stress. Naerheim et al.[13] have evaluated the maximum operating surface temperature of the bearings to be in the range of 600 °C, based upon the postmortem Cr/Fe ratio of oxides found on the wear tracks. Dolan[14] analyzed conditions and requirements for cooling of the bearings and suggested that a "vapor blanket" may form around some balls thereby worsening dissipation of the internally generated heat from the bearings. He also updated the status of the NASA-MSFC ongoing test program[15] which employs MSFC's own BSMT facility.

Analysis of the cage stability[16] for the bearings has indicated that inadequate lubrication under some conditions may lead to an increased risk of unstable oscillations. These could result in an overload leading to cage failures (documented) and/or irreversible (anticipated)[14] vapor insulation of balls, producing a "thermal runaway" which may cause an imminent bearing failure.

Failures of lubricated rolling bearings have been studied very extensively.[17,18] Consequently, the combined body of knowledge on pitting, smearing, fretting, etc., is usually sufficient to design reliable bearing systems. However, wear of rolling element bearings remains largely unexplored in general,[19] and particularly wear dynamics and participation of recognized modes of surface wear and effects of variables remain unknown.

Wear of the HPOTP bearings has been investigated in a macroscale, using the engineering approach[14,15] and the existing BSMT facility. Recently, the phase II HPOTP bearing wear problem has

been approached by the author in microscale, using the actual HPOTP spent flight bearings and a broad range of surface analytical tools and instruments.[20] To date, there has been no data base for comparisons on wear of high-speed, angular contact ball bearings operating in the lox environment, other than NASA and their contractors' files and related disassembly reports. Likewise, there has been no literature on the subject discussed here in application to the actual space hardware. This report presents the dominant wear modes discovered on the turbopump bearings.

B. Bearing Environment and Operating Conditions

A simplified cross section of the HPOTP showing the main shaft support configuration is given in figure 1. The bearing studied in this report is the second bearing from the left (marked (2)) which works in a back-to-back preloaded tandem arrangement with an identical bearing to the left of it (marked (1)). A carefully controlled axial preload is exerted by a custom design beam spring placed between the outer rings of the bearings as shown. Both bearings are cooled by the same steady stream of lox passing axially through them from the pump end, left to right.

Operating conditions for the No. 2 bearing of the phase II HPOTP are shown in table 1. The data listed in it are believed to average and approximate the overall conditions of operation as they pertain to the bearing population being examined in this paper. They do not represent a coherent set of recorded "test data" as most readers are accustomed to seeing in strictly controlled experiments because each test specimen in this study comes from a different turbopump and a different flight of the space shuttle and not from a controlled tribology experiment. Direct measurements for some variables listed in table 1 were impractical (e.g., loads) or even impossible (e.g., ball temperatures) to accomplish due to a lack of access to these bearings in the flight service and/or their explosive environment (lox). Also, there is no single source of information on which to rely in re-creating the conditions of operation for the particular features related to bearing malfunction and/or proposed remedies, while operational variables are treated as incidental information to the issues. Consequently, there is considerable disagreement among experts on the operating conditions. This is an open issue in itself, too broad for an exhaustive treatment and out of scope in this context. The "best" plausible estimates are shown, considering all the available information, in order to provide a feel for the extraordinary severity of this application. The following comments are offered in order to provide more insight.

High power (30,000 hp), high speed (30,000 r/min), and short duration of the HPOTP work cycle render many important variables of its operation highly time dependent due to the thermal transients inherent in the turbopump and/or those which are generated in the bearing itself. Likewise, bearing operating conditions, except for the shaft speed, are transient. Also, individual variations in some component dimensions of the HPOTP, despite a strict scrutiny and individual certification, are probably sufficient to substantially influence bearing loads, especially if thermal effects are considered. Thus, a considerable scatter of bearing operation variables is unavoidable.

The angular velocity and acceleration of the bearing's inner ring are virtually certain and precise, although they vary with the power level. The oxygen environment is believed to locally change[14] from liquid (lox) to gas (gaseous oxygen (gox)) on and near the hot surface tracks of balls. This upsets the heat balance within the bearing and is believed to be a major cause of a potential thermal instability. Surface temperatures (table 1) of the race tracks and balls may reach 600 °C,[13] while the outer race surface temperature in contact with the seat may remain at –150 °C. Thermally induced radial expansion of the inner ring and balls may cause a loss of bearing operational clearance, resulting in an interference overload which generates more heat, and further thermal expansion, until the ongoing and thus

accelerated wear processes restore the bearing clearance. The initially applied coating of dry lubricant film wears away very rapidly, within a few seconds perhaps, and the PTFE transfer film produced by attrition from the ball retainer seats is not quite sufficient to keep the ball wear in check. Since solid lubricants cannot prevent the solid-solid interaction of the load bearing surfaces, a surface distress and the resulting mechanical wear are unavoidable. This is a favorite wear scenario for the HPOTP bearings related to their cooling and lubrication.

The radial load consists of constant and alternating parts (fig. 1). The constant radial load is due to the rotor weight and static fluid pressure. The alternating part is induced by the fluctuating fluid pressure and a dynamic unbalance. The axial load consists of a design preload component (approximately 1,000 lb) which is superposed on the load components due, primarily, to differential axial displacements of the bearing caused by the combined actions of the balance piston (fig. 1), thermal expansion, and changes in fluid pressure. Contact stresses have been shown[3] to be exceedingly high in comparison to conventional applications,[10 11] disregarding the effect of asperity interaction. In addition, these stresses vary as bearing wear occurs.

C. Materials

Cryogenic applications like this one require careful selection of materials for rolling bearing components. High strength, hardness, fracture toughness, and stress corrosion resistance are the usual prerequisites for rolling elements and rings which must withstand repetitive applications of high contact stresses and the resulting wear and rolling contact fatigue. In addition, dimensional stability at cryogenic and elevated temperatures, corrosion resistance, and compatibility with the lox environment, as measured by the NASA autoignition test, are required. The AISI 440C martensitic stainless steel (table 2) satisfies these requirements reasonably well except for the wear resistance. All bearings analyzed here are made of the 440C.

Other materials involved include Armalon ball retainers, solid lubricants, and lox. They influence lubrication and cooling and thereby affect all tribological features of this very unique and technologically critical application, wherein weight limitations and potential exposure to the vacuum environment[4] impose special constraints on the lubrication system and lubricants. The current HPOTP bearings are lubricated with an initial coating of dry lubricant and a transfer film of PTFE from the ball retainers. The retainers are made of Armalon, a composite material, made of the polytetrafluoroethylene (PTFE, Teflon) reinforced with glass fibers whose chemistry is composed of the following oxides: 54.3 percent silicon (Si), 17.2 percent calcium (Ca), 15.2 percent aluminum (Al), 8 percent boron (Bo), 4.7 percent magnesium (Mg), and 0.6 percent sodium (Na). Load bearing surfaces of these bearings are initially sputter-coated and cured with a dry lubricant composed of 35 percent Mo-S_2 and 65 percent antimony-oxide (Sb_2-O_3).

Undesirable, yet present on most bearing surfaces, as shown by the EDT diagrams, are the contaminant particles carried by the stream of lox flowing through the bearings. Liquid oxygen is the process fluid of the HPOTP as well as the coolant for the bearings.

VIII. DETAILED EXPLANATIONS: RESULTS

A macroscopic (low magnification) investigation of the spent turbopump bearings has revealed the existence of a variety of wear patterns on balls (fig. 2). Wear patterns of rings and cages did not vary as much. Lightly worn (fig. 2(4)) balls, below 0.0025 mm (0.0001 in) diameter loss, usually had a golden background marked with several crisscrossing narrow wear tracks. Heavily worn (fig. 2(6)) balls, above 0.0125 mm (0.0005 in) diameter loss, usually were gray and had one or two wide wear tracks and a polar cap, all indicative of a stable operation resulting from stable dynamic behavior. This behavior is related to the growing dynamic unbalance of worn balls with wear which leads to the stable orbit of a ball in an inertial space because the wear track of the ball in an angular contact ball bearing under axial load is shifted from the equatorial position, thereby creating an unbalance. Kawamura and Touma[21] have demonstrated this effect.

A great majority of the SSME flight bearings consistently show ball wear in the range of 0.0025 to 0.0075 mm. The most heavily worn bearing presented in this report is a developmental one which sustained 19 starts and 132 min of HPOTP operation on the ground and whose diametral loss reached 0.048 mm. It was included in this study for the sake of broadening the wear investigation.

Microscopic examination of bearing wear tracks has revealed a wealth of surface features. Races of heavily worn inner rings (IR) usually carry three or four distinct wear patterns like those shown in figure 3. High axial loads leave evidence of plastic flow on the high shoulder (fig. 3(1)), followed by a rough band of adhesive/shear peeling (fig. 3(2)). Interestingly, Averbach and Bamberger[22] found a strikingly similar wear pattern on marginally lubricated bearings of a gas turbine, as shown in figure 3 of their report, which they blamed on ball skidding. A featureless, highly polished (by rolling) area is next (fig. 3(3)), followed on the cylindrical portion of the race by a band of rolling contact microfatigue caused by a radial overload. This band has been further studied in figure 4. Spall sizes varied from 20 to 200 micrometers, their depth usually ranging a few micrometers.

A large spall in figure 4(2) shows a nearly straight edge on the left (fig. 4(3)), a grainy bottom, and a thin chip (fig. 4(3)) still hanging on. An EDS diagram in figure 4(6) shows an unusually heavy concentration of chromium (Cr) inside the spall, which may indicate a high subsurface temperature (compare Naerheim[10]) or a presence of a large subsurface carbide. An EDS diagram for the baseline 440C is shown in figure 4(6).

Lightly worn rings do not show microfatigue on their surfaces, but adhesive/shear peeling can always be identified on them. All rings and balls displayed some evidence of contamination damage in the form of indentations, scratches, and punctures. This evidence has been shown on the photographs in the appendix.

Ball surfaces (fig. 5) whose patterns radically change from place to place are particularly rich in wear morphology. Apparently, the load-speed-temperature history in a microscale varied dramatically on ball surfaces due to changes in relative rolling and sliding motions, as well as an occasional skidding and/or colliding with a cage. There is evidence on balls of many wear modes, including the adhesive/shear peeling, macrospalling, abrasion, contamination, oxidation, plastic deformation, and some corrosion. The predominant wear mode is the adhesive/shear peeling of the oxide scale. It has been found in all the bearings studied regardless of the length of their service or the extent of wear (compare appendix).

A series of microphotographs in figure 5 shows this mode. The dark areas are shallow spalls from which wear flakes were removed. Only the flat bottoms of those spalls are in focus, due to some technical limitations of the optical microscope whose depth of focus at the magnification of × 1,000 was less than the depth of the spalls. However, when focused on the upper layer (not shown here), the general surface morphology remained unchanged. This fact proves that the same wear mechanisms, namely scale formation-breakdown-and-removal, have formed both lower and upper layers.

Cracking of the upper oxide layer, i.e., scale, is shown in figure 6(1), peeling in figure 6(2), and wear debris inside the spall in figure 6(3). The elemental composition by EDS of the bottom of the spall is shown in figure 6(4). It can be seen that it contains elements foreign to the base 440C and the cage material, like zinc (Zn) and titanium (Ti) which may have entered the bearing with the lox as contaminants. The XFS and SEM/EDS analyses (see appendix) of the solid residue found on the inlet filters to the BSMT have confirmed participation of many contaminants, including Ti and Zn, in the lox stream. An overall EDS analysis (fig. 6(5)) of the ball surface did not show Zn or Ti, so their presence seems limited to mostly spall cavities. That is because a mechanical removal of small particles from inside a spall by any microscopic events occurring on the ball surfaces is unlikely. It can be seen on microphotographs that wear debris shows up inside cavities rather than on the top layers.

Figure 7 shows a sequence of photos which helped in resolving a major wear mode active on a ball surface during an early stage of service. This ball had negligible wear, beyond detection by a mechanical micrometer. However, a destructive mode of adhesive/shear peeling of the upper layers (oxide scale, usually) has already begun on its surface, as can be seen at a magnification of × 1,000. This wear mode has been identified not only in all the examined turbopump and BSMT bearings operating in lox but also in bearings tested in liquid nitrogen, and even on the surfaces of the brand new 440C balls. That is so because their superfinish relies upon the mechanical wear by an abrasive material, and light abrasion of the 440C stainless steel shows adhesive shear and not plastic plowing as a major wear mechanism.

Figures 8(1) and 8(2) show the original machining marks as fine dot-lines still visible on the surface of the lightly worn ball, and figure 8(3) shows a shiny surface of a brand new ball. Under a × 1,000 magnification, these well-aligned dots proved to be very shallow pits just like those produced by the adhesive/shear wear mode discussed earlier. Obviously, the finish marks come from the sliding (shear) wear in which adhesion plays a major role. Thus, the adhesive/shear peeling mode is quite universal. The difference between high and low wear in this mode lies in the relative size and depth of spalls and their number on the surface, i.e., on the wear kinematics. Wear dynamics is another matter, and it needs further investigation.

A heavy wear goes together with large and deep spalls densely packed upon the surface, while a light wear is characterized by small and shallow spalls, which are rather sparsely populated on the track surface.

Some heavily worn balls show coexistence of adhesive/shear mode with shallow pitting mode. It seems very likely that the adhesive/shear peeling may lead to rolling contact fatigue (pitting, spalling), as both of these modes seem to rely upon crack propagation in the upper layers whose structure, composition, and mechanical properties are heavily affected by contact stresses.[18] A reduction in adhesion and shear stress, e.g., by a more effective lubricant, may alleviate adhesive/shear peeling at the expense of pitting, or vice versa, depending on the respective wear rates.

Figure 9 shows surface profilograms of a heavily worn outer ring. Since its wear track exhibited the adhesive/shear peeling mode, and since figure 9(2) gives a good measure of asperity heights on the track, an estimate for an average depth of the peeling spalls of the order of 1 to 2 micrometers seems quite reasonable. An estimate for the lightly worn balls (fig. 2(4)) is of the same order of magnitude, while that for the heavily worn balls (fig. 2(6)) is an order of magnitude higher.

An XPS study in conjunction with ion sputtering of a heavily worn ball has been carried out in order to establish depth profiles of particular elements of interest on the surface. Figure 10(1) shows the presence of a very shallow layer of fluorine (F) which quickly vanishes with the depth below the surface, thereby indicating the definite possibility of inadequate lubrication with the PTFE. Actually, the abscissa in figure 10 is the sputter time, but this translates directly into the depth of sputter and that into a depth below the surface. Figure 10(2) shows a very short transition zone of the iron oxides with depth, and that may indicate a relatively high rate of oxide removal from the surface by wear. Oxygen (O) and fluorine (F) peaks in figure 10(3) are very close to the surface, as expected from the conditions of operation of the bearings.

Wear debris collected from the BSMT outlet filters after bearing tests in lox (fig. 11) consisted of fragmented glass fibers, PTFE specks from the cage, contaminant particles, and some very thin and fragile wear flakes coming from the bearing balls and rings. Usually, these flakes were approximately 50 or more micrometers in size and a few to several tens of micrometers in thickness, which had a lot to do with the filter grade. However, some very large particles (fig. 11(1)) had a surface morphology very closely resembling that of the rings (fig. 11(4)), or balls, thereby confirming the predominance of the adhesive/shear peeling mechanism described in this paper. The fact that wear flake surfaces bear an unmistakable resemblance to the wear surface of balls and/or races is a clear indication of their origin. In addition, combined with other observations and analyses, it allows for a significant simplification regarding modeling wear under the circumstances, namely that a third body life[2] of wear debris is exceedingly short here.

A more detailed analysis of wear debris, and modeling the wear dynamics, will be forthcoming with an application to the BSMT of the particle collection system (PCS) which has been designed and implemented by MSFC in close cooperation with the author.

IX. RECOMMENDATIONS FOR FURTHER STUDY

As shown in the preceding sections, this study involved a number of surface science and material science techniques in application to tribology of wear of the SSME's HPOTP bearings. However, it seems in order to caution here that most of these techniques have not been well tuned to the tasks of this project, for a variety of reasons and causes, analysis of which is beyond the scope of this report.

Also, the extent of the study has out-of-necessity been limited to only about 5 percent of the bearing population, and further curtailed by the workload capacity of the Materials Laboratory to only about 1 percent of the available wear surface. Nevertheless, the major conclusions reached in this study (section VI) are fully justified by the quality, if not the volume, of evidence. To clarify this statement, it is worthy of mention that all elements of the available bearings were carefully examined by the author using optical microscopy.

Undoubtedly, there is a lot more information stored on the surface tracks of the remaining 95-percent population of the flight bearings, and it could possibly be recovered if more emphasis is put on application of the analytical capabilities of the MSFC's Materials and Processes Laboratory.

The following are some of the author's major recommendations for further study, aimed at completion of the project and reaching its major objectives (section I) and conceived in an accord and consultation with the sponsor.

1. Collect more evidence on and further study the dominant wear mode mechanisms. Include ceramic materials.

2. Introduce a math model for the dominant wear mode in terms of operating conditions in a microscale, and relate them to the overall operating conditions.

3. Introduce a mathematical model for the mechanical interaction between elements of the bearing with respect to the film transfer mechanism.

4. Design and implement a test program to validate the mathematical wear model in terms of wear rate versus operating conditions. A new design of a single-bearing tester and/or a single-contact apparatus is needed. The existing gox tester may be adaptable.

REFERENCES

1. Lancaster, J.K.: "Material Specific Wear Mechanisms: Relevance to Wear Modeling." Wear, vol. 141, 1990, pp. 159–183.

2. Keer, L.M., and Worden, R.E.: "A Qualitative Model to Describe the Microchipping Wear Mode in Ceramic Bearings." Tribology Transactions, vol. 33, No. 3, 1990, pp. 411–417.

3. Todd, M.J.: "Modeling of Ball Bearings in Spacecraft." Tribology International, vol. 23, No. 2, 1990, pp. 123–128.

4. Buckley, D.H.: "Friction, Wear, and Lubrication in Vacuum." NASA, Washington, DC, NASA SP-277, 1971.

5. Zaretsky, E.V.: "Liquid Lubrication." Tribology International, vol. 23, No. 2, 1990, pp. 75–94.

6. Roberts, E.V.: "Thin Solid Lubricant Films in Space." Tribology International, vol. 23, No. 2, 1990, pp. 95–104.

7. Douglas, H.W.: "Liquid Rocket Engine Turbopump Bearings." NASA, Cleveland, OH, NASA SP-8048, 1971.

8. Bhat, B.N., and Dolan, F.J.: "Past Performance Analysis of HPOTP Bearings." NASA, Huntsville, AL, NASA TM-82470, 1971.

9. Maurer, R.E., and Pallini, R.A.: "Development of New Materials for Turbopump Bearings." SKF, King of Prussia, PA, Report. AT85D010, 1985.

10. Kannel, J.W., et al.: "Development of Improved Self Lubricating Cages for SSME HPOTP Bearings." Advanced Earth-to-Orbit Technology, NASA Conference Publication No. 3012, Huntsville, AL, vol. 1, 1988, pp. 175–189.

11. Cannon, J.L., et al.: "Marshall Space Flight Center Bearing Tester Results." Advanced Earth-to-Orbit Technology, NASA Conference, Huntsville, AL, September 1990.

12. Armstrong, E.S., and Coe, H.H.: "Bearing Optimization for SSME HPOTP Application." Advanced Earth-to-Orbit Technology, NASA Conference Publication No. 3012, vol. 1, Huntsville, AL, 1988, pp. 159–174.

13. Naerheim, Y., et al.: "Determination of the SSME High Pressure Oxidizer Turbopump Bearing Temperature." Advanced Earth-to-Orbit Technology, NASA Conference Publication No. 3012, vol. 1, Huntsville, AL, 1988, pp. 102–109.

14. Dolan, F.J., et al.: "Cryogenic, High Speed, Turbopump Bearing Cooling Requirements." Advanced Earth-to-Orbit Technology, NASA Conference Publication No. 3012, vol. 1, Huntsville, AL, 1988, pp. 110–141.

15. Cody, J.C., et al.: "Evolution and Use of Combined Mechanical and Thermal Codes for Cryogenic Turbopump Bearings." Advanced Earth-to-Orbit Technology, NASA Conference Publication No. 3012, vol. 1, Huntsville, AL, 1988, pp. 88–101.

16. Merriman, T.L., and Kannel, J.W.: "Cage Stability Analysis for SSME HPOTP Bearings." Advanced Earth-to-Orbit Technology, NASA Conference Publication No. 3012, vol. 1, Huntsville, AL, 1988, pp. 200–212.

17. Tallian, T.E.: "On Competing Failure Modes in Rolling Contact." ASLE Transactions, vol. 10, 1967, pp. 418–426.

18. Czyzewski, T.: "Changes in the Stress Field in the Elastohydrodynamic Contact Zone Due to Some Operating Factors and Their Possible Role in the Contact Fatigue of Cylindrical Surfaces." Wear, vol. 31, 1975, pp. 119–140.

19. Quinn, T.J.F.: "Role of Wear in Failure of Common Tribosystems." Wear, vol. 100, 1984, pp. 399–436.

20. Chase, T.J.: "Wear Modes Active in Angular Contact Bearings Operating in Liquid Oxygen Environment of the Space Shuttle Turbopumps." STLE paper No. 91153, in press.

21. Kawamura, H., and Touma, K.: "Motion of Unbalanced Balls in High-Speed Angular Contact Ball Bearings." Journal of Tribology, vol. 112, 1990, pp. 105–110.

22. Averbach, B.L., and Bamberger, E.N.: "Analysis of Bearing Incidents in Aircraft Gas Turbine Mainshaft Bearings." Tribology Transactions, vol. 34, No. 2, 1991, pp. 241–247.

Table 1. Operating conditions.*

Radial load	2.56 to 7.13 (kN)
Axial load	6.46 to 10.24 (kN)
Angular velocity, inner ring (IR)	3,141.6 (rad/s)
Angular acceleration (IR), (average, start to FPL)	785.4 (rad/s^2)
Environment (coolant) 2.1 kg/s axial mass flow rate, pressure and temperature	lox 2 MPa and –162 °C
Lubricant: transfer film from ball separator seats dry film lube coating on race tracks	solid PTFE Mo-S_2/Sb_2O_3
Hertz contact stress (IR)	2.5 to 3.5 (GPa)
Surface temperature: ball and inner race track	up to 600 °C
outer ring on O.D., approximately	–150 °C

*Compiled by the author from NASA and contractors' files.

Table 2. AISI 440C stainless steel.

	Fe	Cr	C	Mo	Mn	Si	Ni	Cu	P
Composition* (in percent weight)	80.25	16.95	1.04	0.50	0.36	0.49	0.28	1.04	0.02

Properties† (hardened and tempered)	
Tensile strength	1.965 GPa (285 ksi)
0.2-percent yield strength	1.896 GPa (275 ksi)
Percent elongation (in 50 mm)	2
Percent reduction of area	10
Hardness (Rockwell C)	57 (to 61)

*Supplier information.
†T. Baumeister (editor): "Marks' Standard Handbook for Mechanical Engineers," (eighth edition).

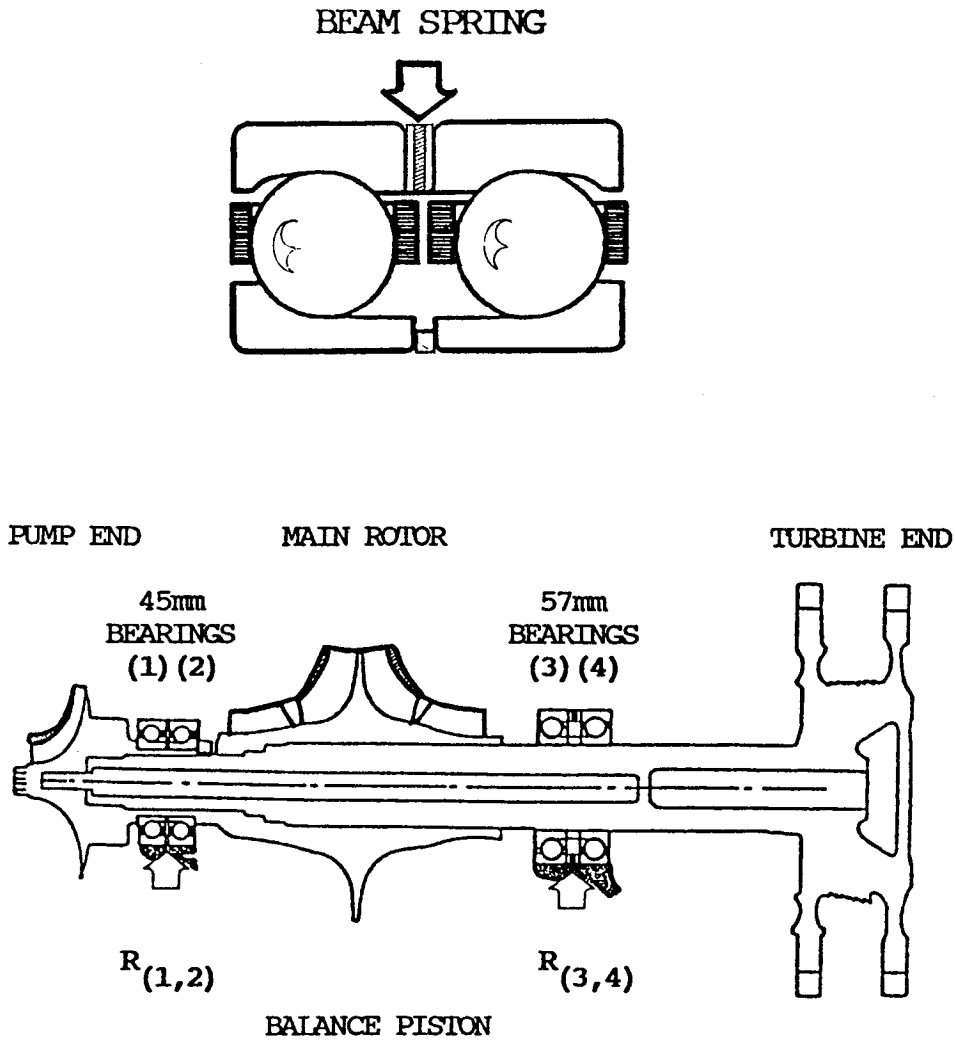

Figure 1. HPOTP shaft support configuration and bearing preload arrangement. The "balance piston" design is supposed to balance major axial loads on the shaft. The bearing studied, marked (2), carries 80 percent of the load on the left support $R_{(1,2)} = 6.06_{(avg.)} + 2.86_{(alt.)}$ (kN).

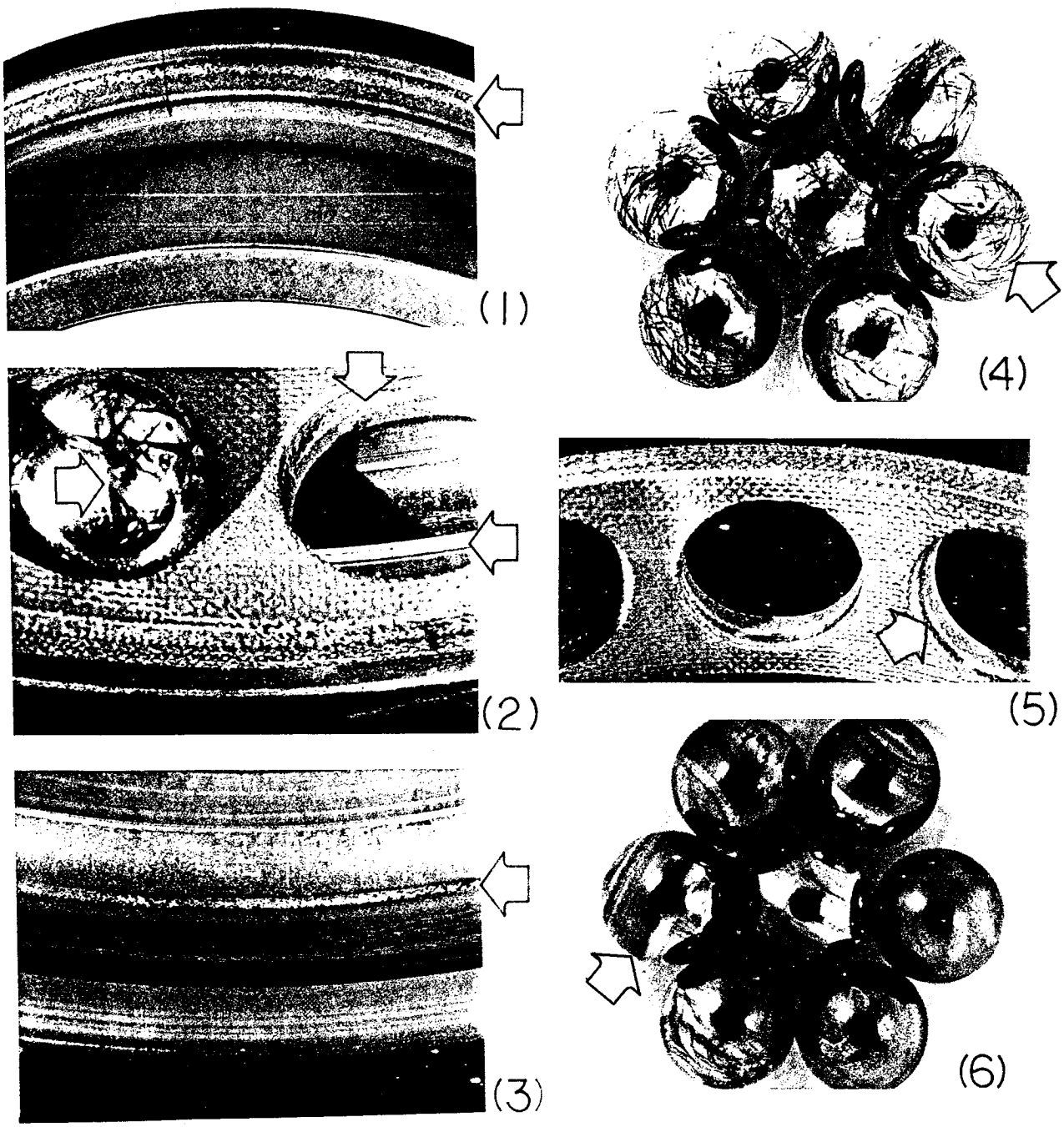

Figure 2. Wear tracks on bearings: (1) inner ring, (2) combined, (3) outer ring, (4) lightly worn balls (note skid marks), (5) cage (note pocket wear), and (6) heavily worn balls.

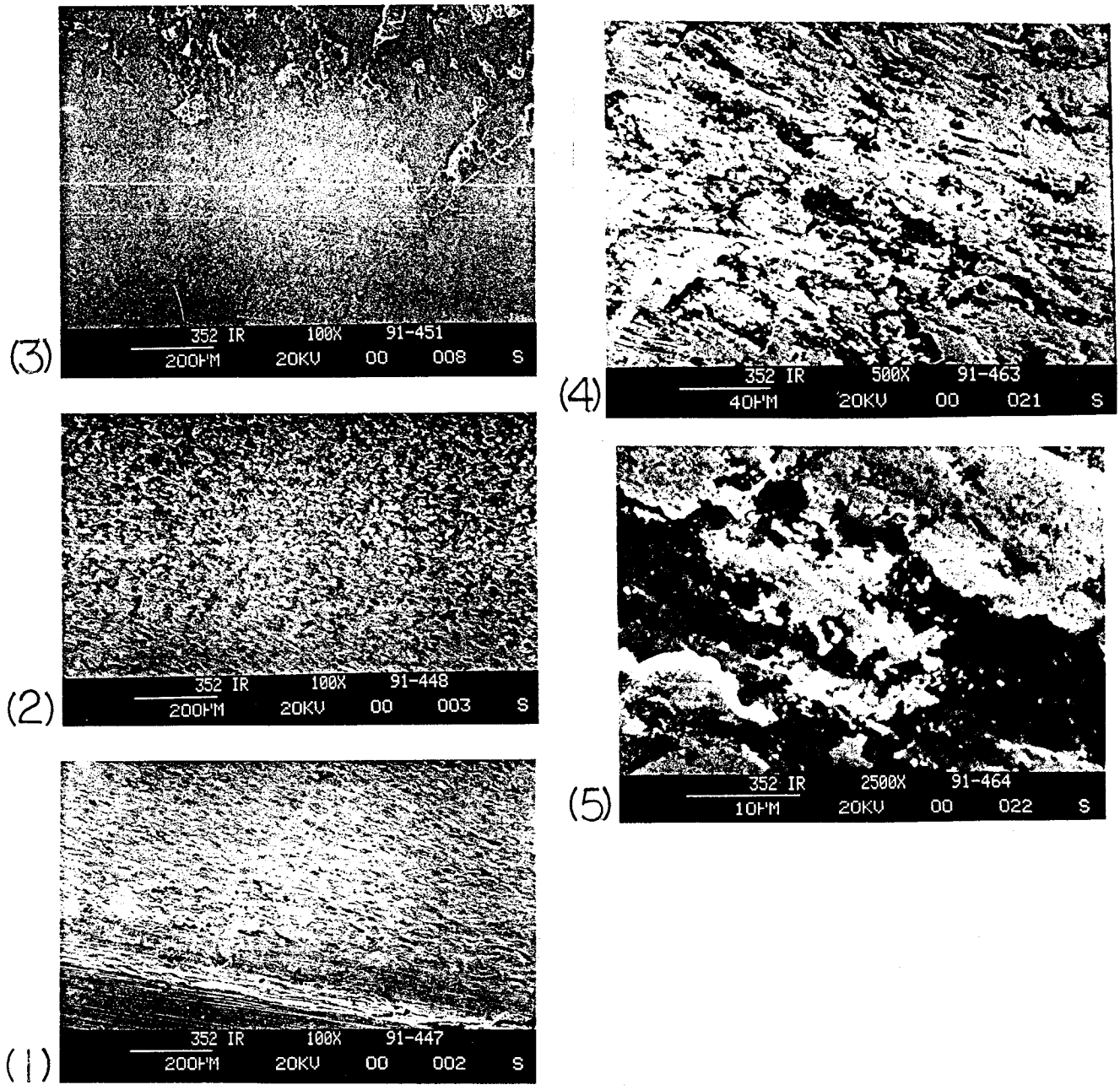

Figure 3. Heavily worn inner ring No. 352. SEM micrographs across the wear track: (1) plastic flow near the land, × 100; (2) adhesive/shear peeling, × 100; (3) contact fatigue, × 100; (4) detail of (2), × 500; and (5) detail of (4), × 2,500.

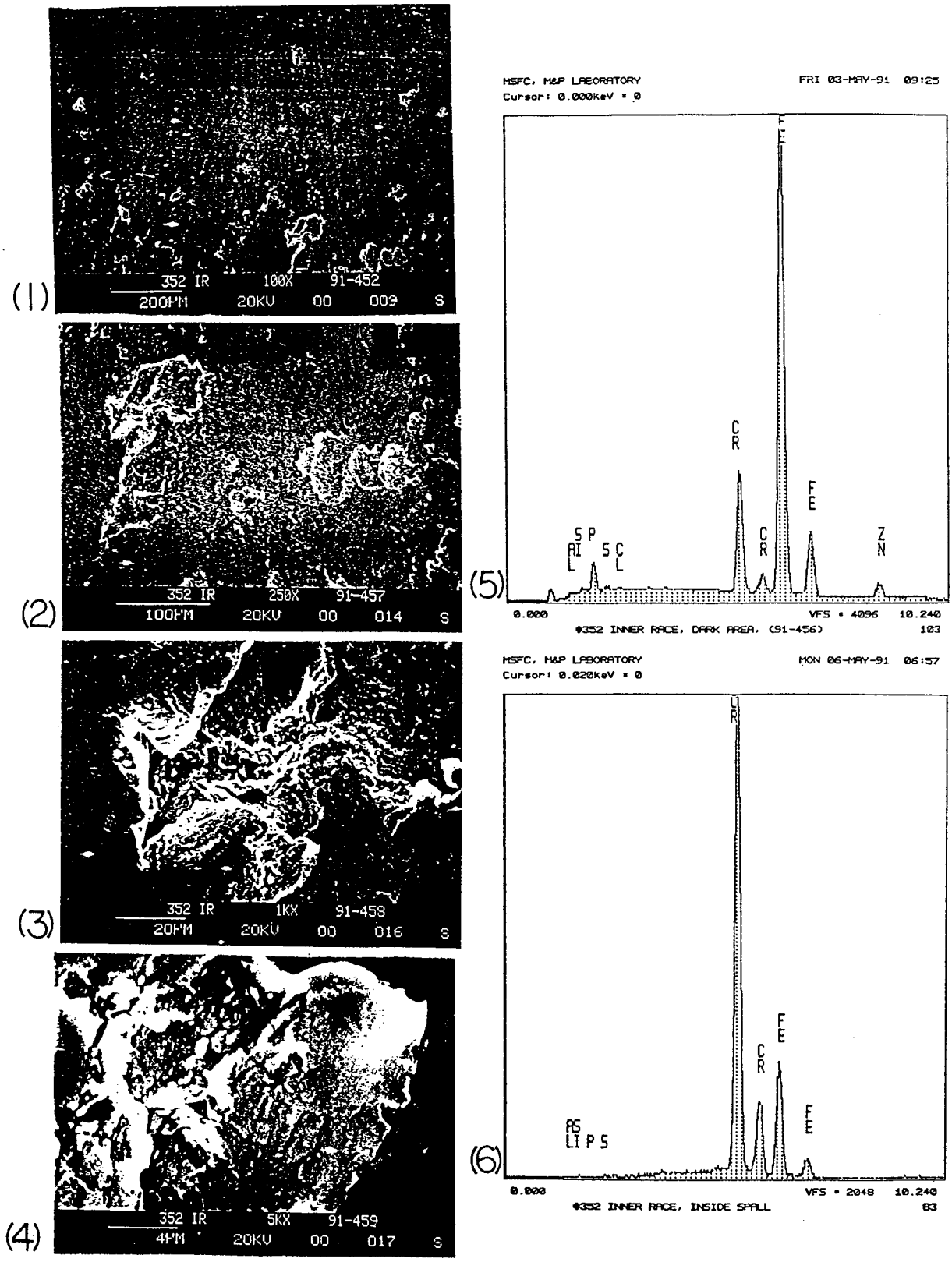

Figure 4. Heavily worn inner ring No. 352 (continued). SEM micrographs across the contact fatigued area of the wear track: (1) spalls, × 100; (2) spalls, × 250; (3) detail of (2), × 1,000; (4) fatigue flake, detail of (3), × 5,000; (5) EDS overall; and (6) EDS inside a spall.

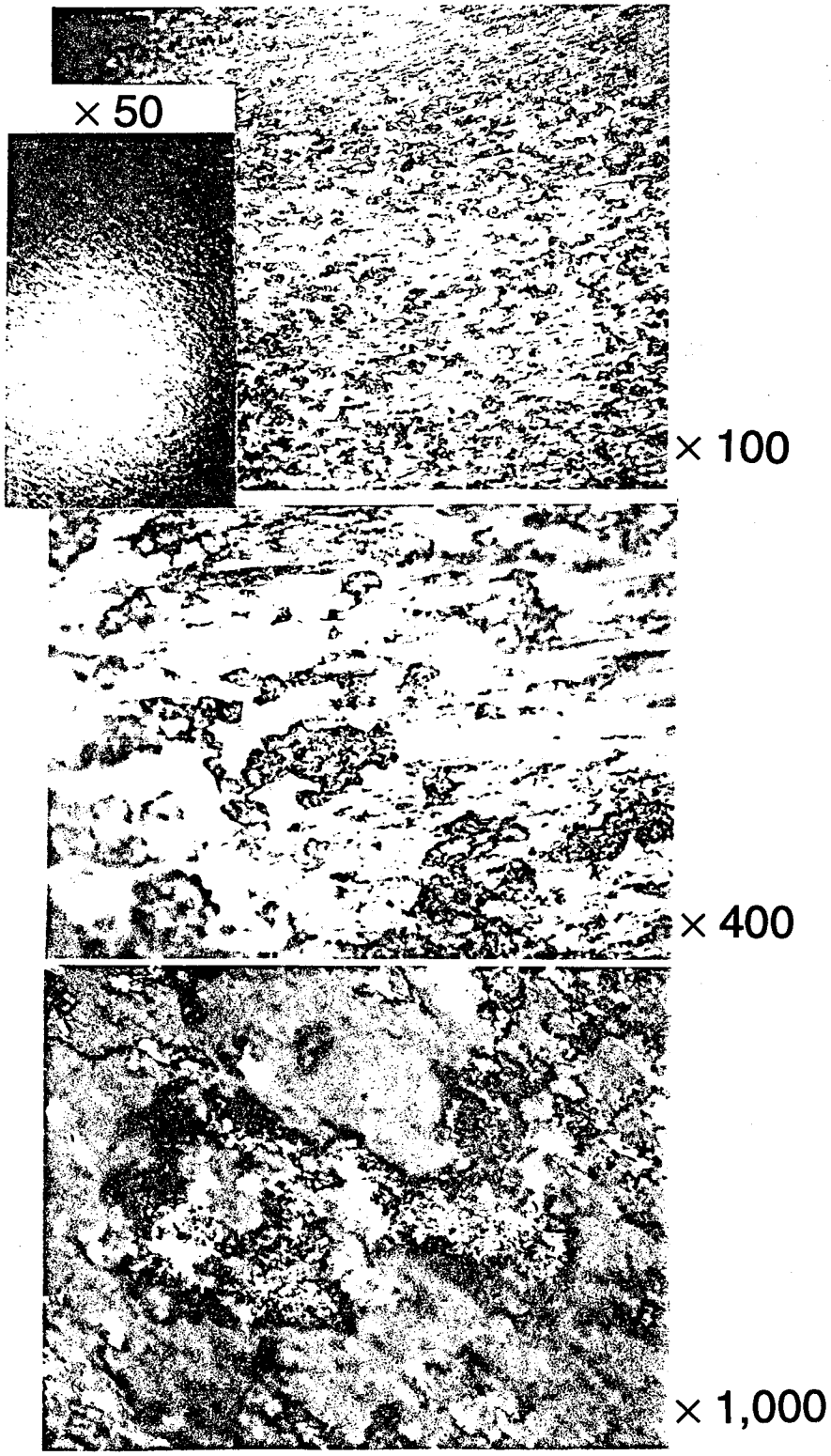

Figure 5. Heavily worn ball No. 3 (bearing No. 352): adhesive/shear peeling wear mode. Optical micrographs at × 50, × 100, × 400 and × 1,000.

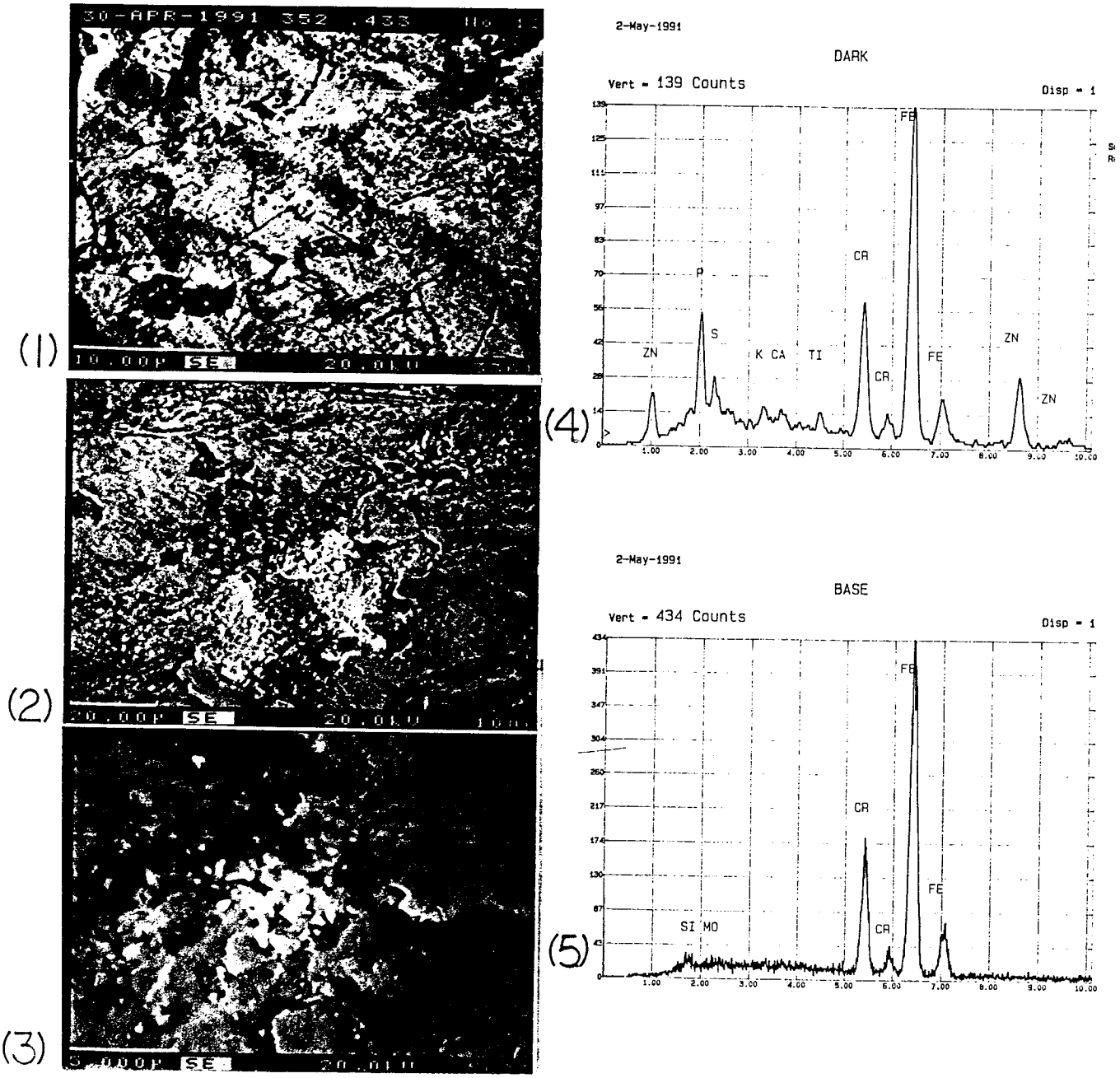

Figure 6. Heavily worn ball No. 12 (bearing No. 352): adhesive/shear peeling wear and early contact fatigue. Microprobe SEM and EDS graphs. (1) Surface cracks, × 3,360; (2) surface peeling and submicron size debris, × 1,000; (3) detail of (2), × 5,000; (4) microprobe EDS inside a spall, and (5) EDS overall.

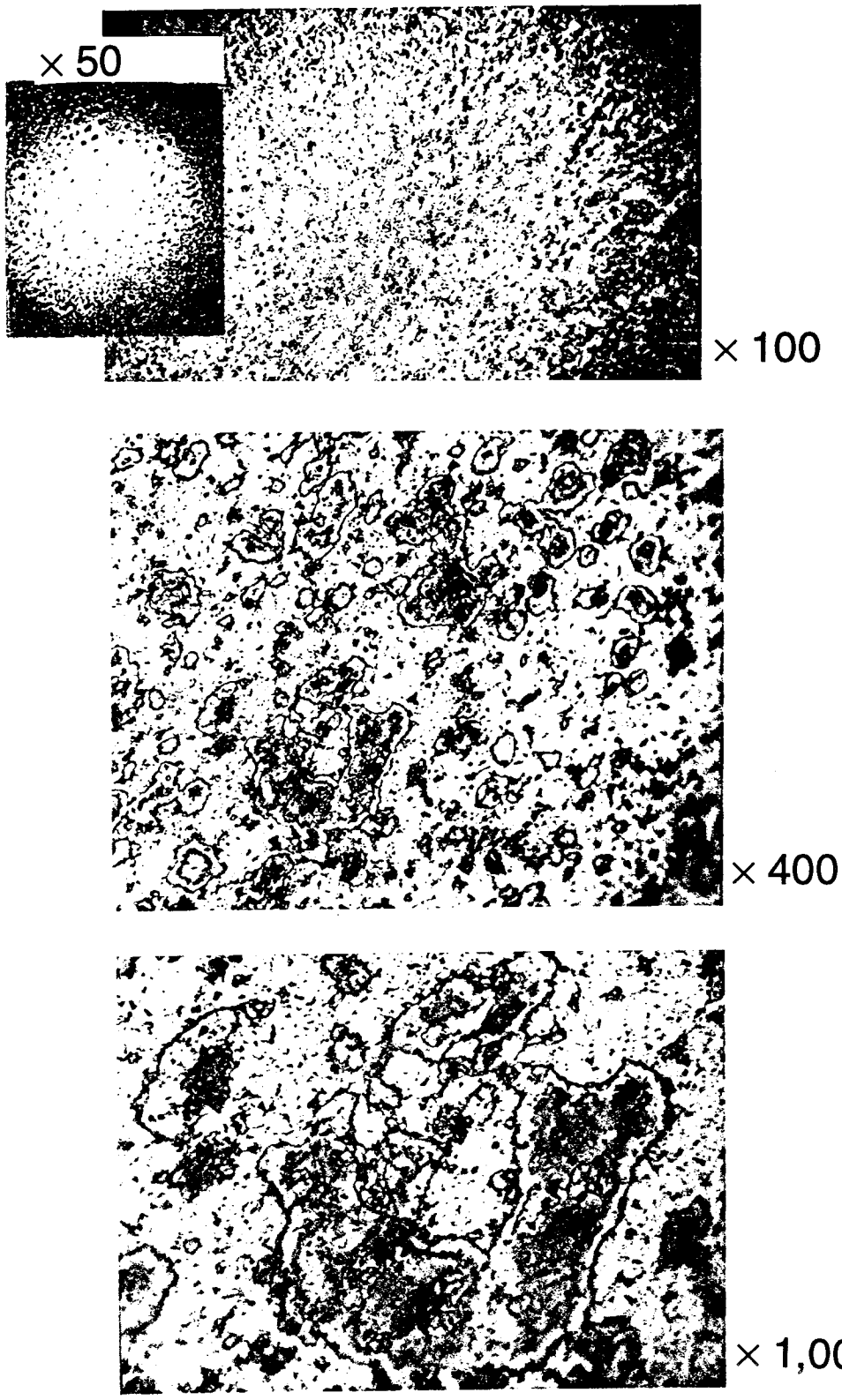

Figure 7. Lightly worn ball No. 10 (bearing No. 611): adhesive/shear peeling wear mode. Optical micrographs at × 50, × 100, × 400, and × 1,000.

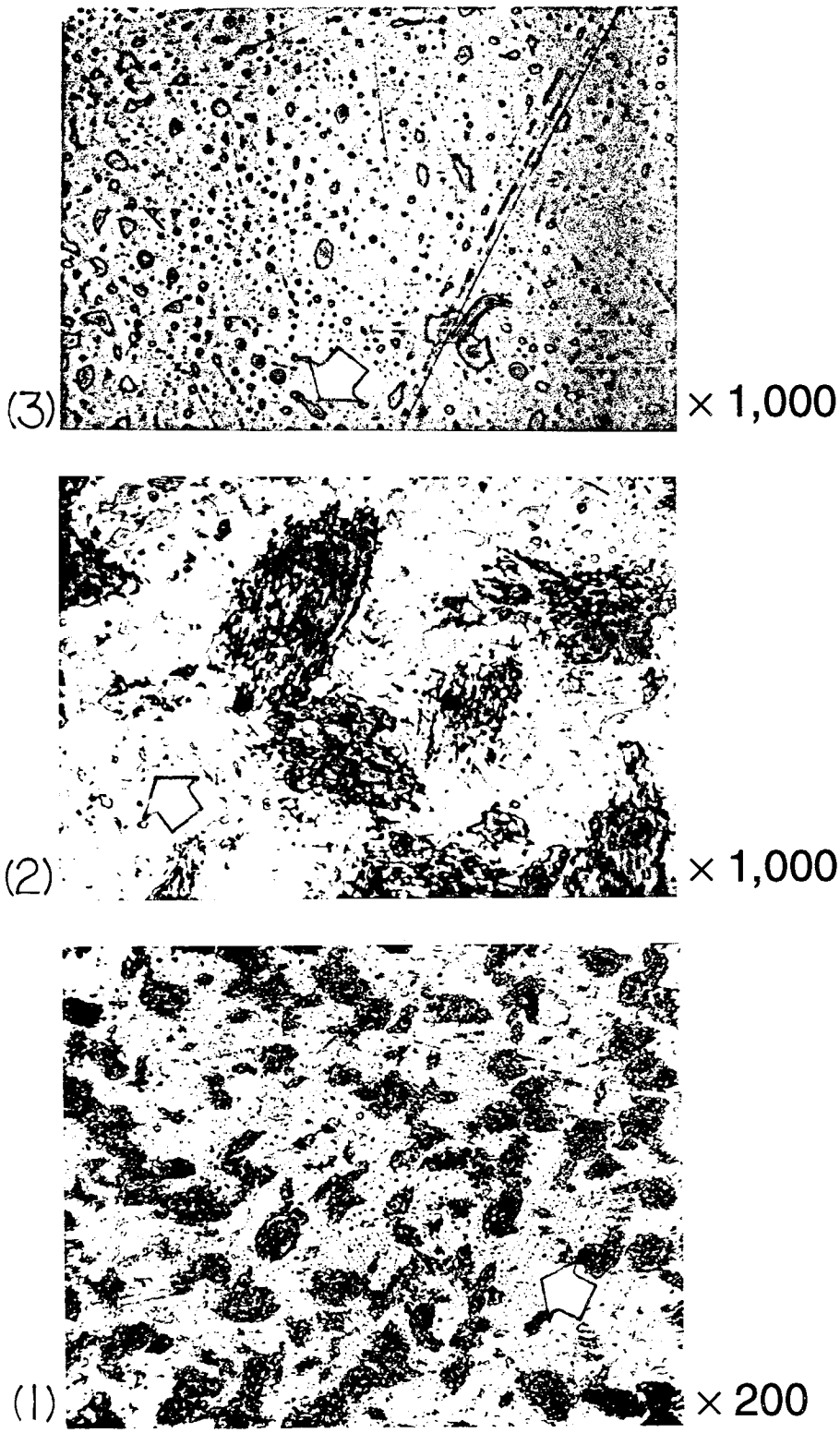

Figure 8. Lightly worn ball No. 1 (bearing No. 500): (1) adhesive/shear peeling (black spots) and virgin surface (white background, actually goldish) with original machining marks (dotted lines) still visible; (2) detail of (1) shows the dotted lines to also have the adhesive/shear origin; (3) finishing marks on a brand new ball. Optical micrographs.

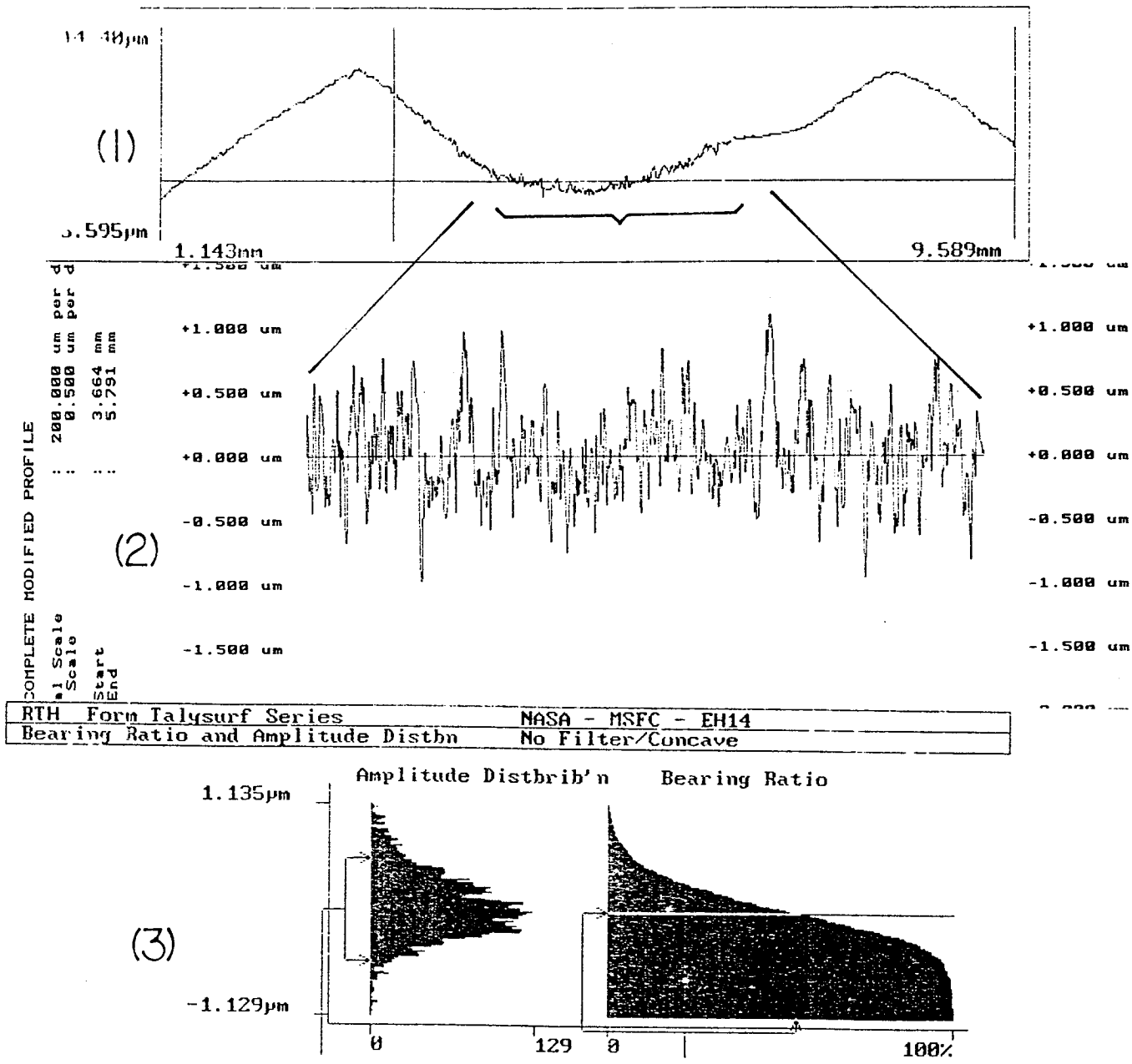

Figure 9. Heavily worn outer ring No. 352. Form Talysurf series (Rank Taylor-Hobson) surface profilograms: (1) modified profile, (2) wear track, detail of (1), roughness statistics of the wear track.

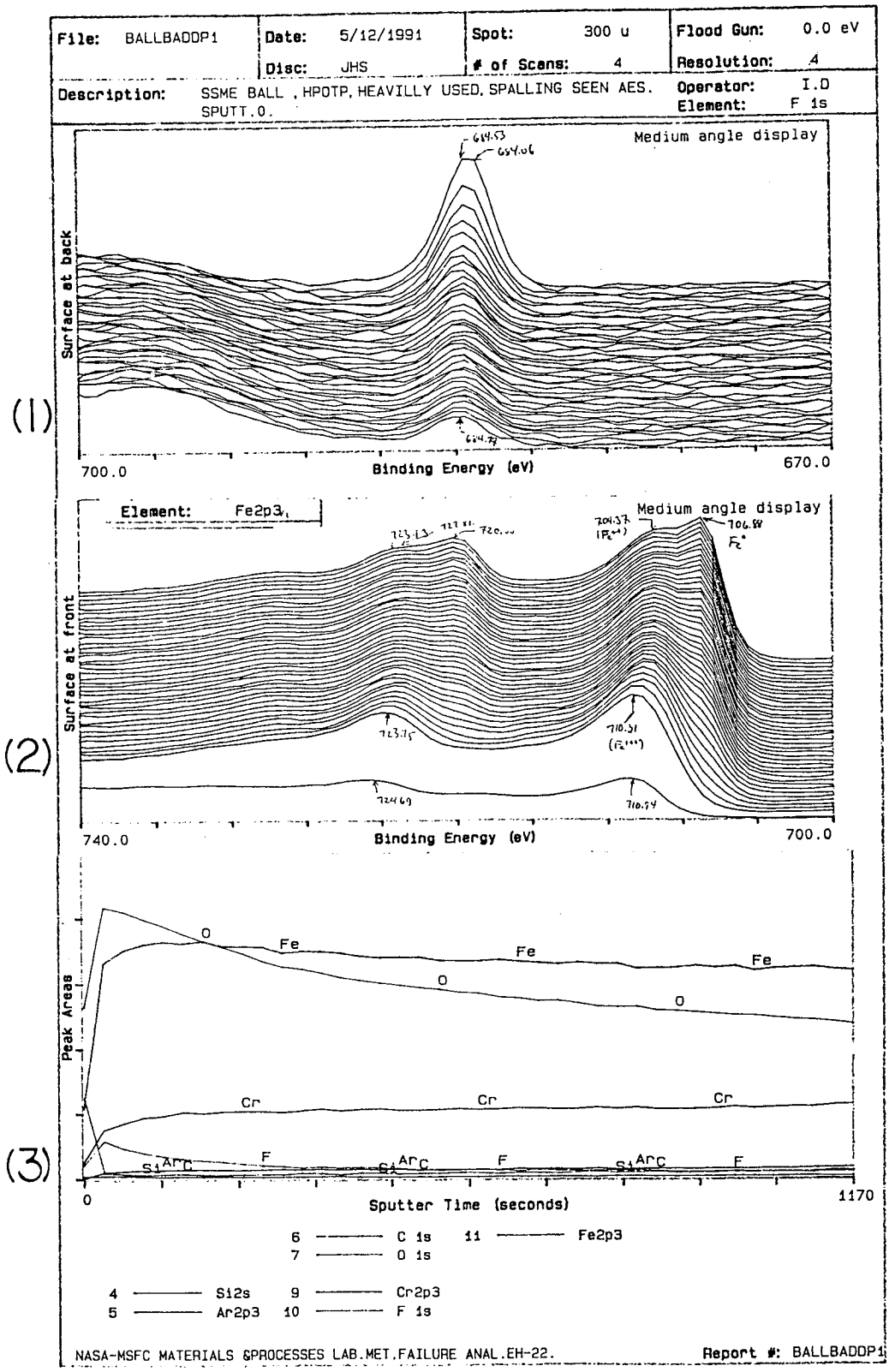

Figure 10. Depth profiling of a heavily worn ball. X-ray photoelectron spectroscopy: (1) fluorine, (2) iron, and (3) combined diagram.

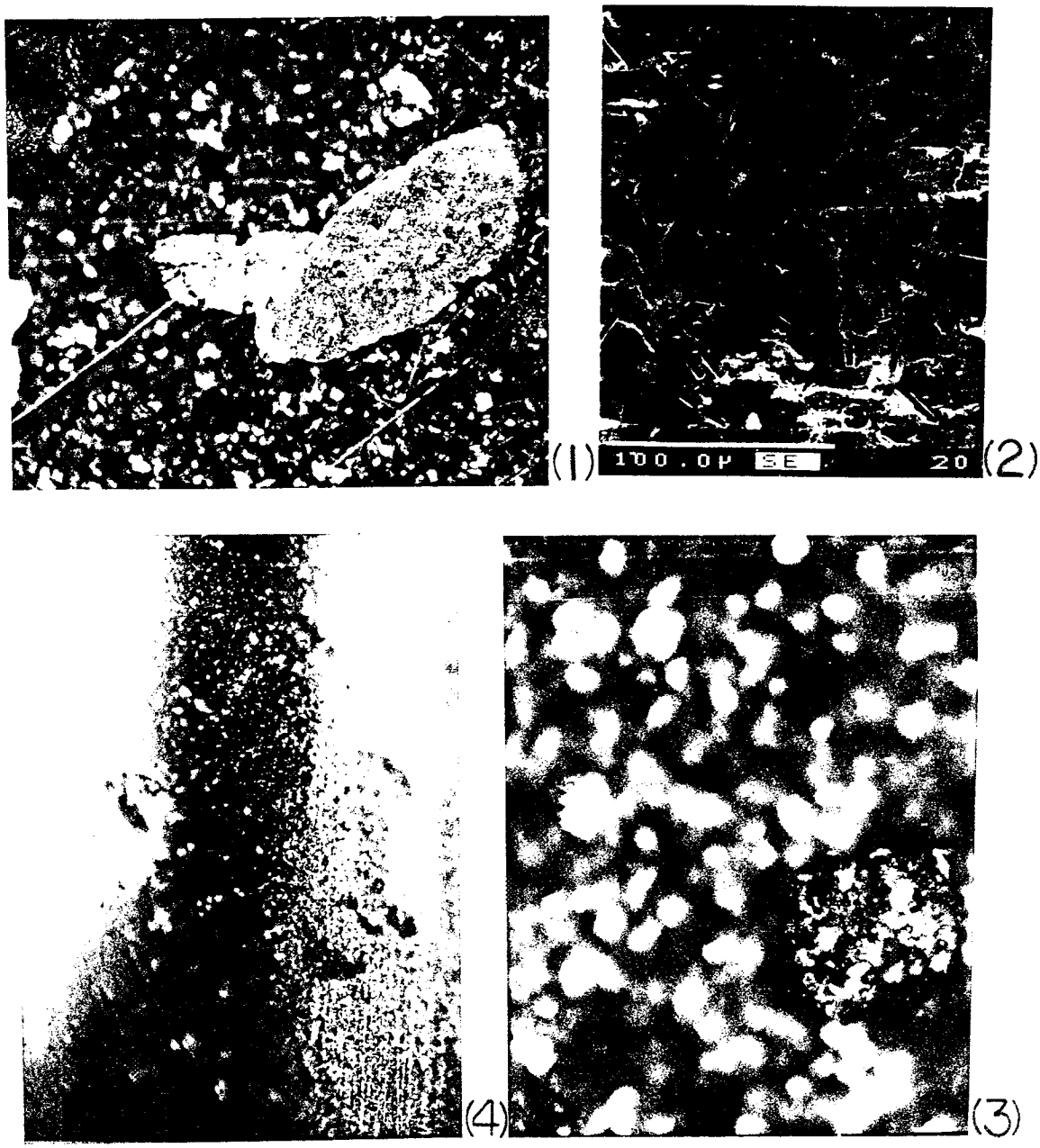

Figure 11. BSMT wear debris (× 100): (1) large flake, (2) overall, (3) composite flake showing secondary peeling, and (4) inner ring wear track.

APPENDIX: EVIDENCE

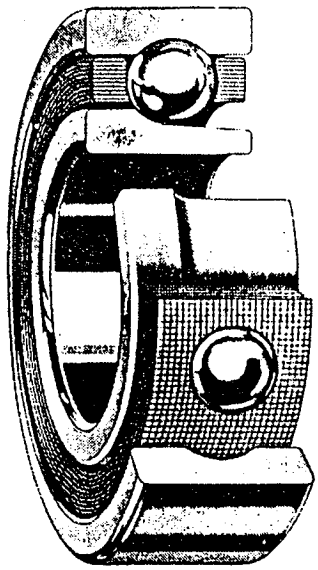

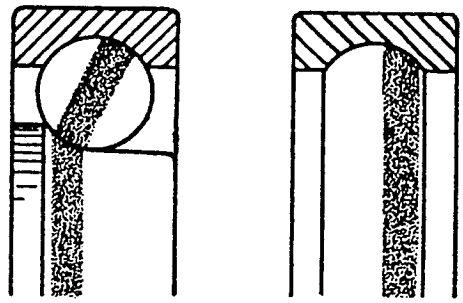

Separable angular contact
ball bearing

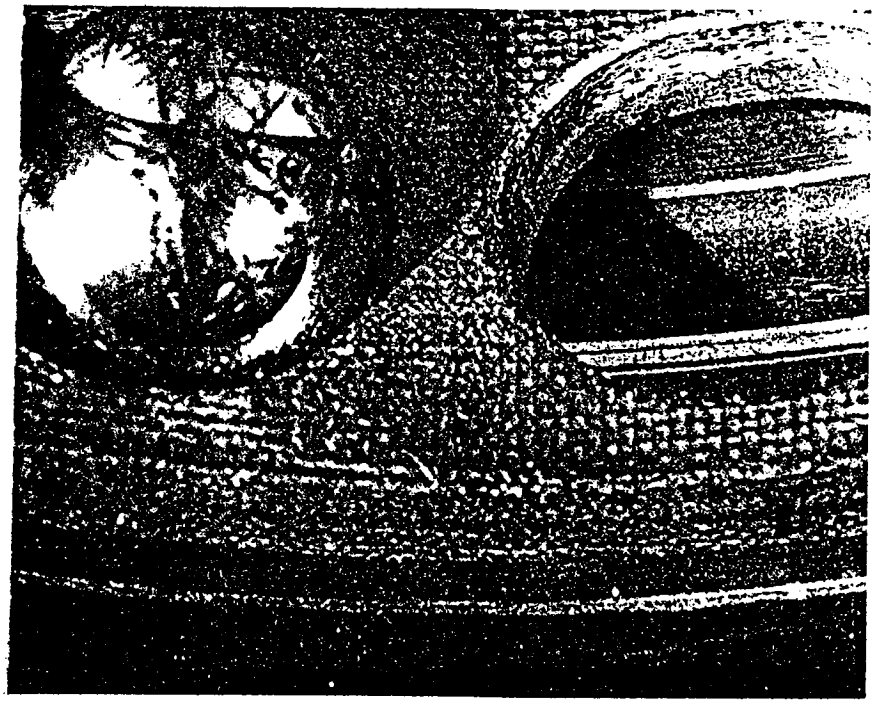

Figure A-1. Angular contact ball bearing. Wear patterns in axial loading.

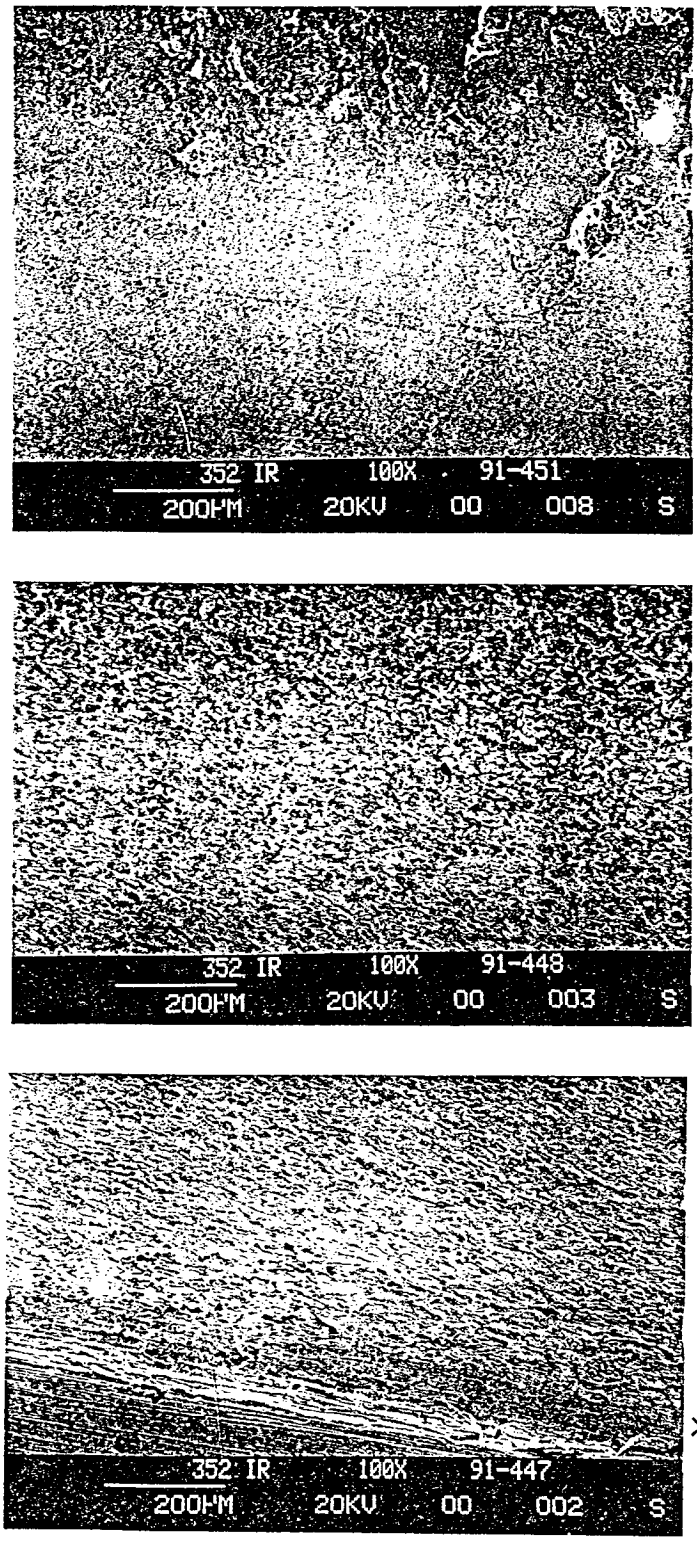

Figure A-2. Surface condition across the wear track. Inner ring of bearing No. 352.

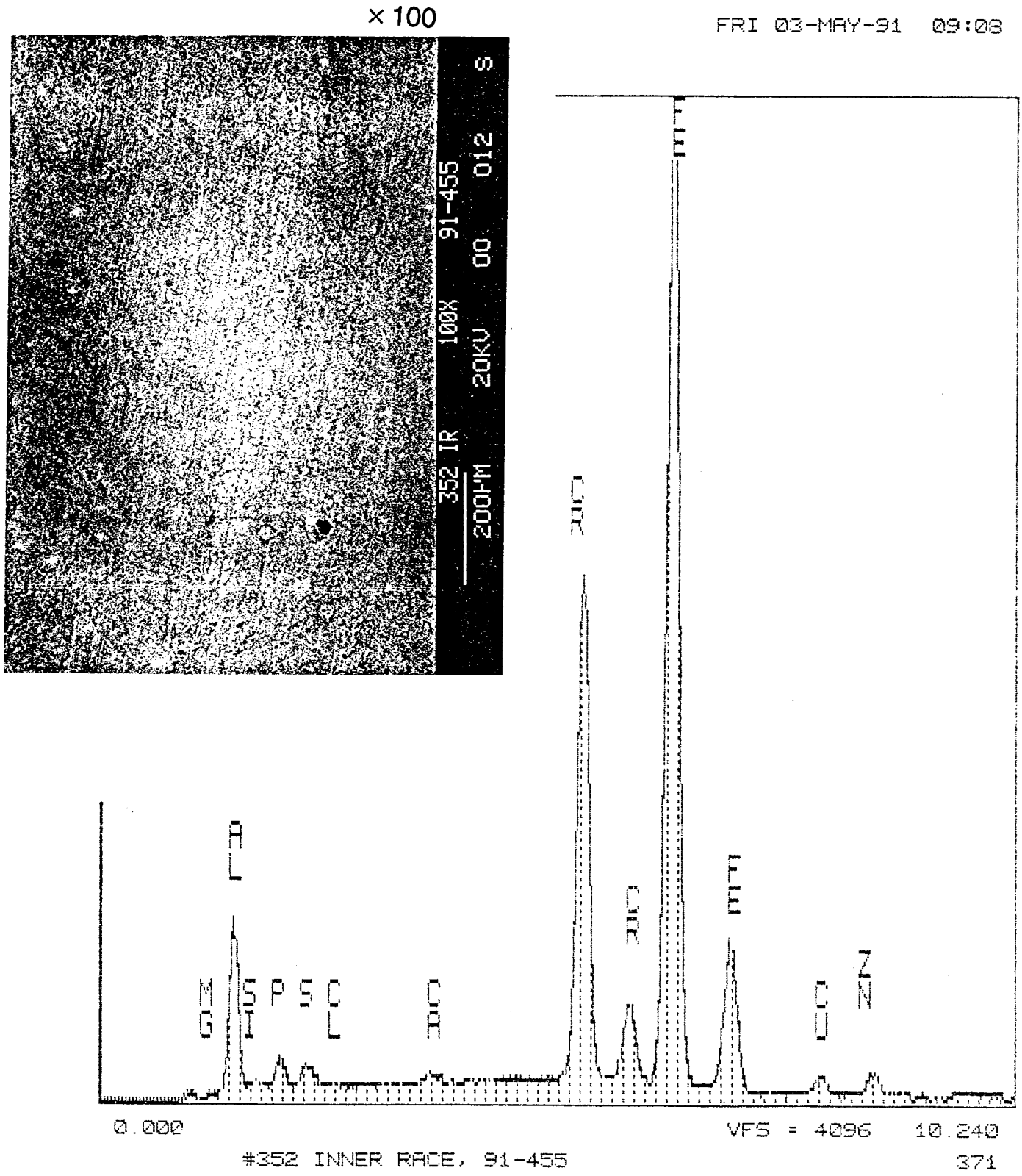

Figure A-3. Overall SEM/EDS of the wear track on the inner ring of bearing No. 352: Note presence of foreign matter like Al, Zn, and Cu. It may have come with the lox stream (compare figs. A-54 through A-62).

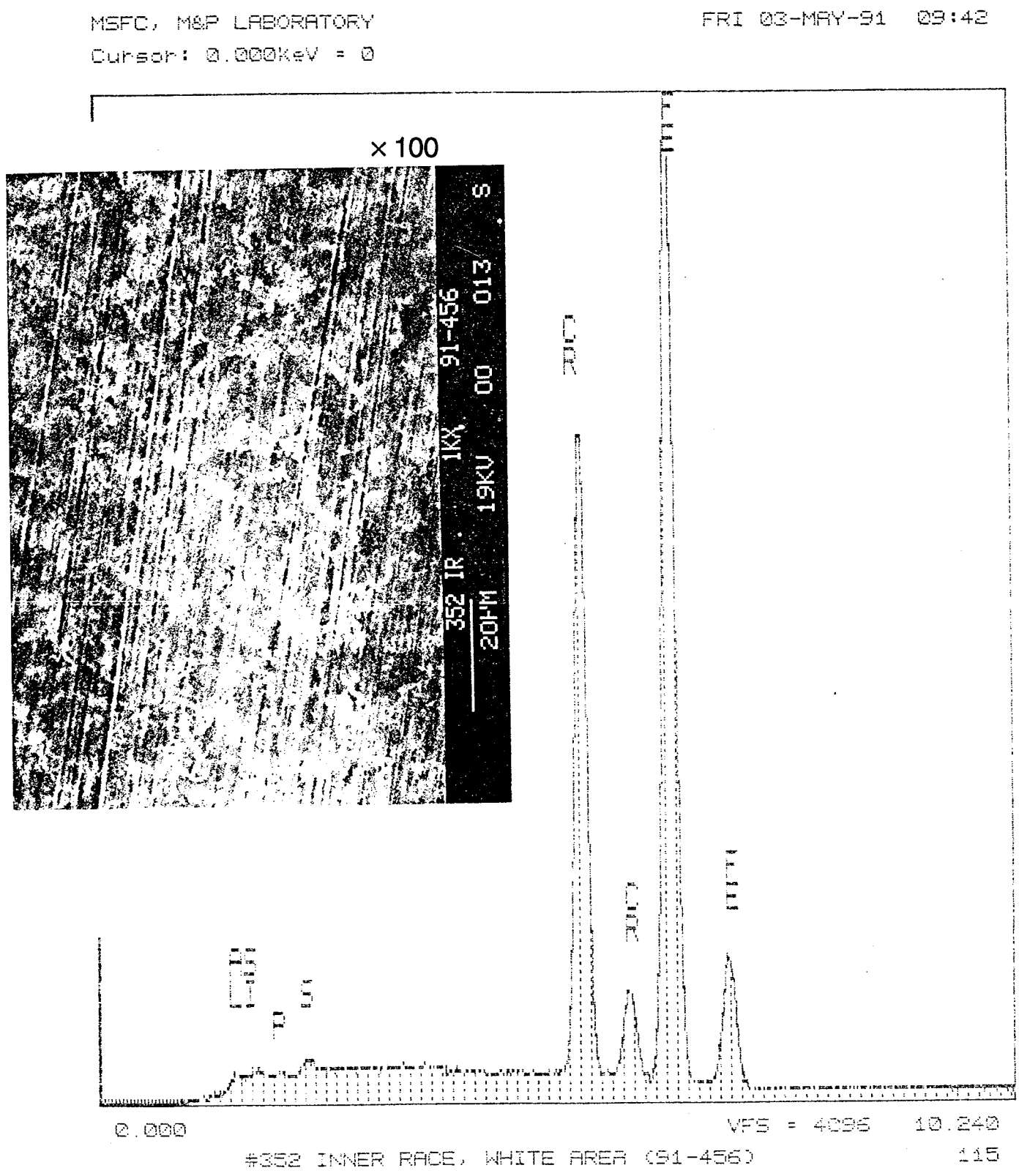

Figure A-4. SEM/EDS of the white area on wear track on the inner ring of bearing No. 352. Note increased Cr/Fe ratio compared to figure A-3.

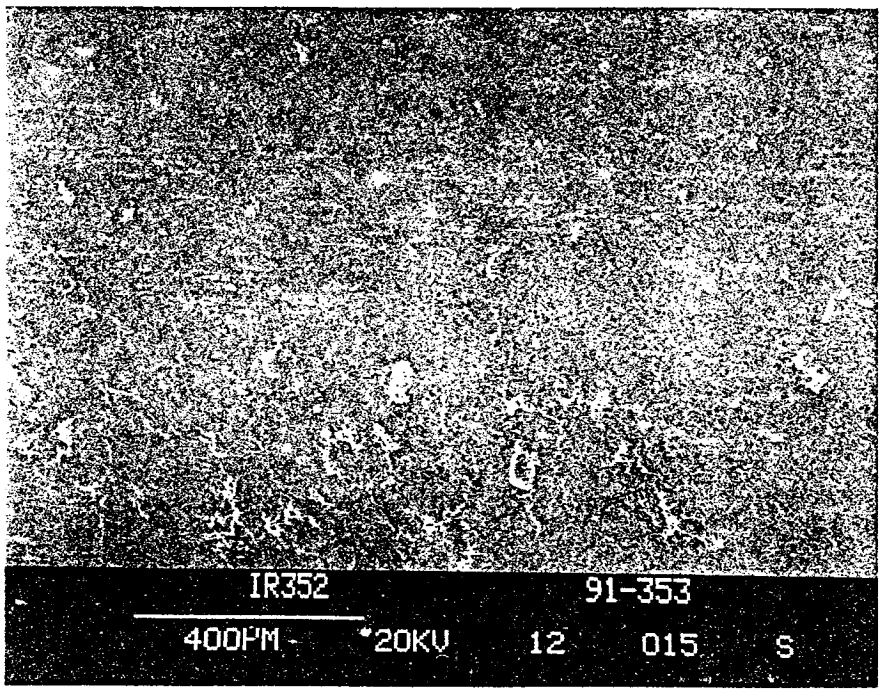

× 100

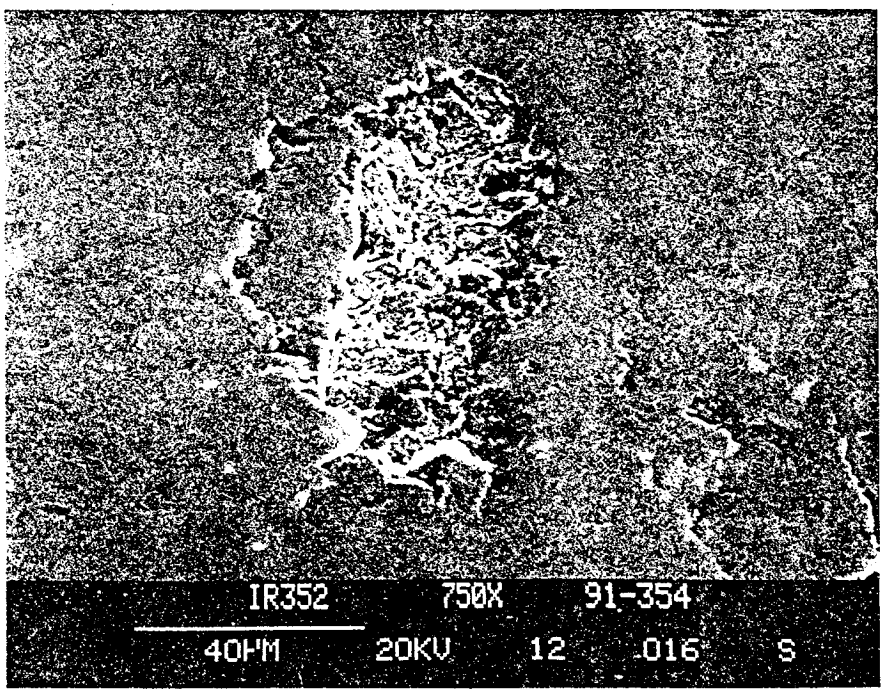

× 750

Figure A-5. SEM of the microfatigued area on wear track of the inner ring of bearing No. 352.

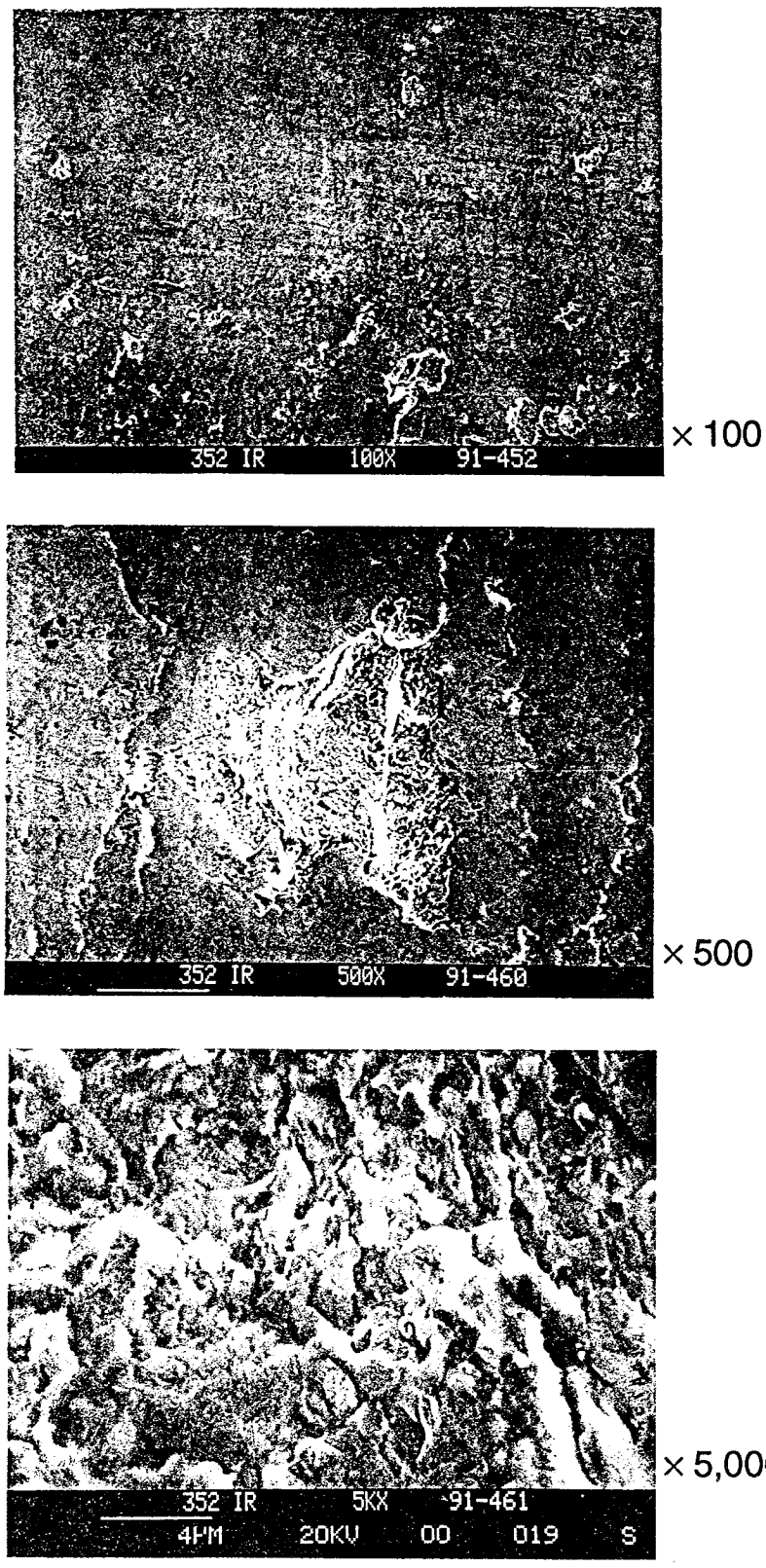

Figure A-6. SEM of the microfatigued area on wear track of the inner ring of bearing No. 352. Note grainy appearance of the spall bottom.

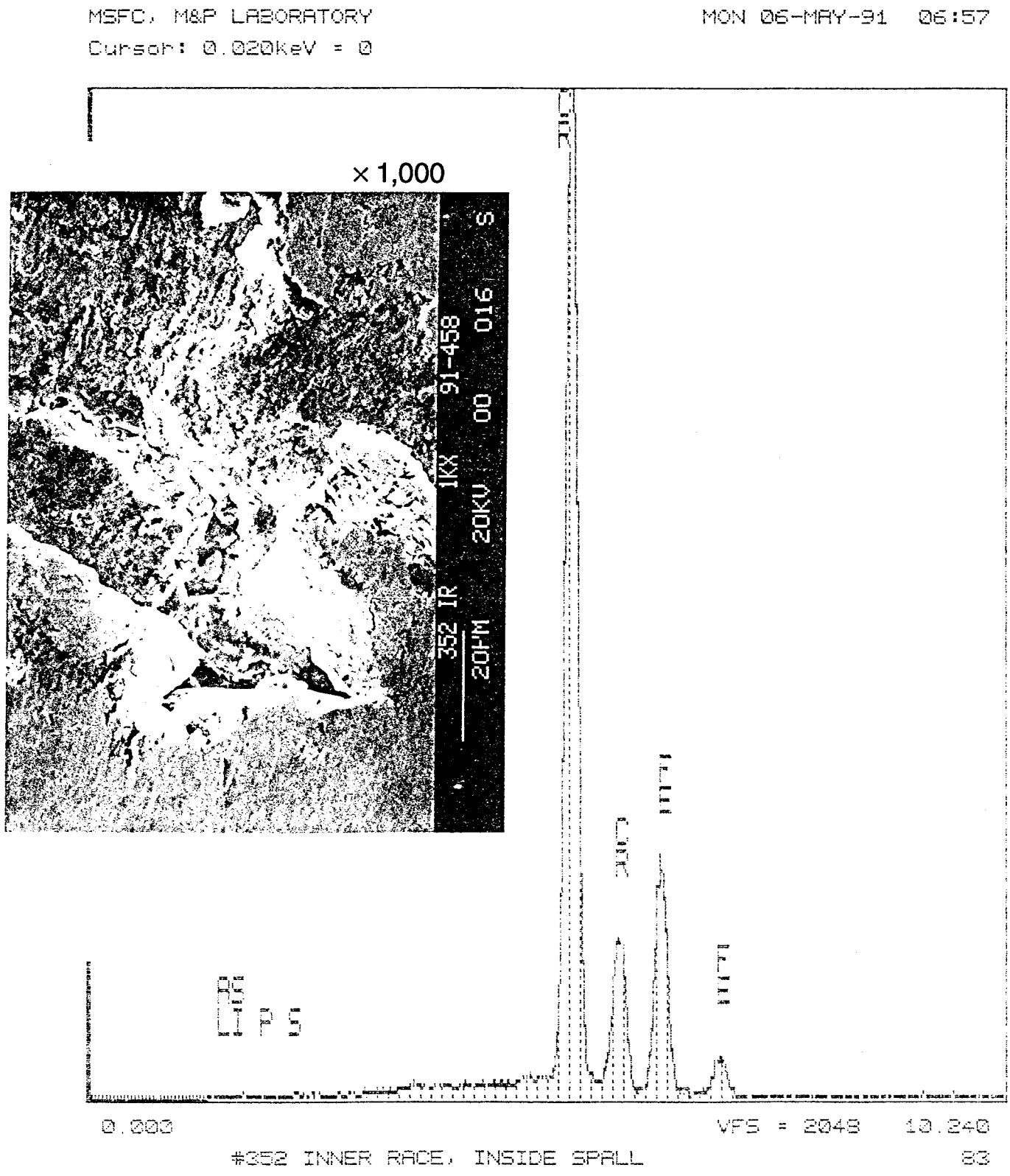

Figure A-7. SEM/EDS on microfatigued area. Wear track of the inner ring of bearing No. 352. Note high Cr concentration inside the spall.

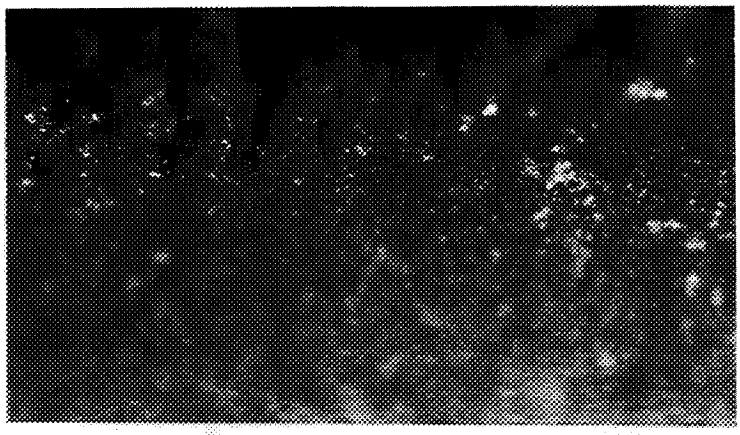

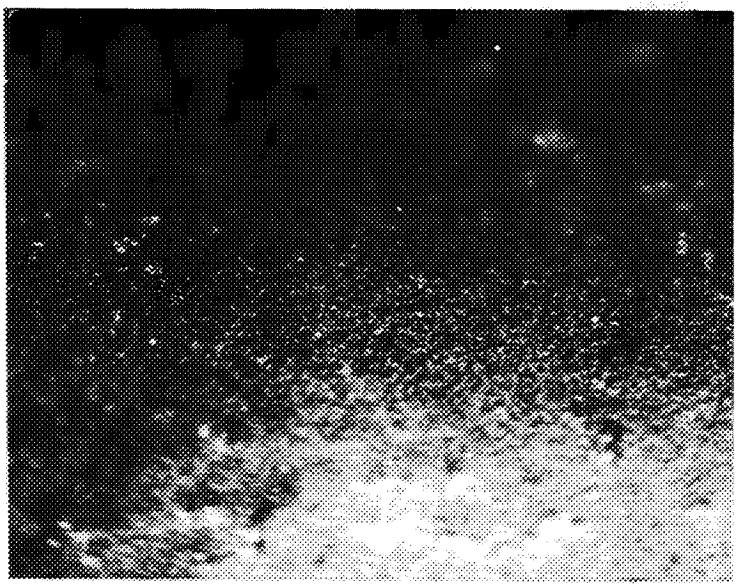

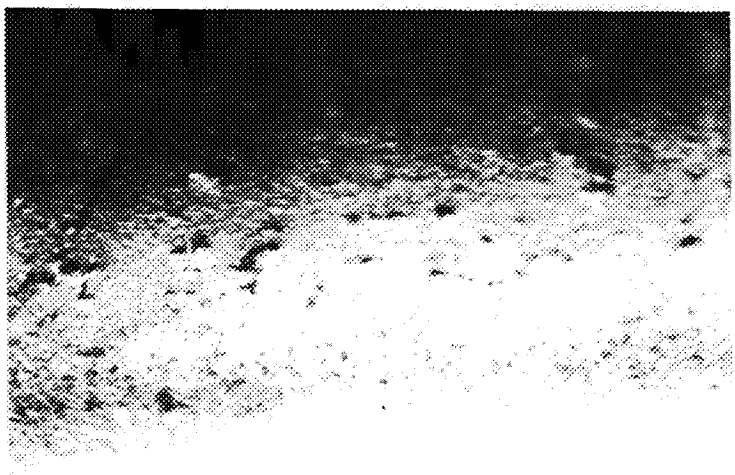

Figure A-8. Optical microscopy (OM) of the wear track on the inner ring of bearing No. 352. Note many spalls, holes, and scratches.

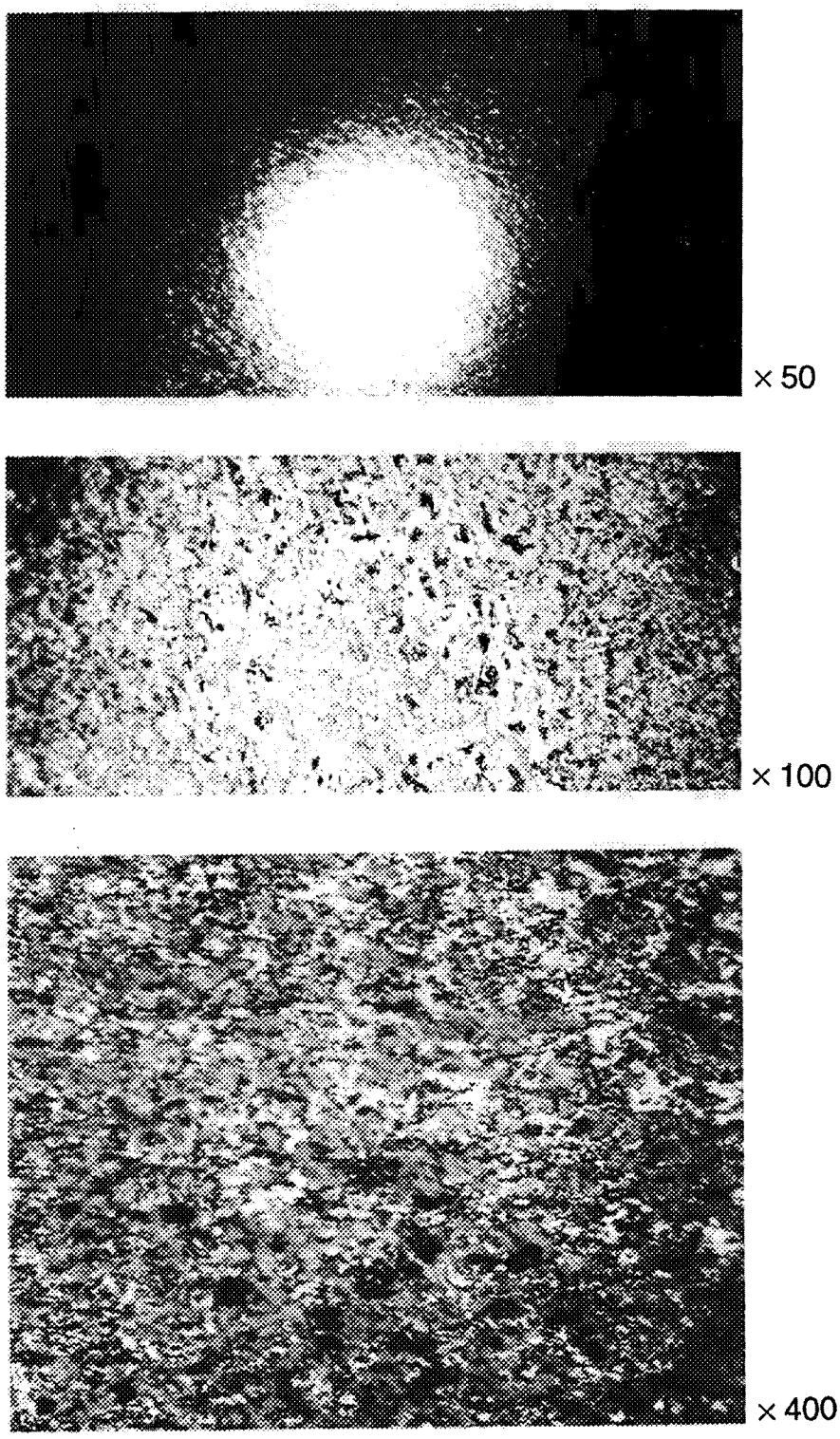

Figure A-9. OM of a ball surface in bearing No. 352. The dominant wear mode is adhesive/shear peeling. Note many dark pits.

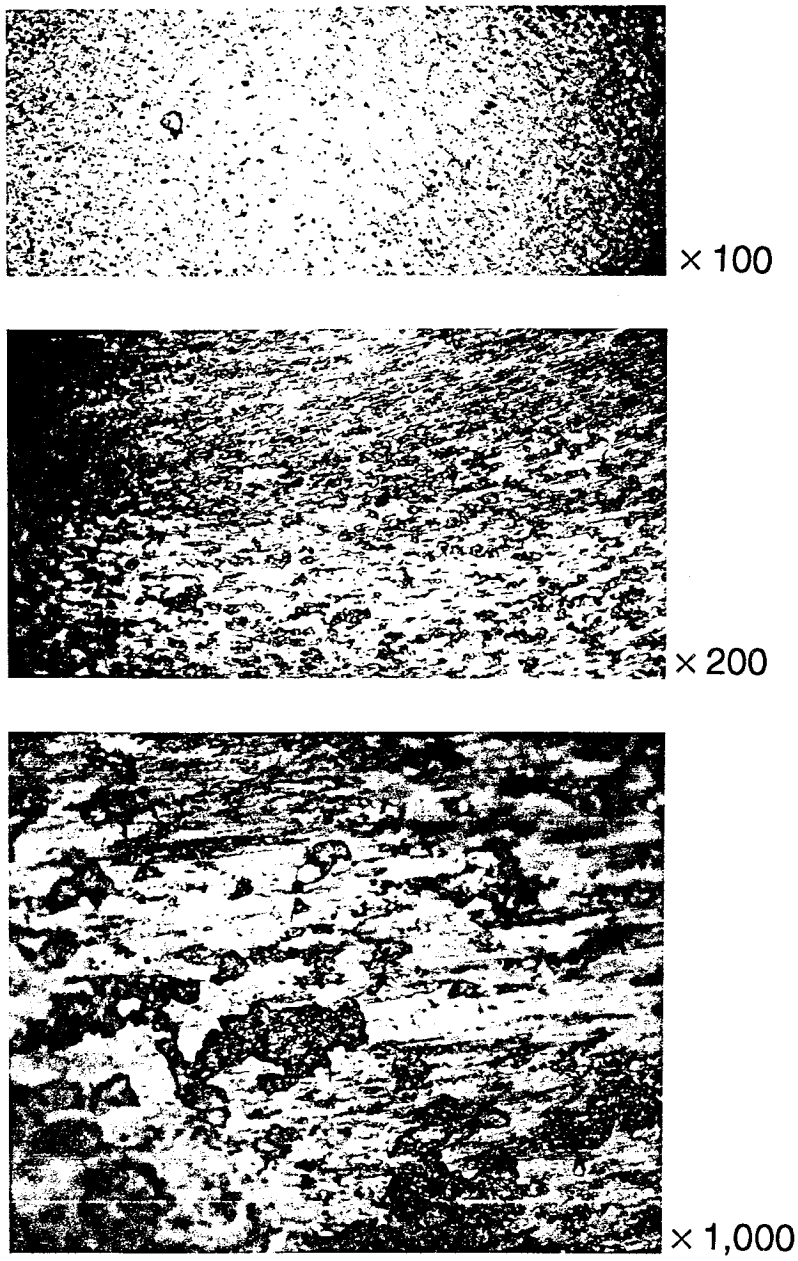

Figure A-10. OM of a ball surface in bearing No. 352. Adhesive/shear peeling of the upper layer may involve brittle fracture or low cycle fatigue. Note many cracks and wear debris inside dark pits.

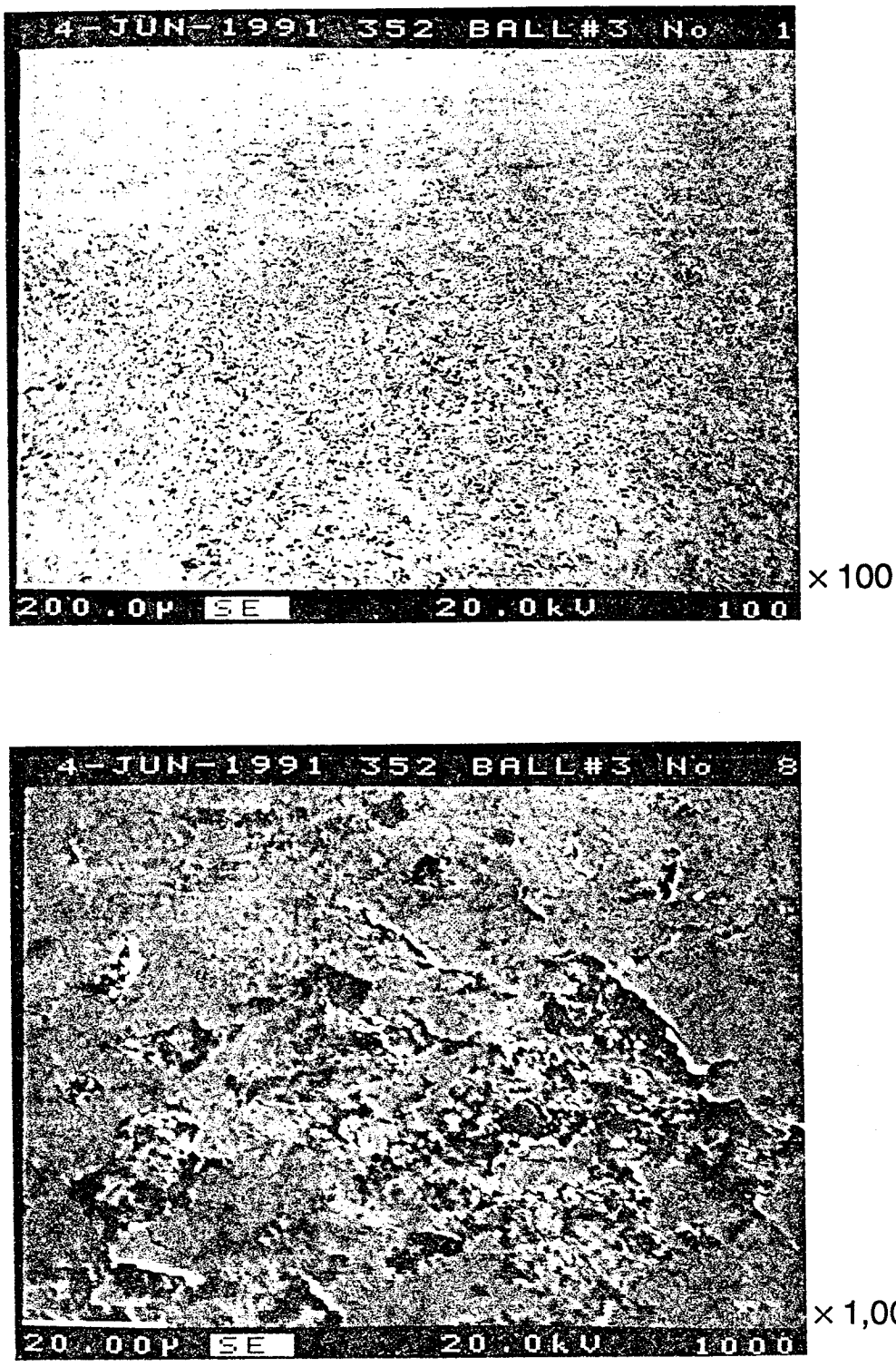

Figure A-11. Microprobe SEM of a ball surface in bearing No. 352. Adhesive/shear peeling of the upper layer. Note many fatigue cracks.

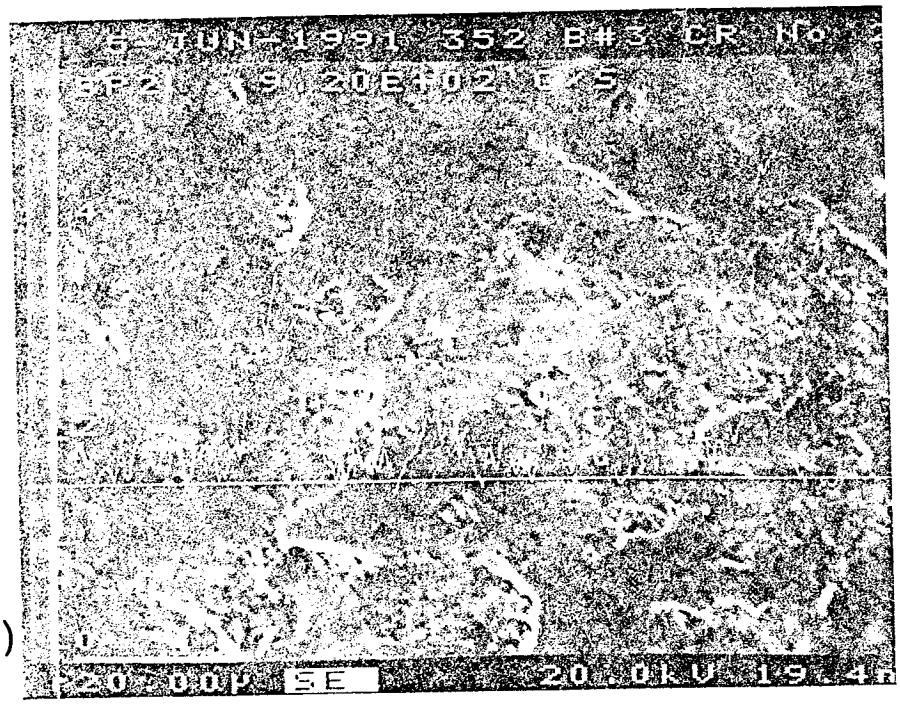

(1) × 1,000

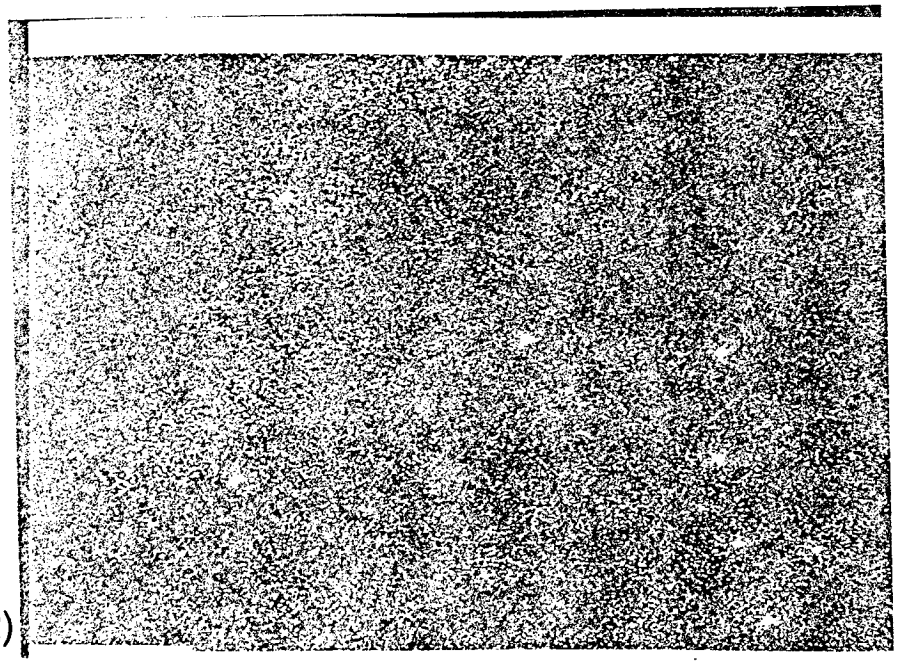

(2) × 1,000

Figure A-12. Microprobe analysis of a ball surface in bearing No. 352 (the same area as in fig. A-11). (1) Cr distribution along the horizontal line, note Cr concentration inside spalls; and (2) overall Cr distribution.

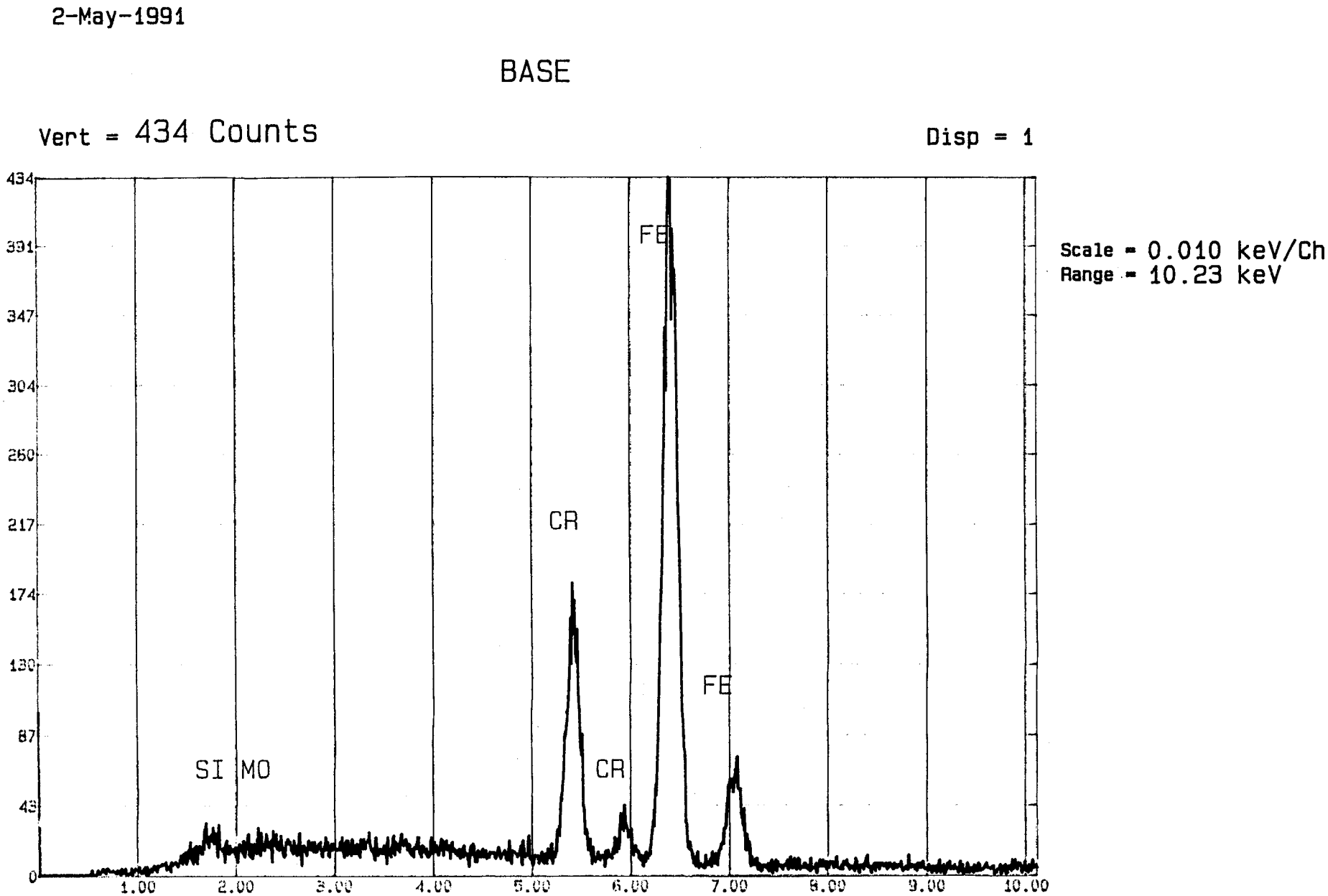

Figure A-13. Microprobe analysis of a ball surface in bearing No. 352. Note presence of Si (ingredient in glass fibers of Armalon cages).

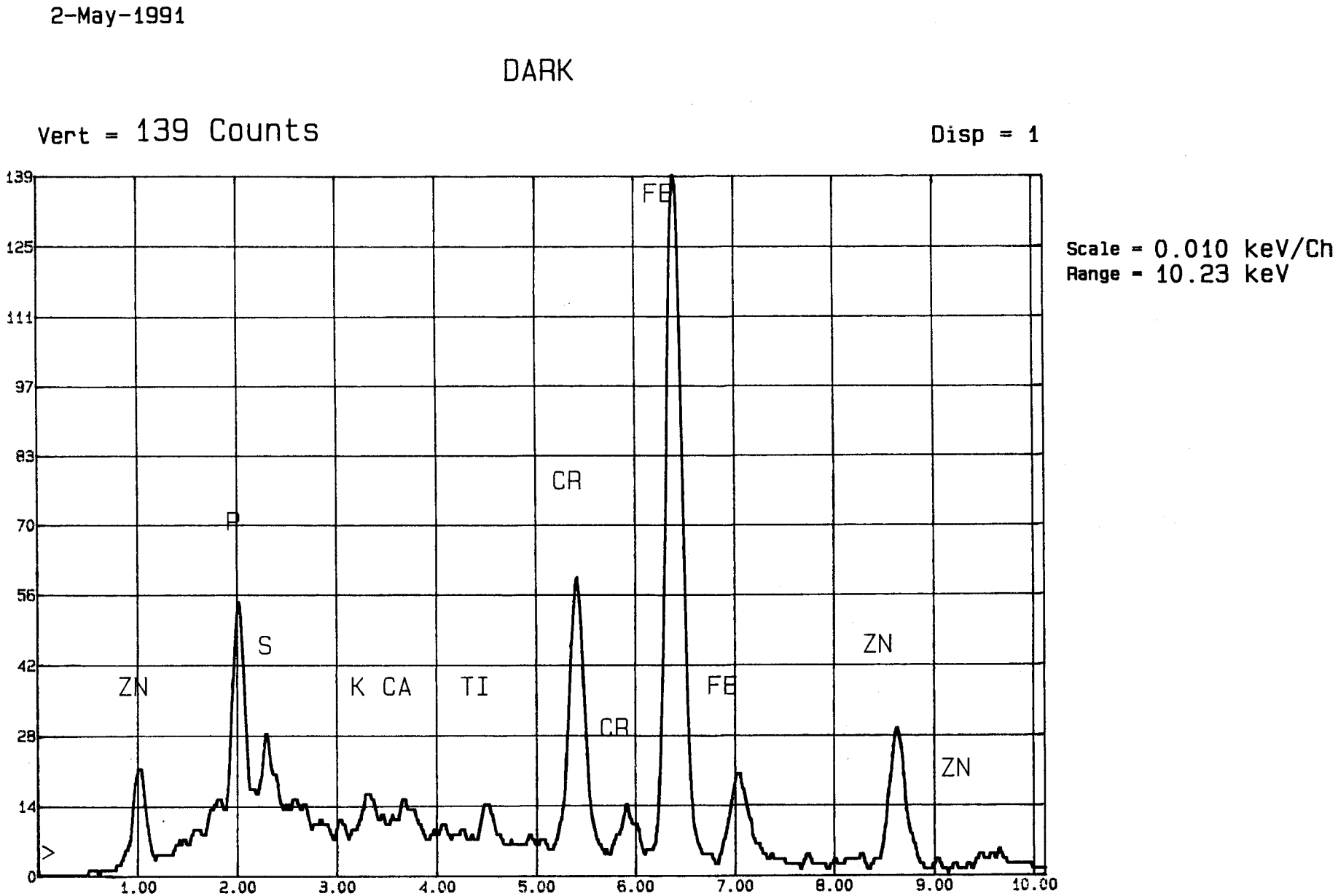

Figure A-14. Microprobe analysis of a ball surface pit in bearing No. 352. Note presence of elements foreign to the system like Zn, Ti and P, all or some of which may have entered the bearing with lox as contaminants. Also compare figures A-54 through A-62.

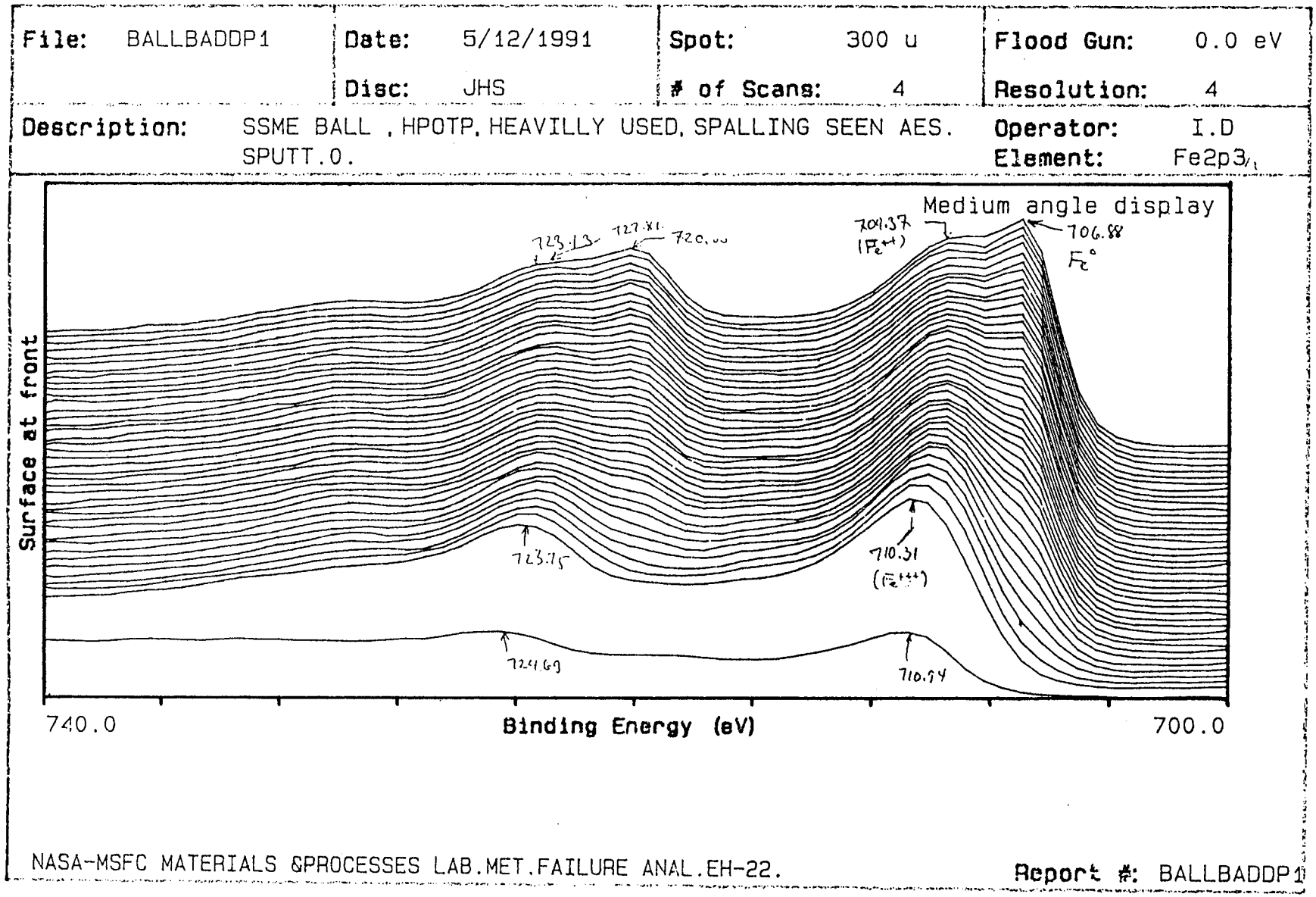

Figure A-15. XPS sputtering for depth profiling on a ball of bearing No. 352. Note iron (oxide) transformation (indicated by the shift of peak of binding energy with time).

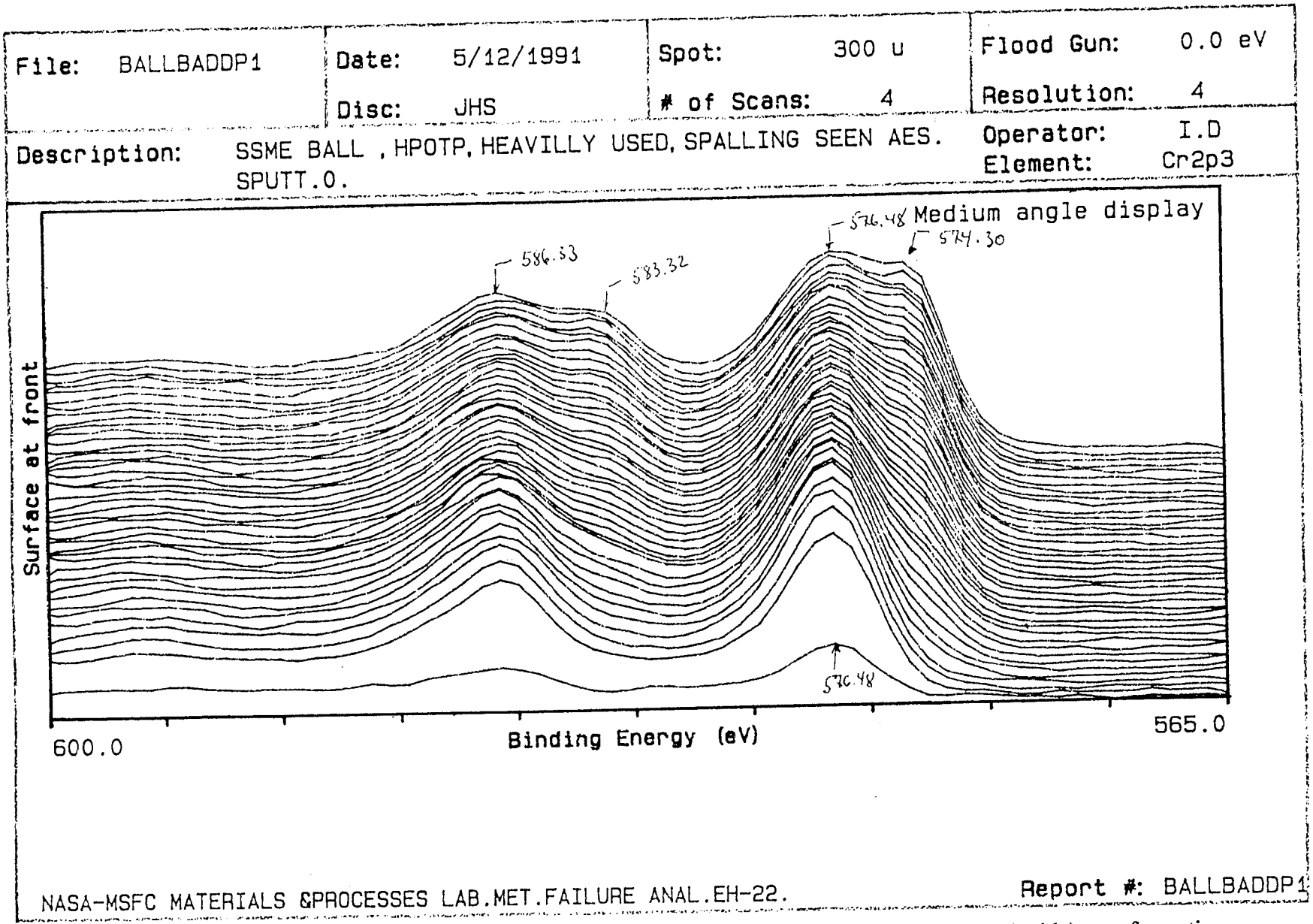

Figure A-16. XPS sputtering for depth profiling on a ball of bearing No. 352. Note chromium (oxide) transformation (indicated by the shift in the position of the peak of binding energy with time).

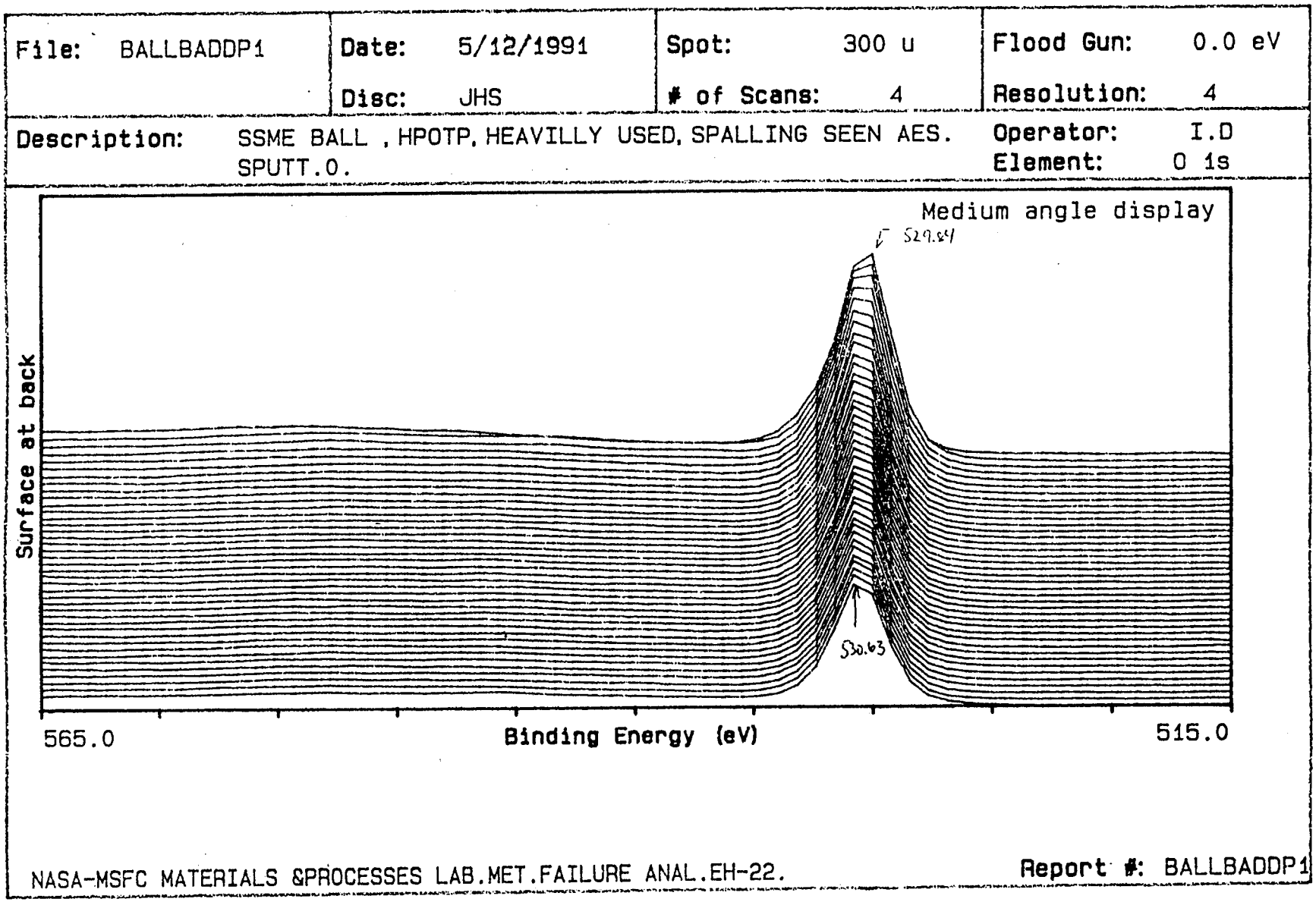

Figure A-17. XPS sputtering for depth profiling on a ball of bearing No. 352. The binding energy peak decreases with depth (sputter time), thus showing a drop in oxygen concentration below the surface. Note the "surface at back" reference.

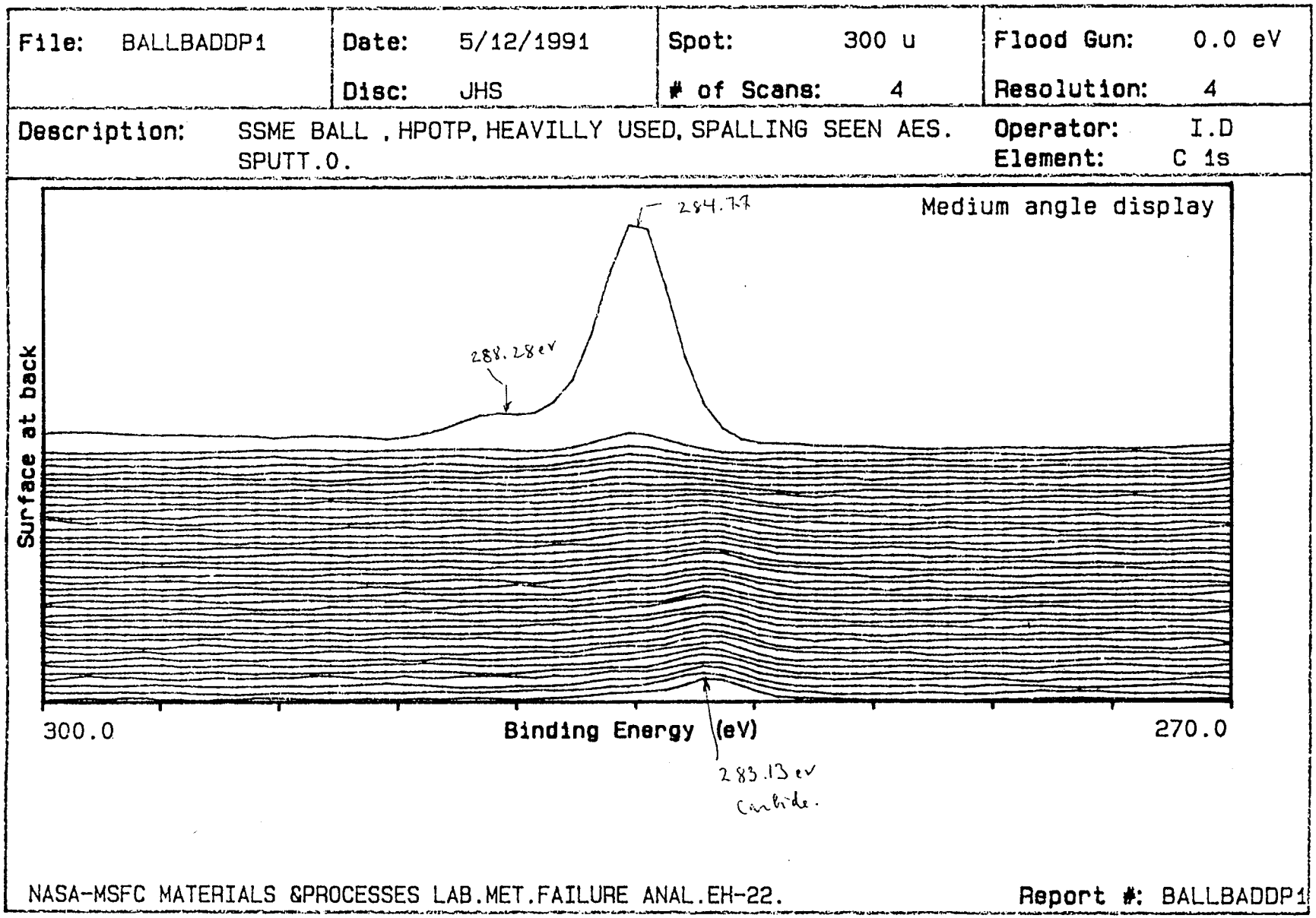

Figure A-18. XPS sputtering for depth profiling on a ball of bearing No. 352. The surface peak indicates carbon absorbed from the air. The lower peak may indicate presence of a subsurface carbide.

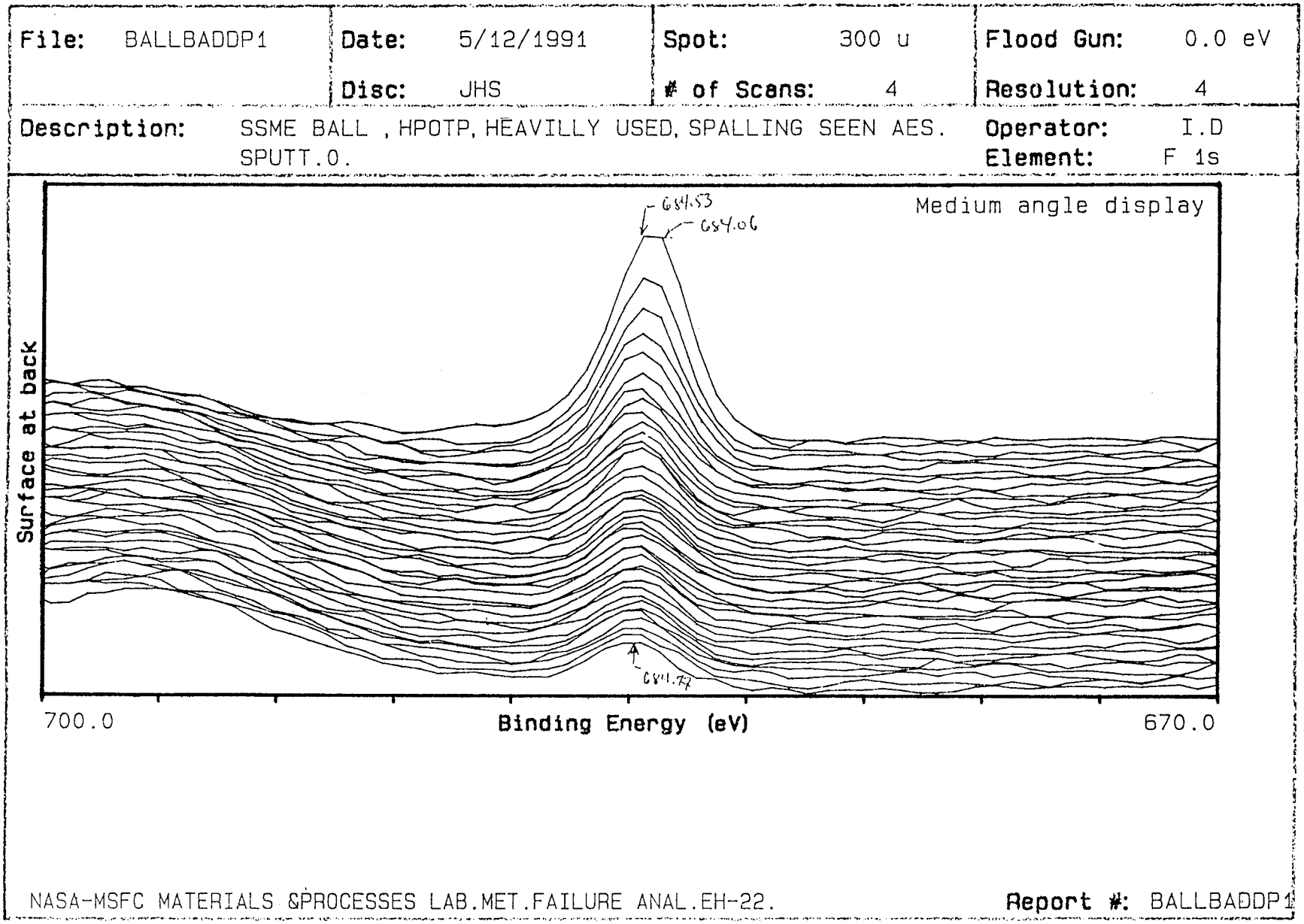

Figure A-19. XPS sputtering for depth profiling on a ball of bearing No. 352. Note how the surface peak of fluorine (basic constituent of PTFE) quickly vanishes with depth, thus indicating that a lubricant layer is very shallow.

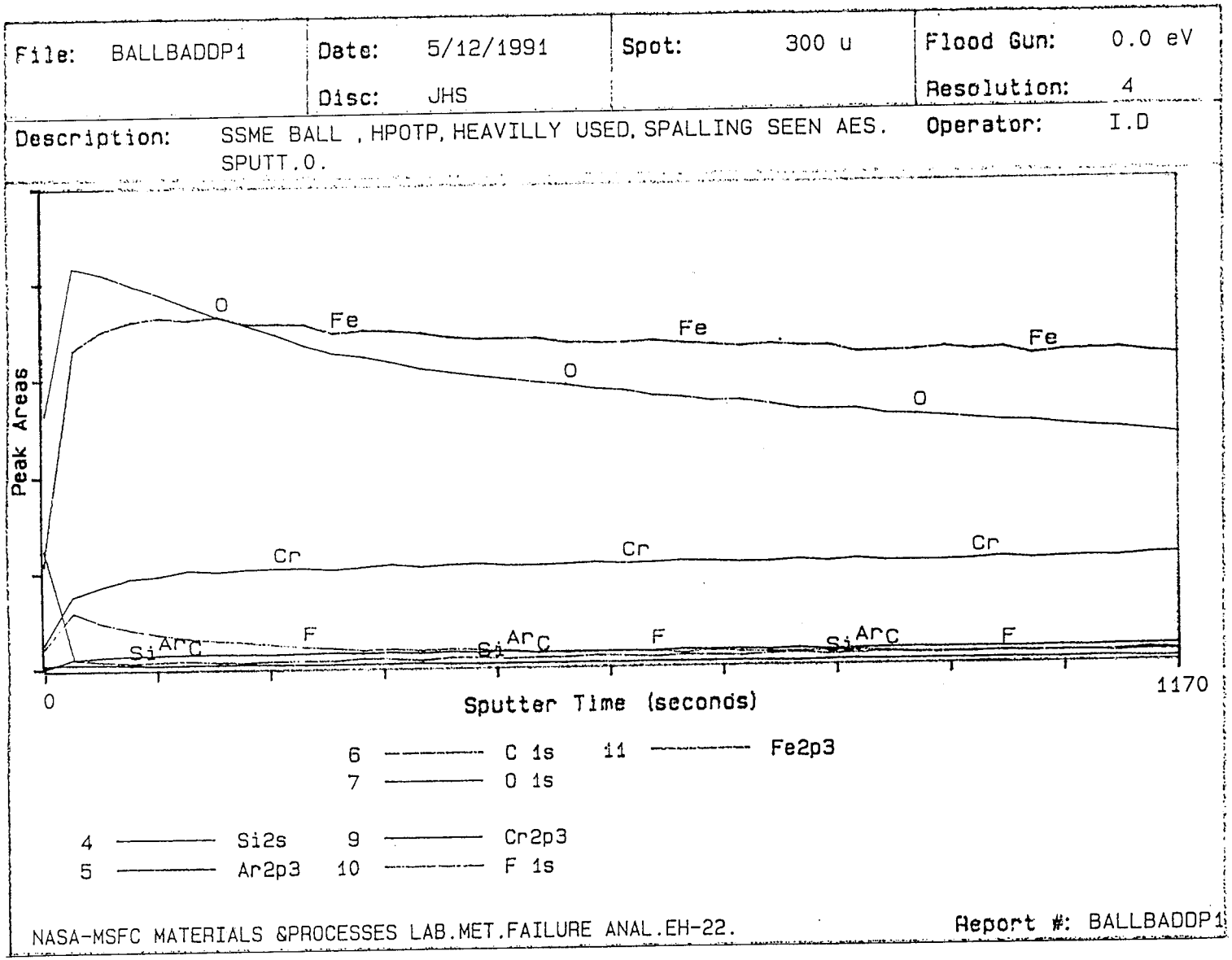

Figure A-20. XPS sputtering for depth profiling on a ball of bearing No. 352. Combined results.

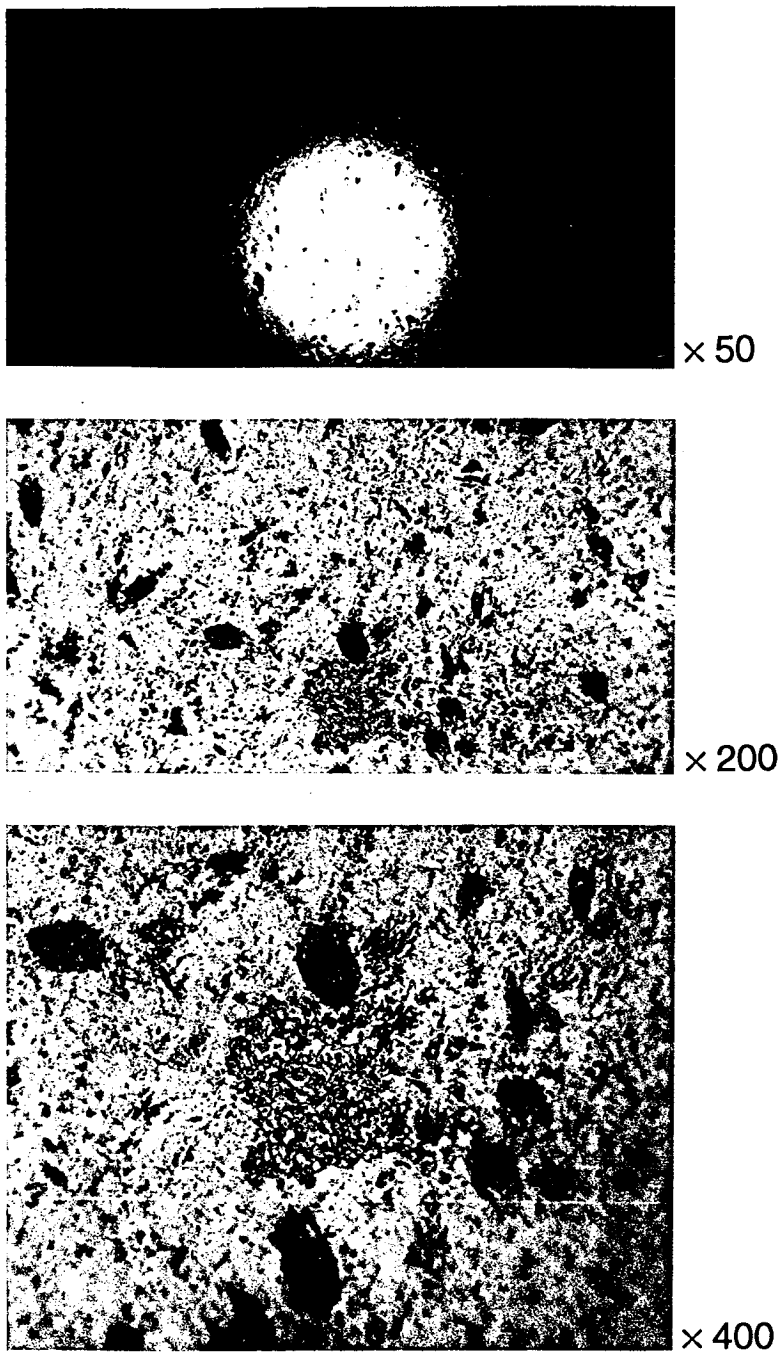

Figure A-21. OM of a very lightly worn ball of bearing No. 611 shows very dark (brown and black) spots on a highly polished golden background. A close-up view of a multicolored area between the two black patches shows very shallow peeling. The red, green, and blue colors are probably chromium oxides.

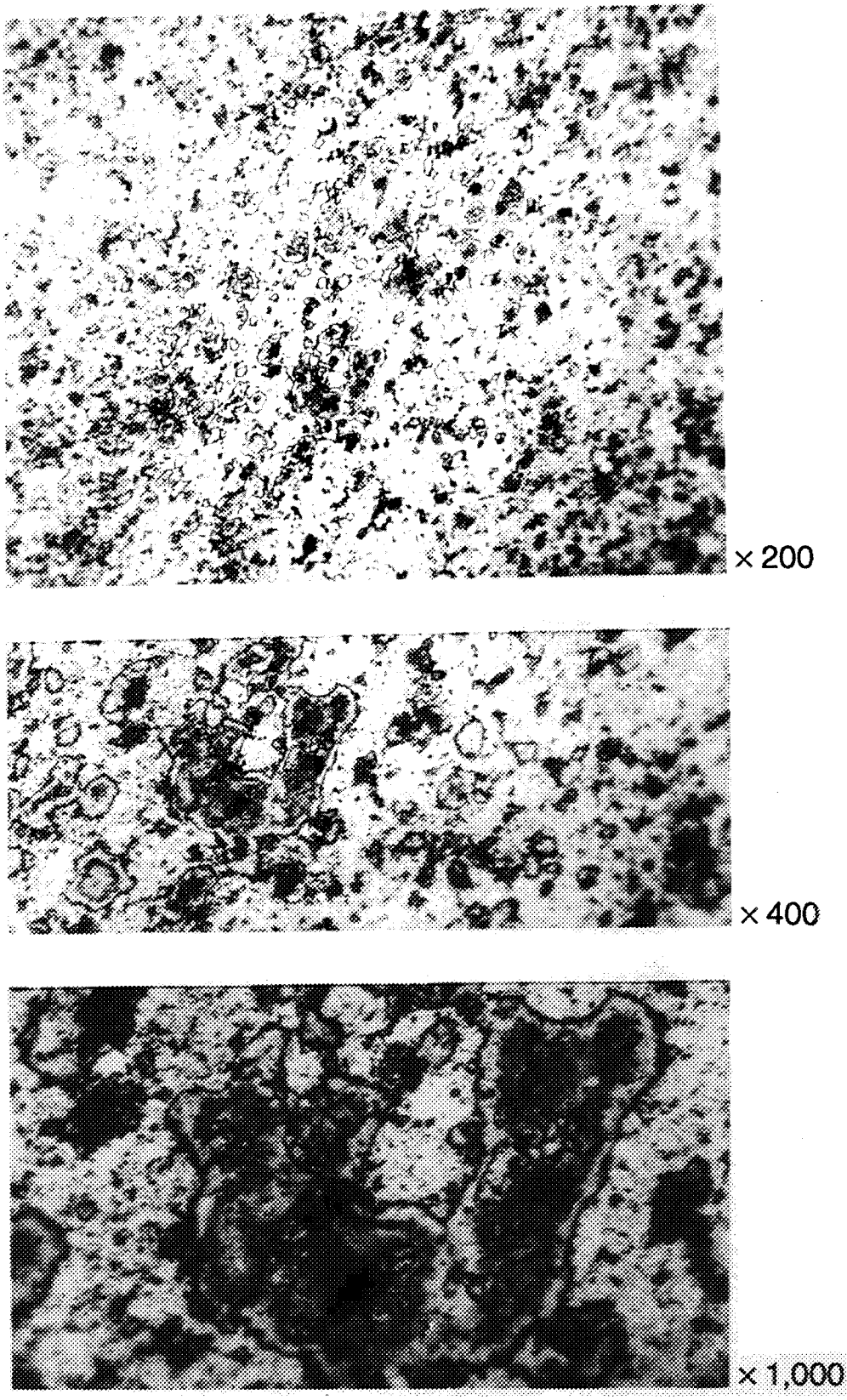

Figure A-22. OM of a very lightly worn ball of bearing No. 611: adhesive/shear peeling wear mode. Compare figure A-10 (very heavily worn ball).

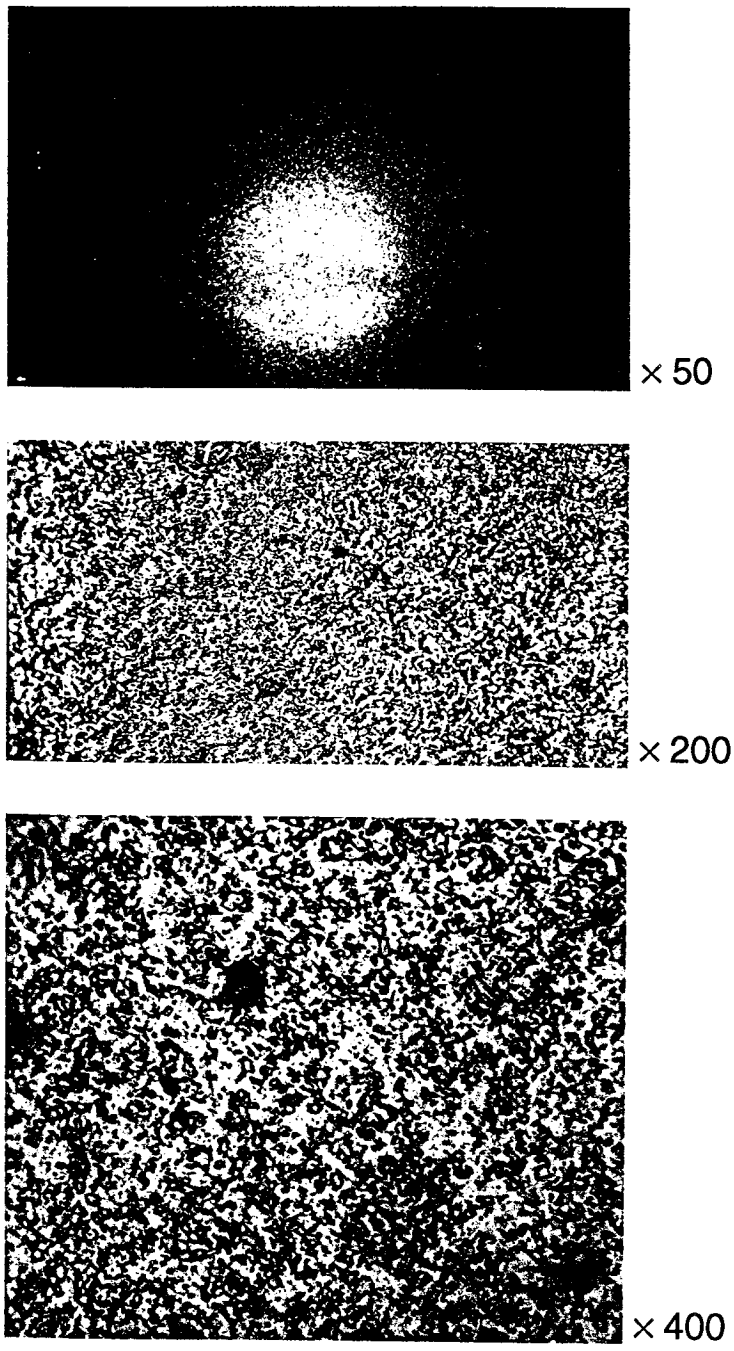

Figure A-23. OM of a representative ball of bearing No. 857 shows the same adhesive/shear peeling wear mode as in figure A-22.

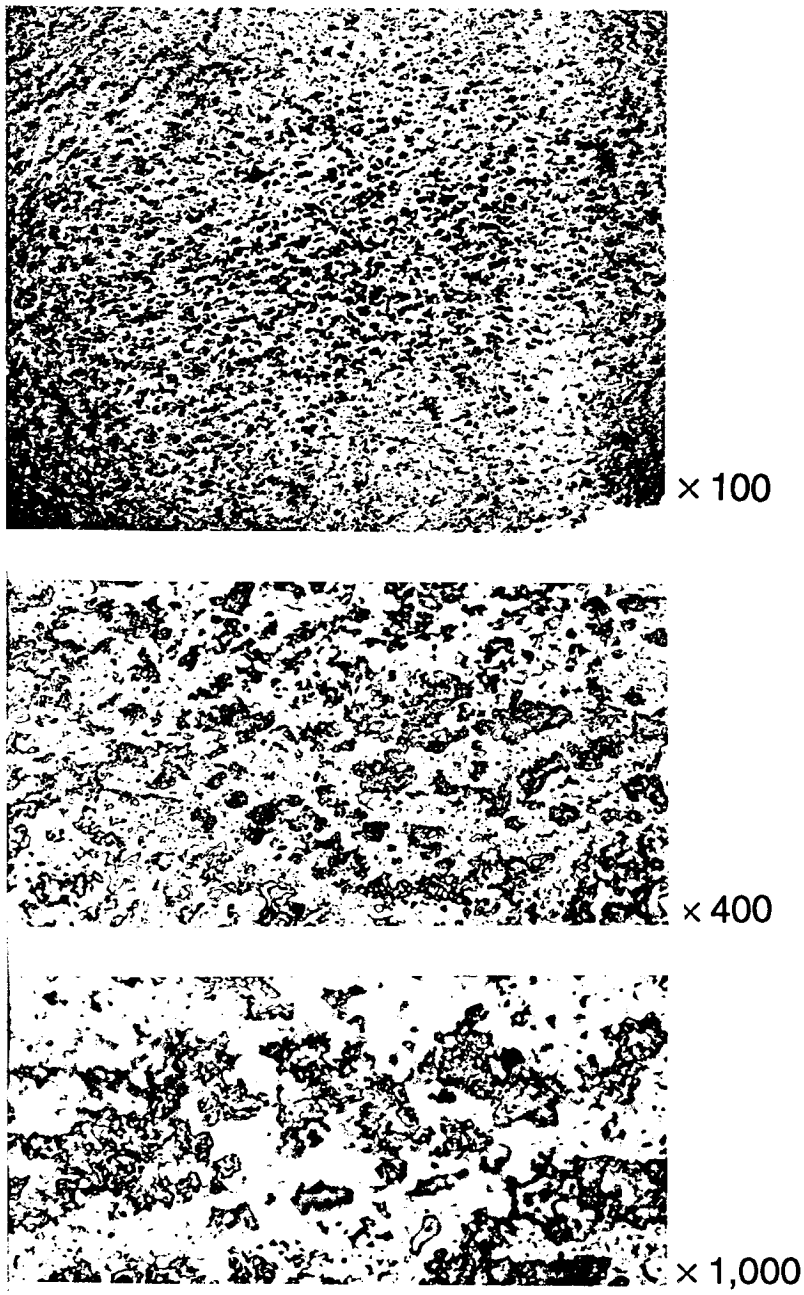

Figure A-24. OM of a lightly worn ball of bearing No. 857. Adhesive/shear peeling mode of wear.

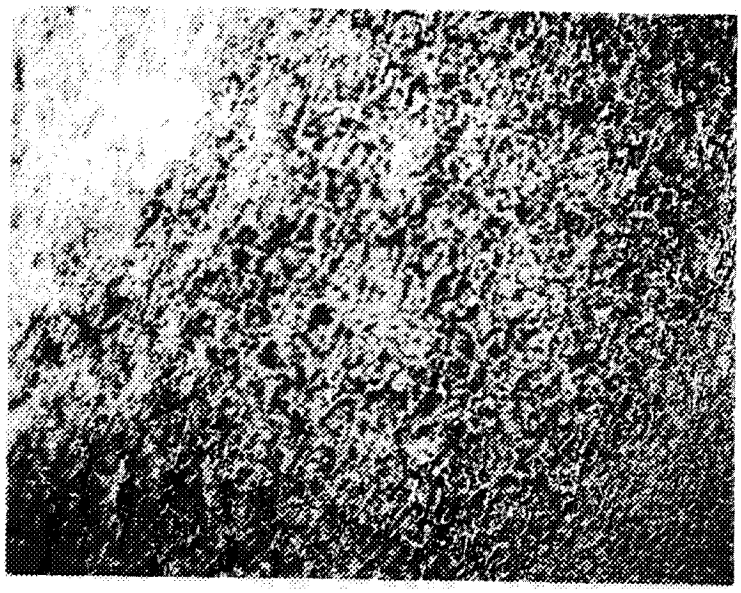

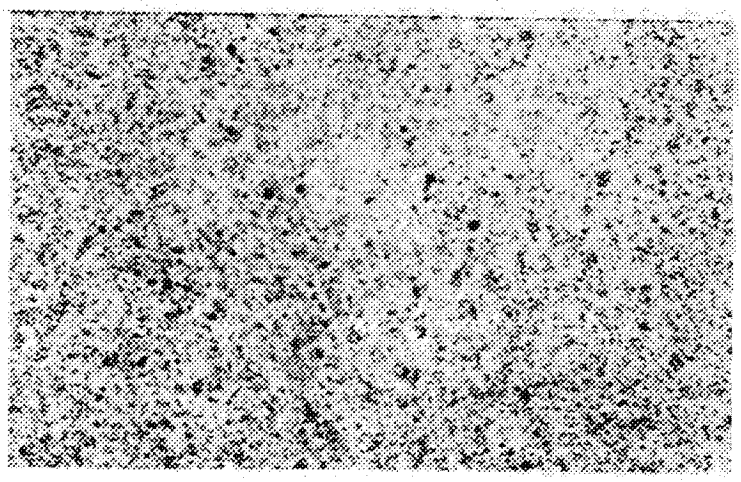

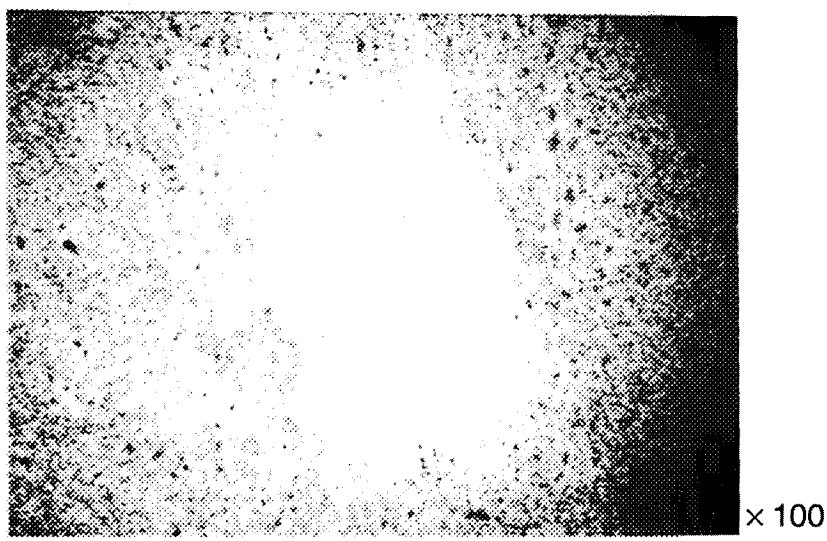

Figure A-25. OM of a worn ball of bearing No. 477. Adhesive/shear peeling mode of wear (on a dark track).

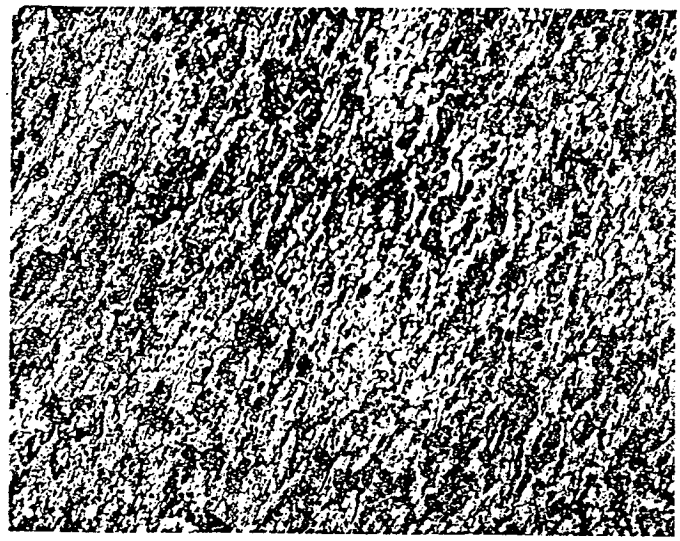

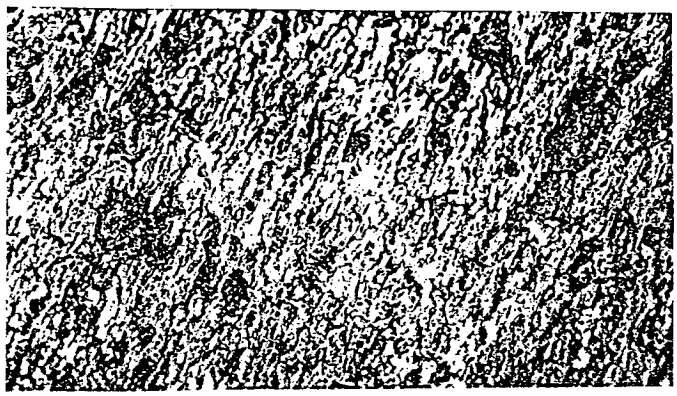

Figure A-26. OM of a worn ball of bearing No. 477. Adhesive/shear peeling mode (heavy wear on a dark track).

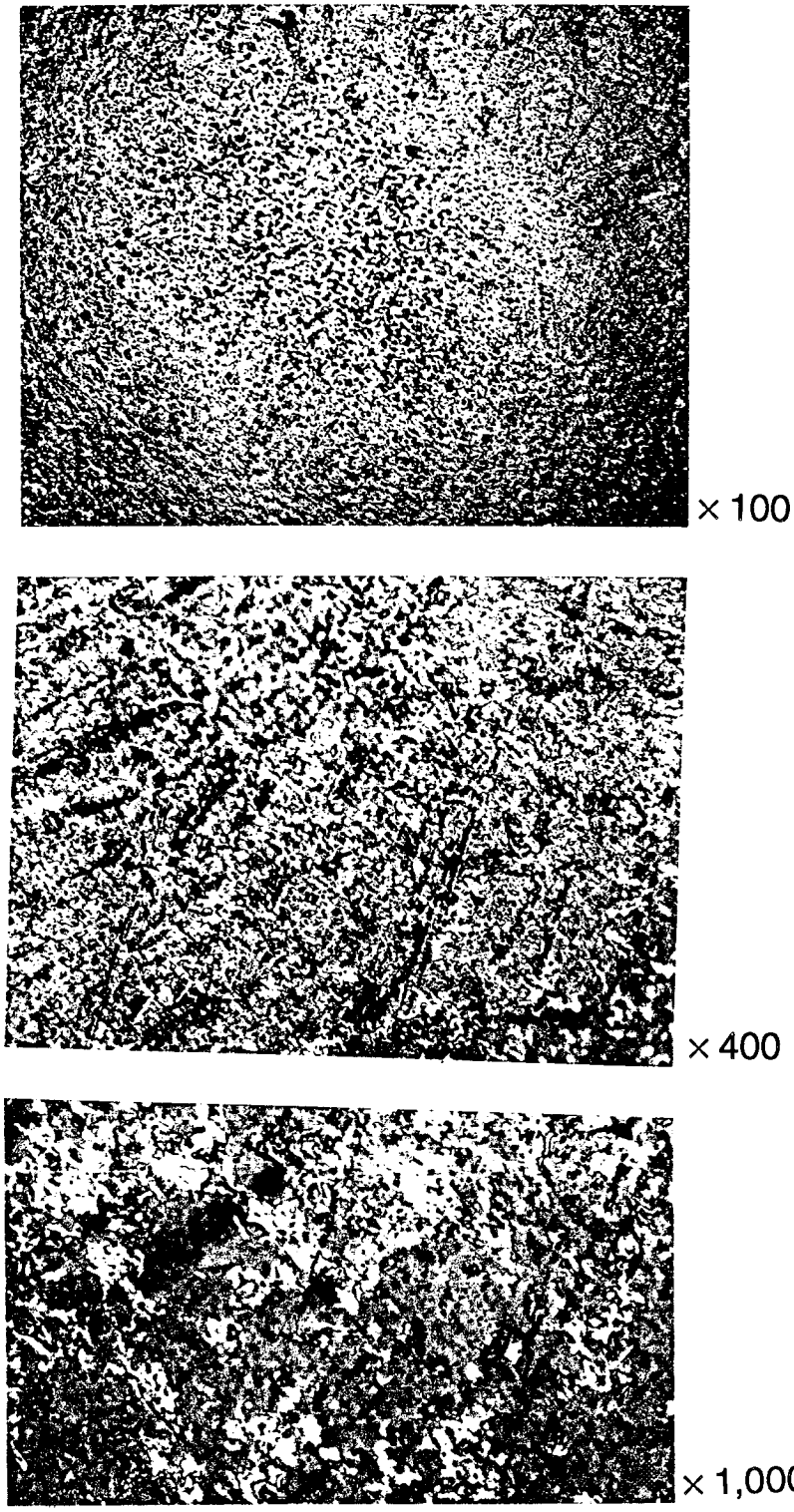

Figure A-27. OM of a very lightly worn ball of bearing No. 500. Adhesive/shear peeling mode (moderately heavy wear on a dark track).

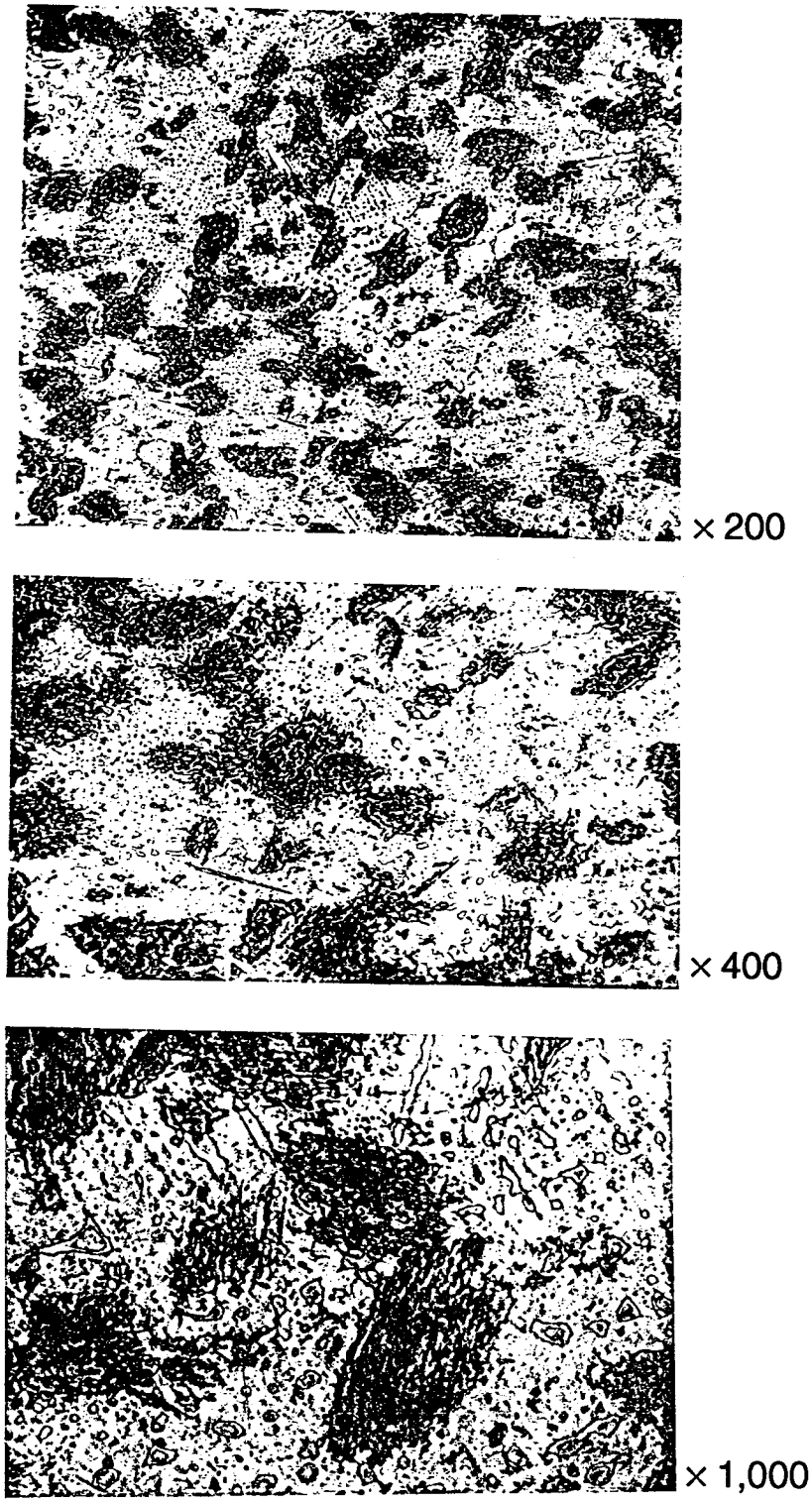

Figure A-28. OM of a very lightly worn ball of bearing No. 500. Note many dark patches on a white (actually golden) background which originated from sliding contacts of the ball with either cage pockets or contaminant particles. Their morphology shows scratch-like features. Also, note original finish marks which look like fine dot lines.

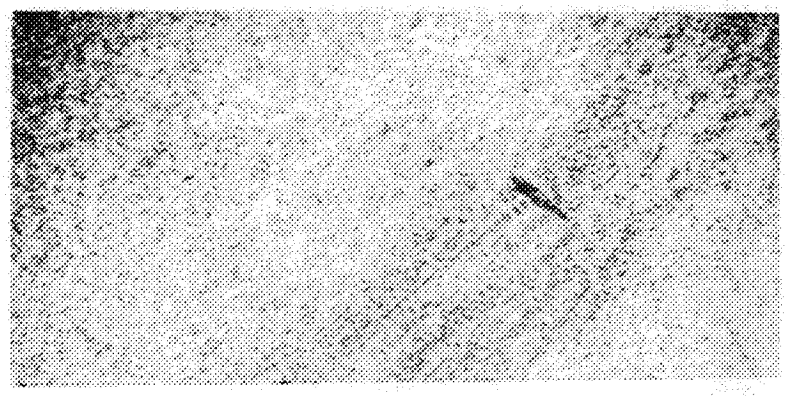

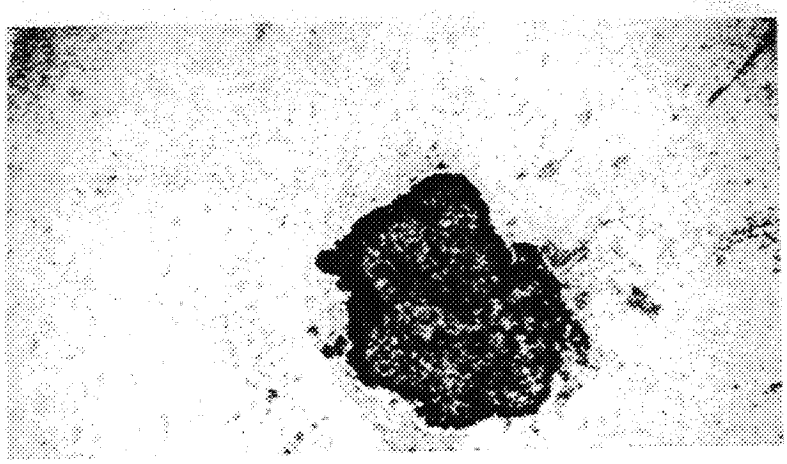

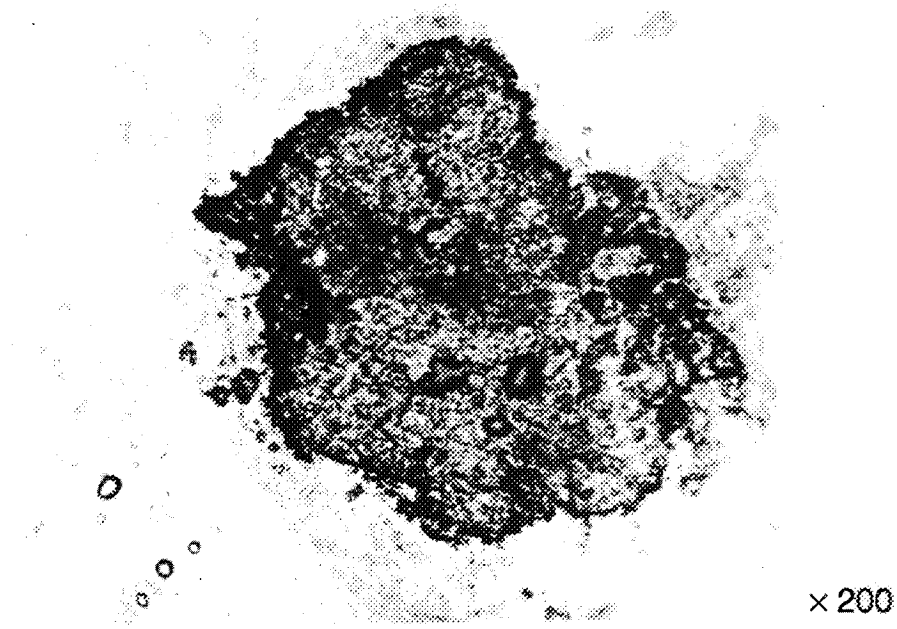

Figure A-29. OM of a very lightly worn ball of bearing No. 493. The focus is on a curious large pit (possibly a skid mark).

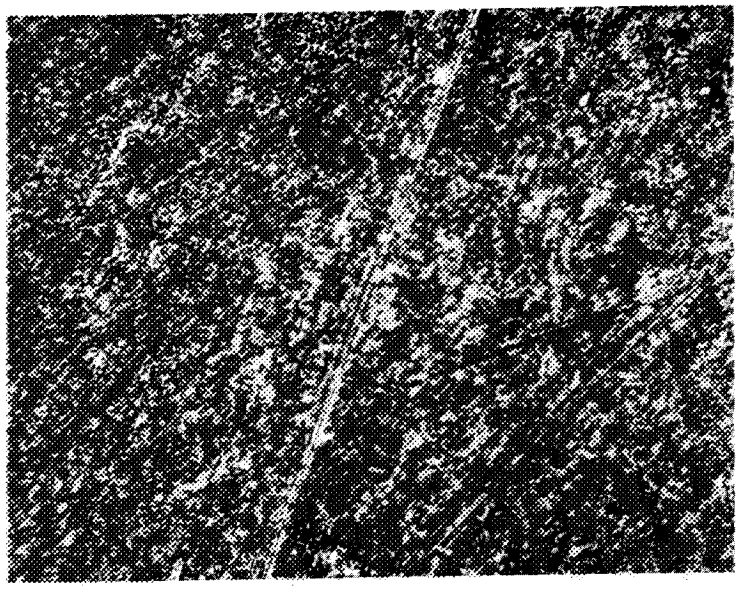

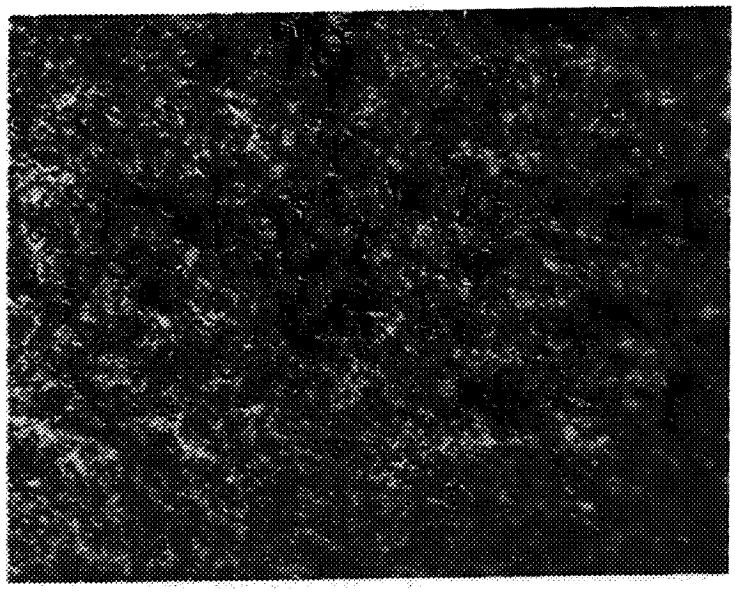

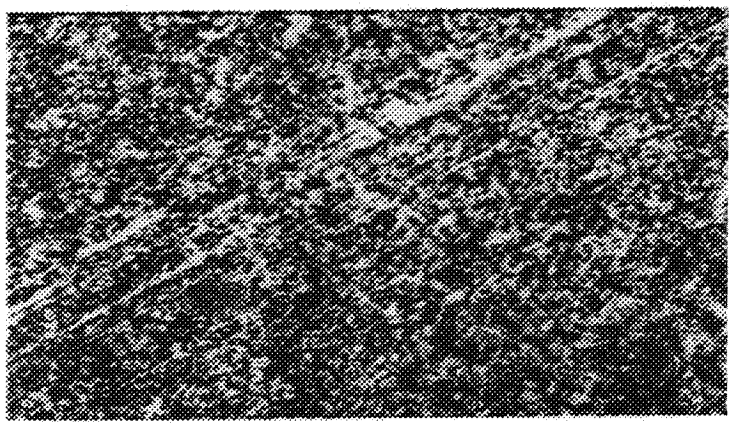

Figure A-30. OM of a very lightly worn ball of bearing No. 493. The predominant wear mode of the track is very light adhesive/shear peeling. Note scratches (probably from contact with the Armalon glass fibers, compare figure A-48).

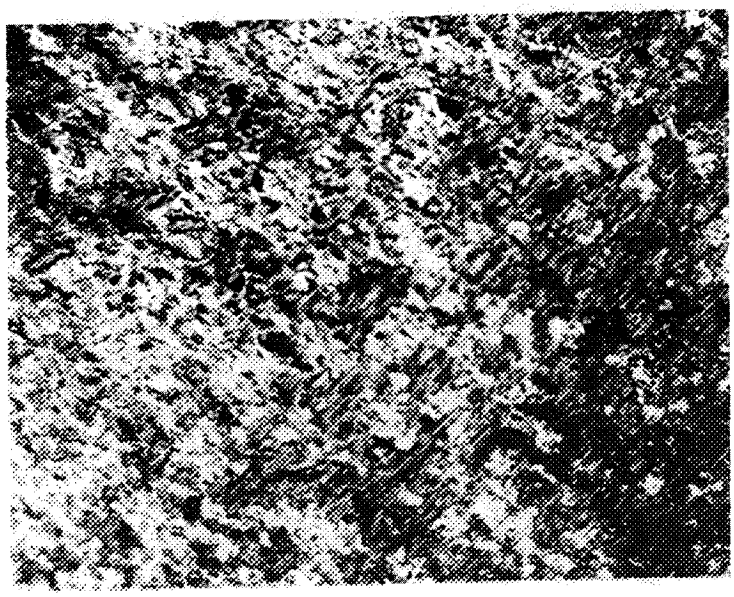

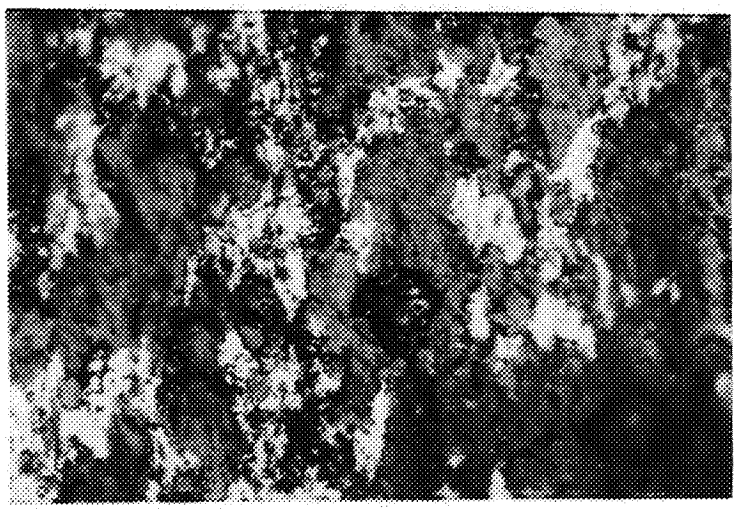

Figure A-31. OM of a worn ball of bearing No. 578. The predominant mode of the wear tracks is adhesive/shear peeling. Many pits are elongated in the direction of the track, most likely due to high traction (shear) stresses, which may also indicate insufficient lubrication.

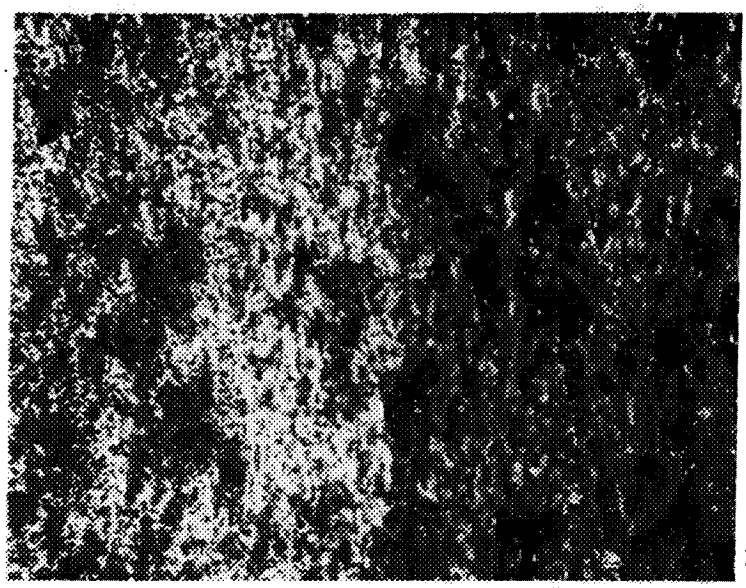

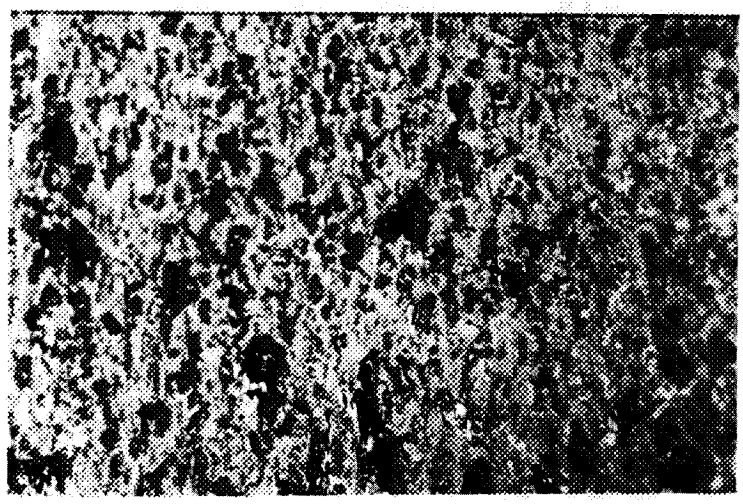

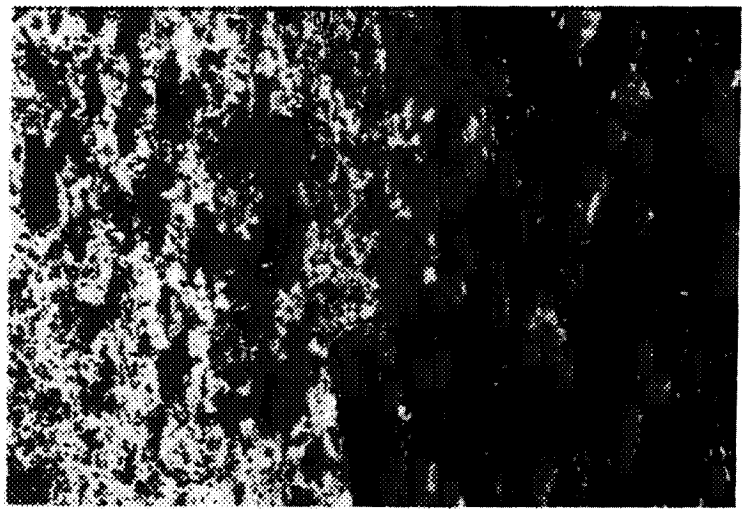

Figure A-32. OM of a worn ball of bearing No. 578. The predominant mode is adhesive/shear peeling. Note many transfer patches.

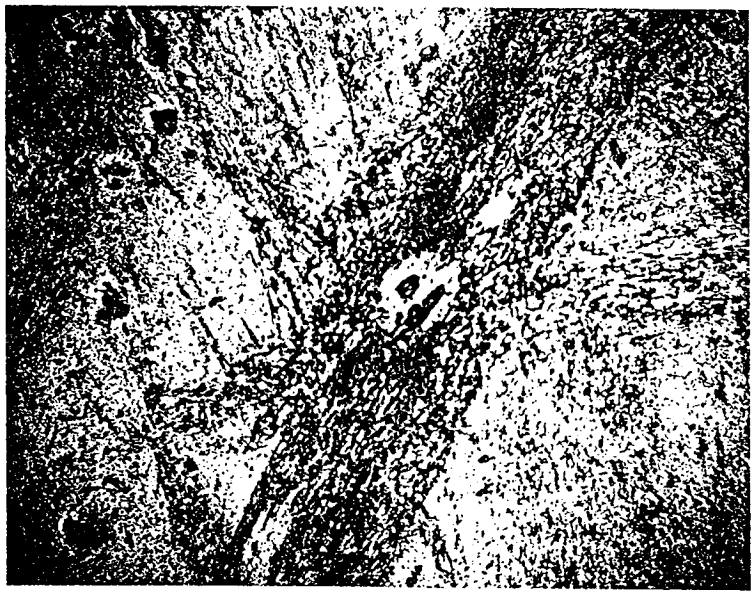

Figure A-33. OM of a lightly worn ball of bearing No. 543. The focus is on the crossing of wear tracks which show adhesive/shear peeling, material transfer, and some deeper pits due to a possibly violent contact with either a cage material or a contaminant debris.

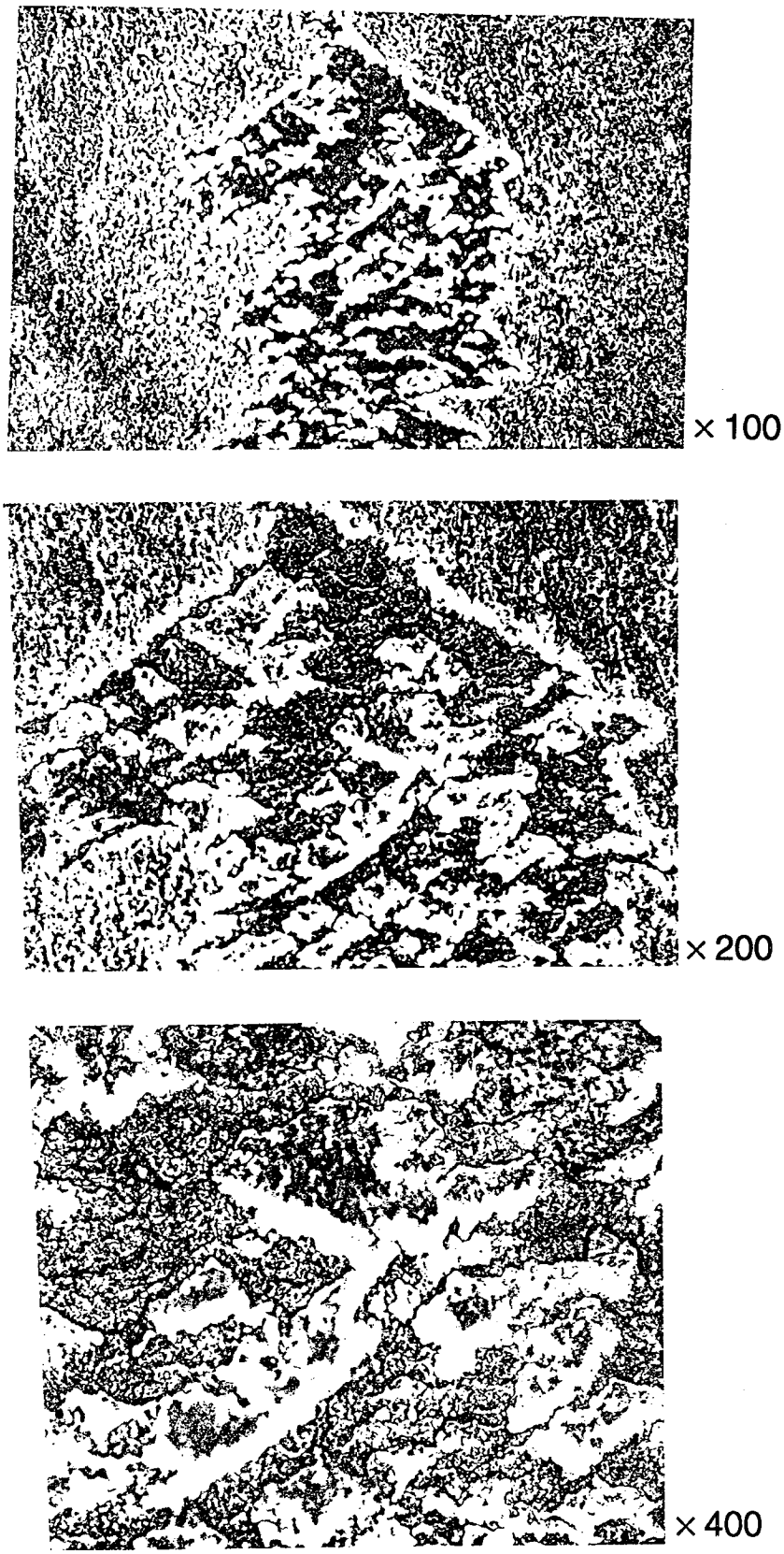

Figure A-34. OM of a lightly worn ball of bearing No. 543. The focus is on an arrow-like scratch, a single event producing the adhesive/shear effects like those of the predominant wear mode in all bearings examined.

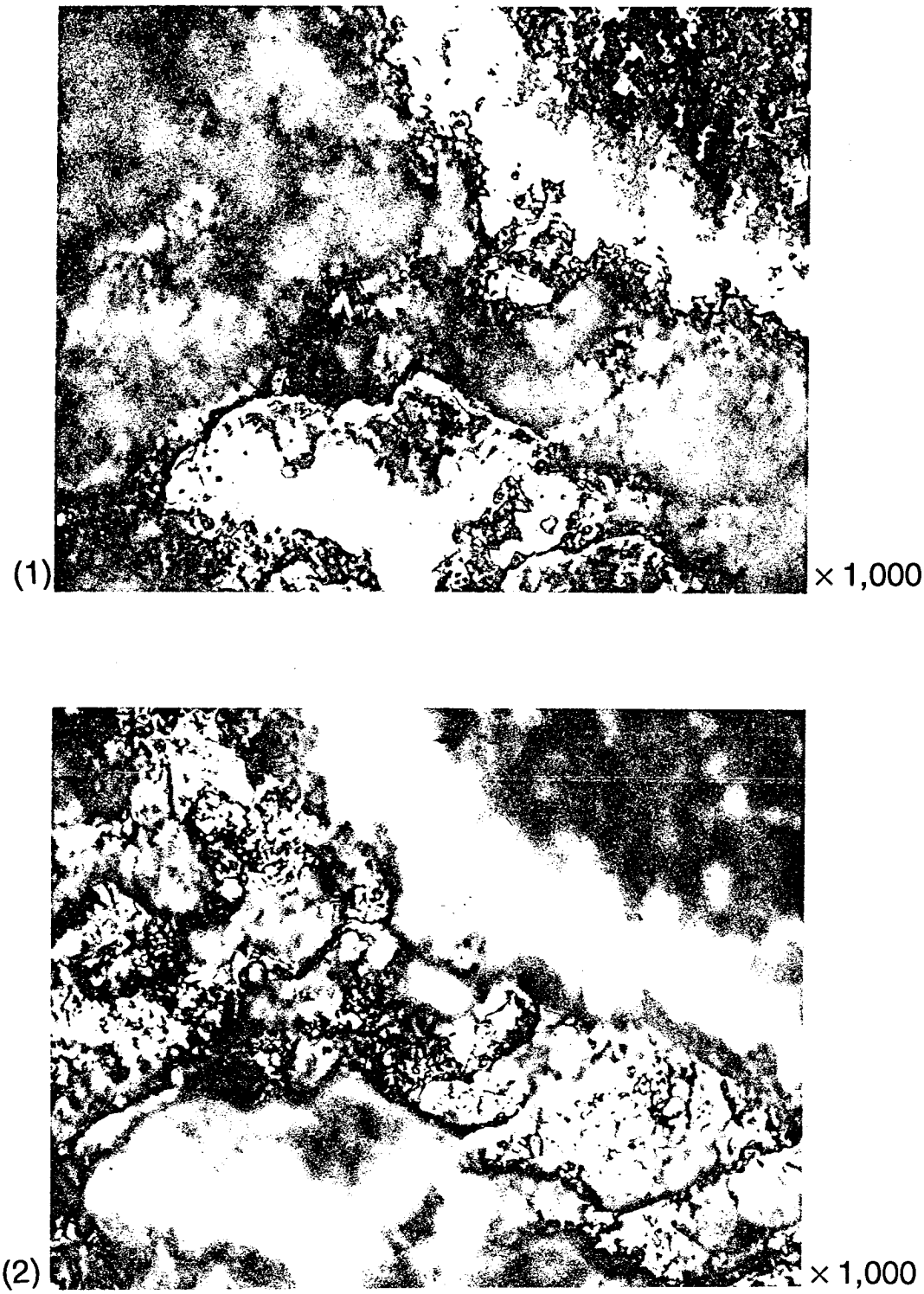

Figure A-35. OM of a lightly worn ball of bearing No. 543 (continued). The focus on top layers (1) shows the same surface morphology as the focus on bottom layers (2) of the scratch area. Thus both layers were formed by the same basic mechanisms, namely the adhesive/shear peeling.

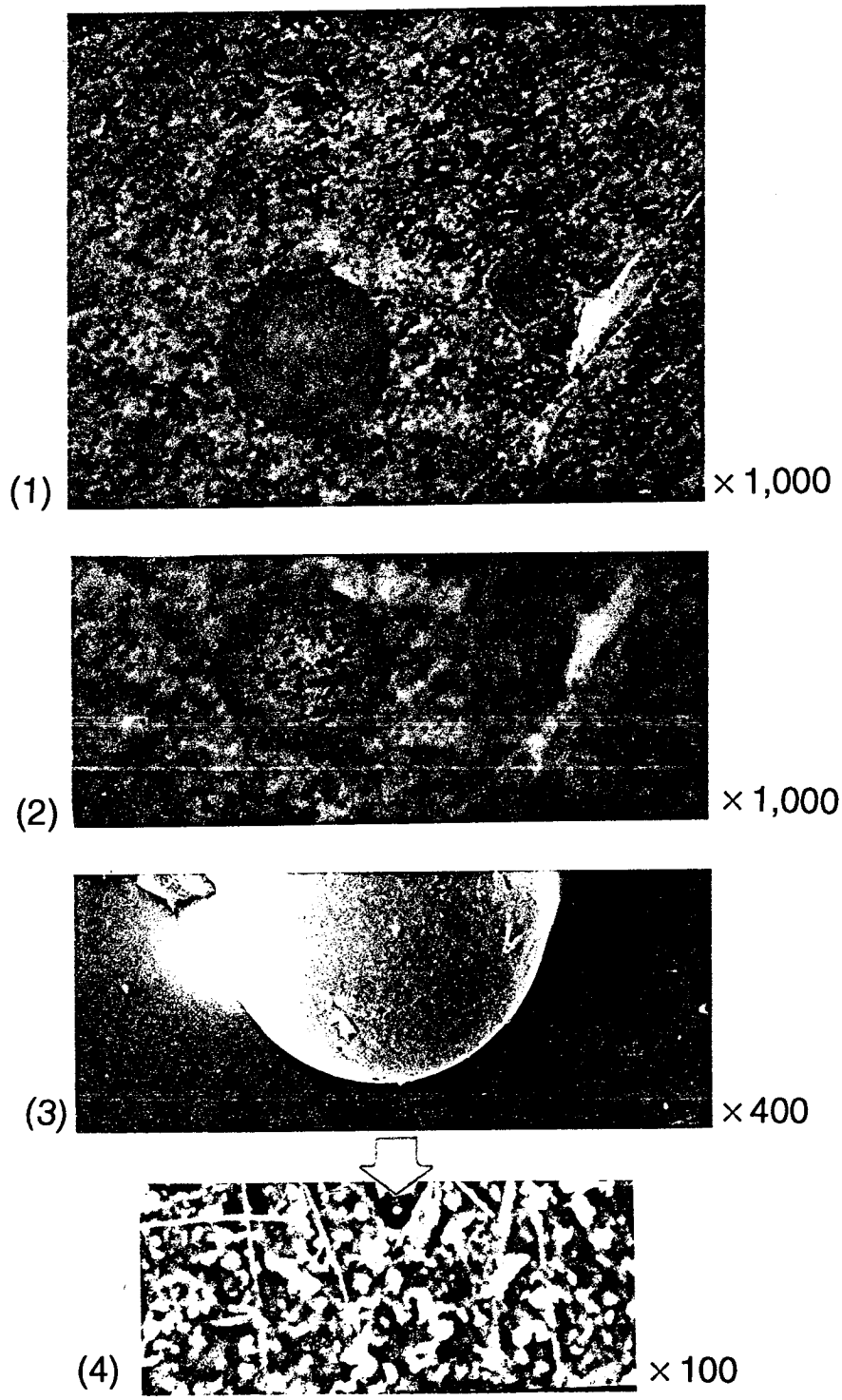

Figure A-36. Surface damage (ball, bearing No. 493) by a spherical contaminant particle: (1) focus on the top, (2) focus on the bottom, (3) a particle found on the BSMT inlet filter, and (4) a black spherical particle found on the BSMT outlet filter. Optical microscopy.

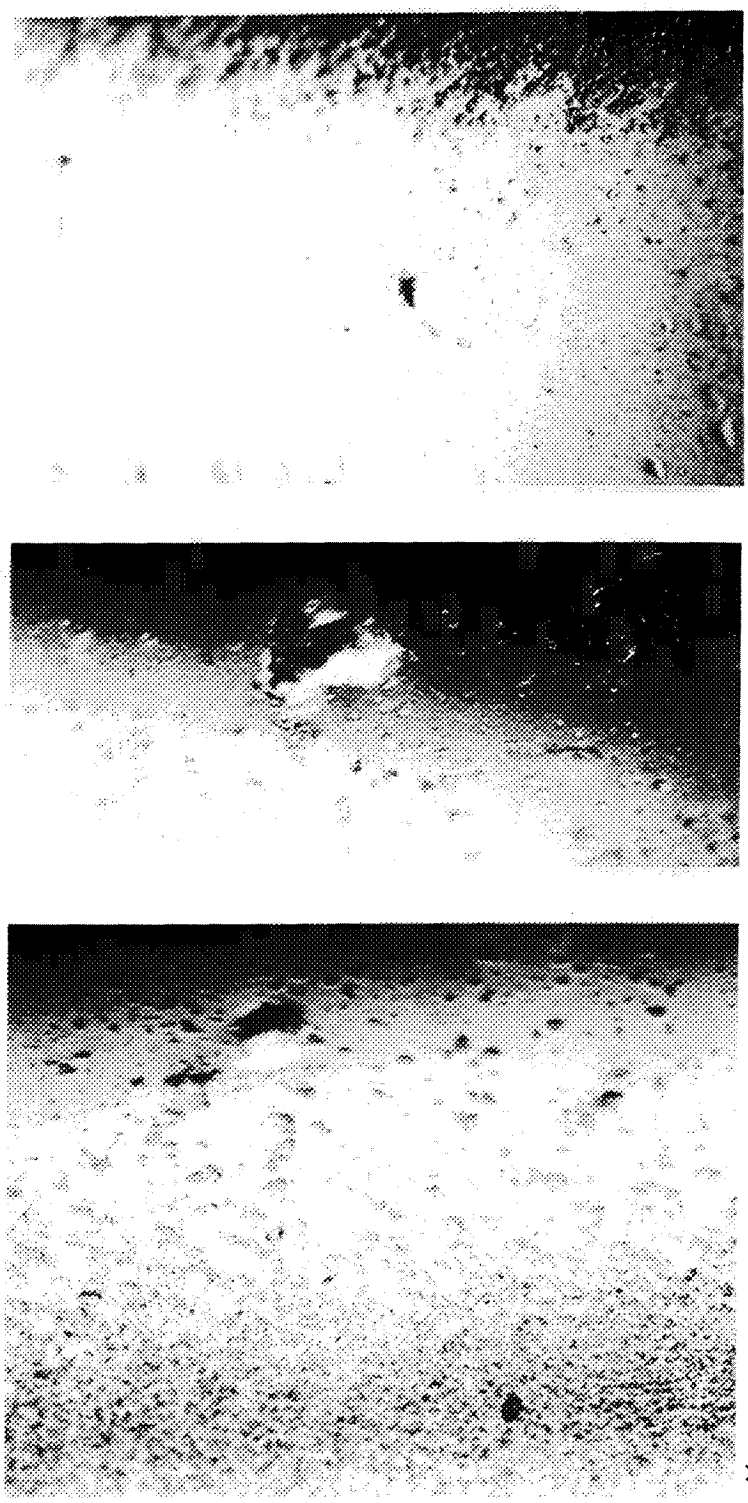

Figure A-37. Surface damage (inner ring, bearing No. 611) by contaminant particles and adhesive/shear peeling. Optical microscopy.

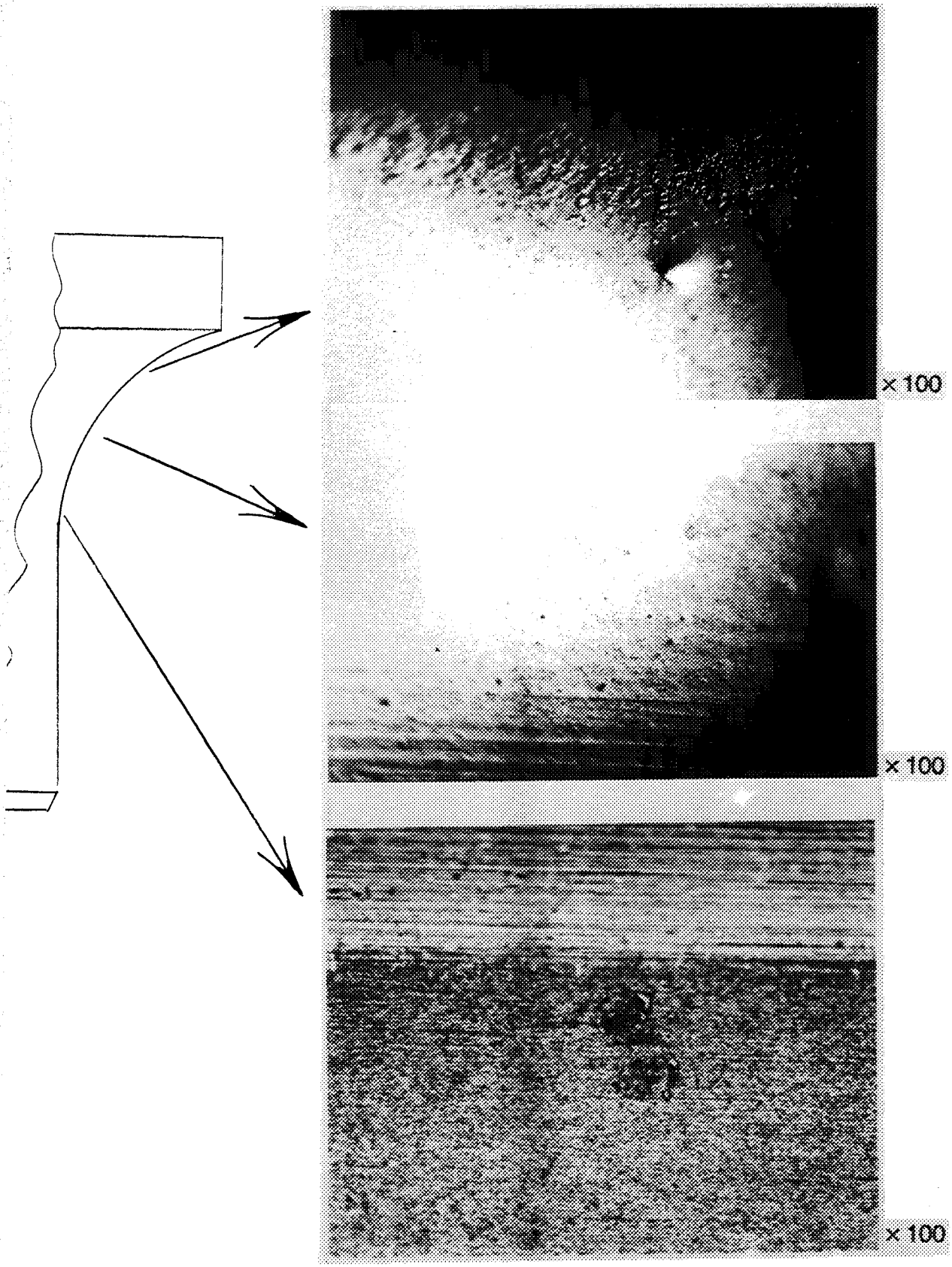

Figure A-38. Surface damage (inner ring, bearing No. 611) by contaminant particles and adhesive/shear peeling. Note a very light corrosion on the unworn surface. Optical microscopy.

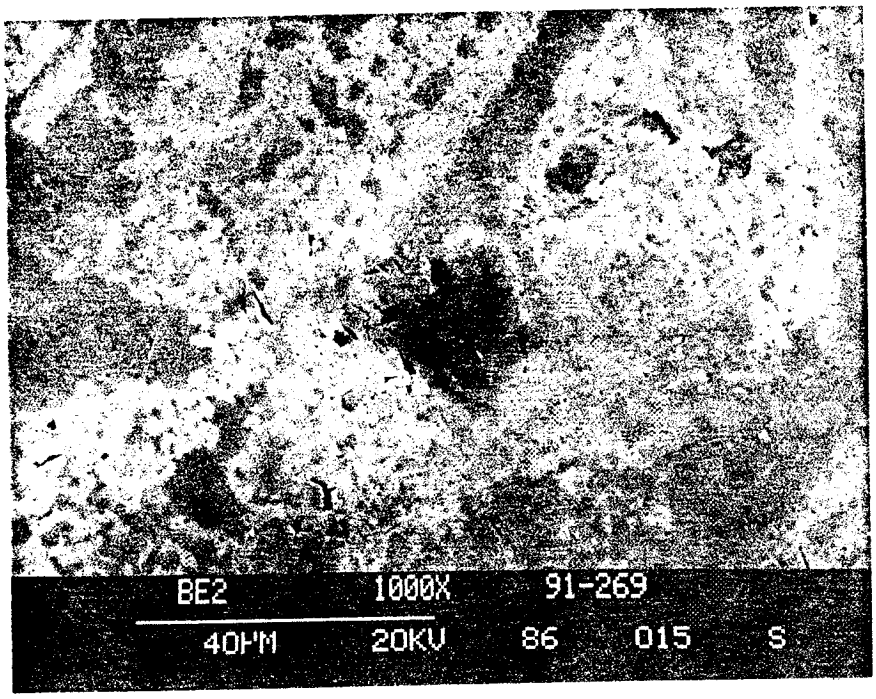

× 1,000

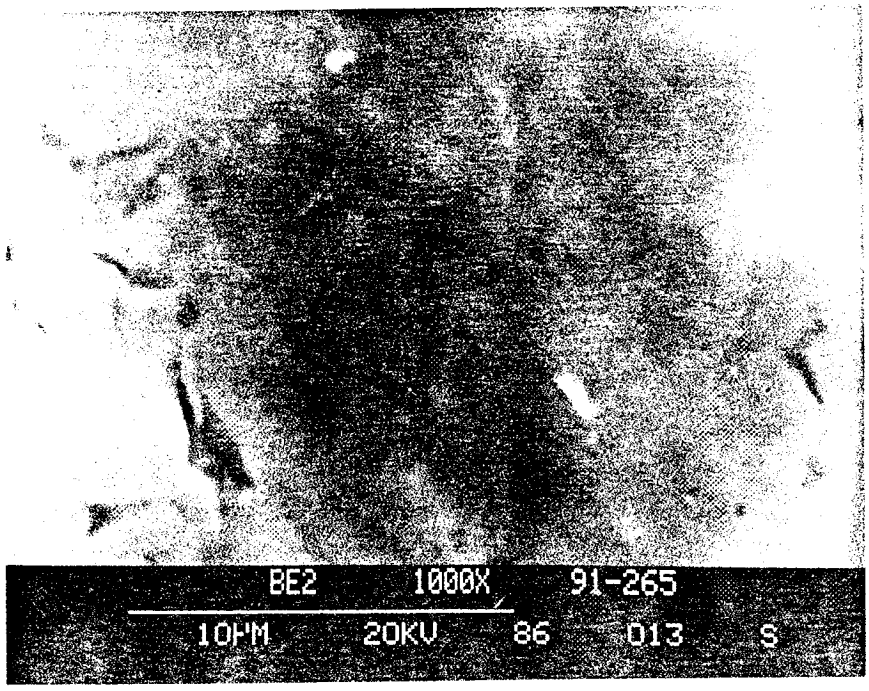

× 5,000

Figure A-39. Surface damage (inner ring, bearing No. 611) by contaminant particles and adhesive/shear peeling (SEM).

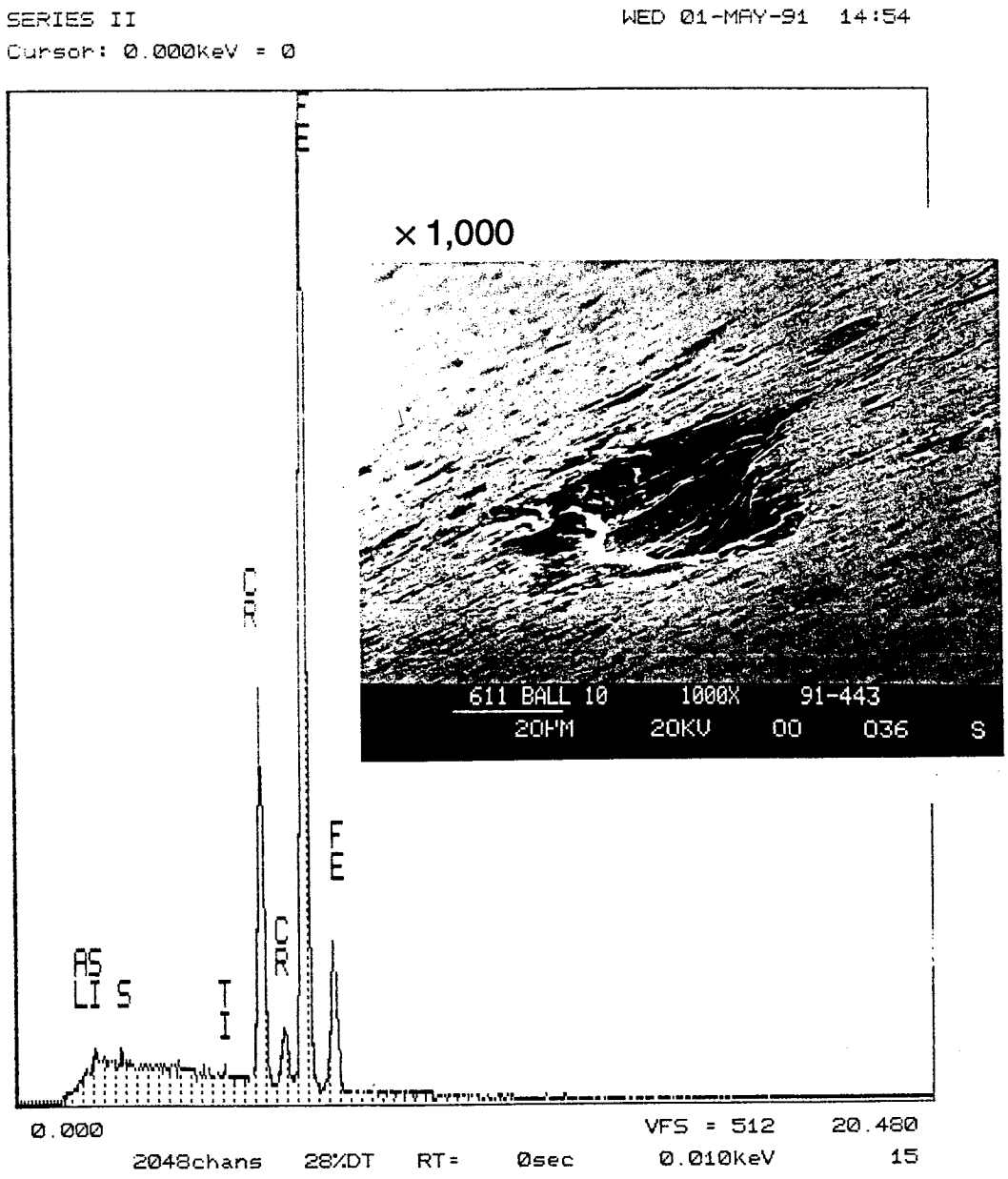

Figure A-40. SEM/EDS of a lightly worn ball of bearing No. 611. A microspall of classic proportions. Note wear debris whose shape and chemistry (Al, Si) are not inconsistent with those of the glass fibers in the Armalon cage.

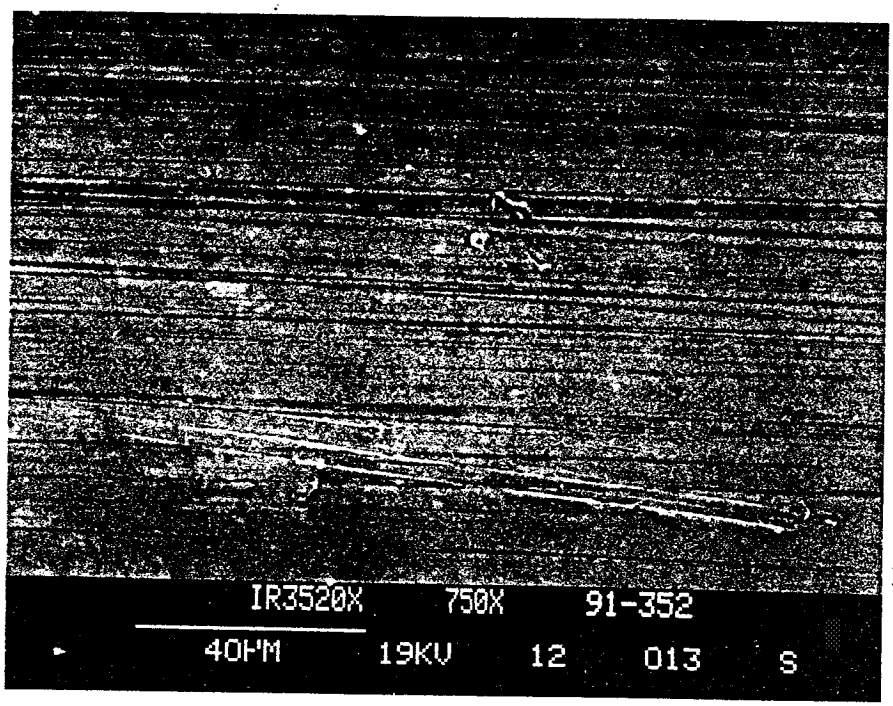

× 750

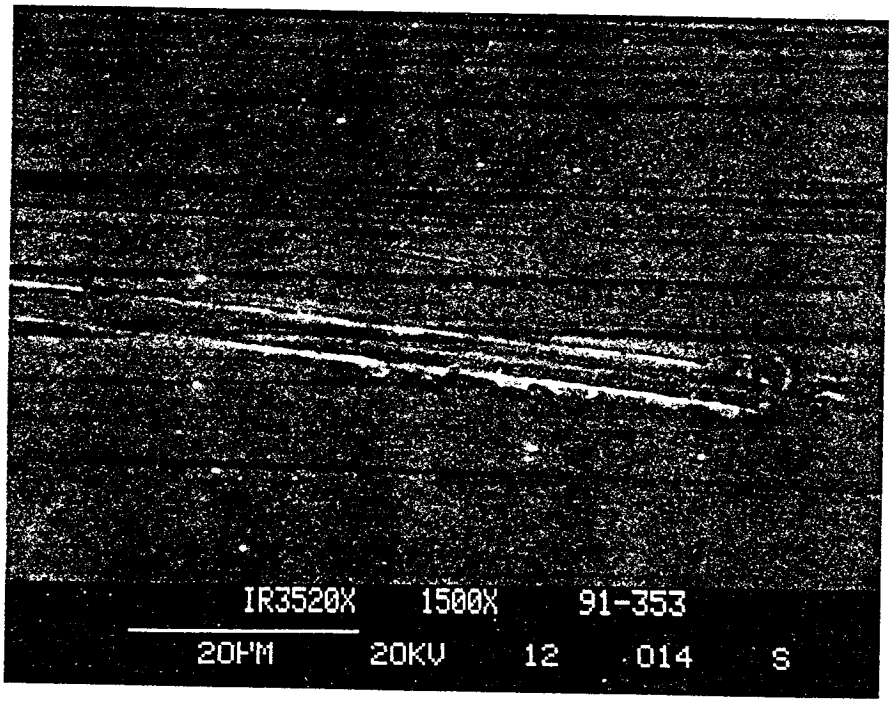

× 1,500

Figure A-41. SEM of the inner ring of bearing No. 352: a scratch mark on the worn surface at an angle to the track. It may have been caused by a contaminant particle or a glass fiber on a ball which changed its running trajectory due to a side-load induced by the particle.

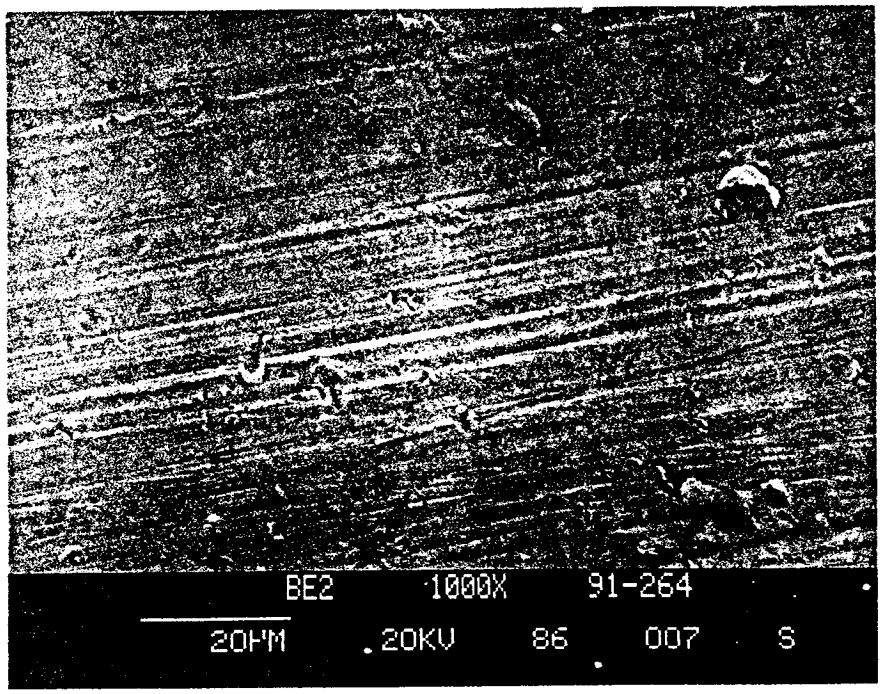

× 1,000

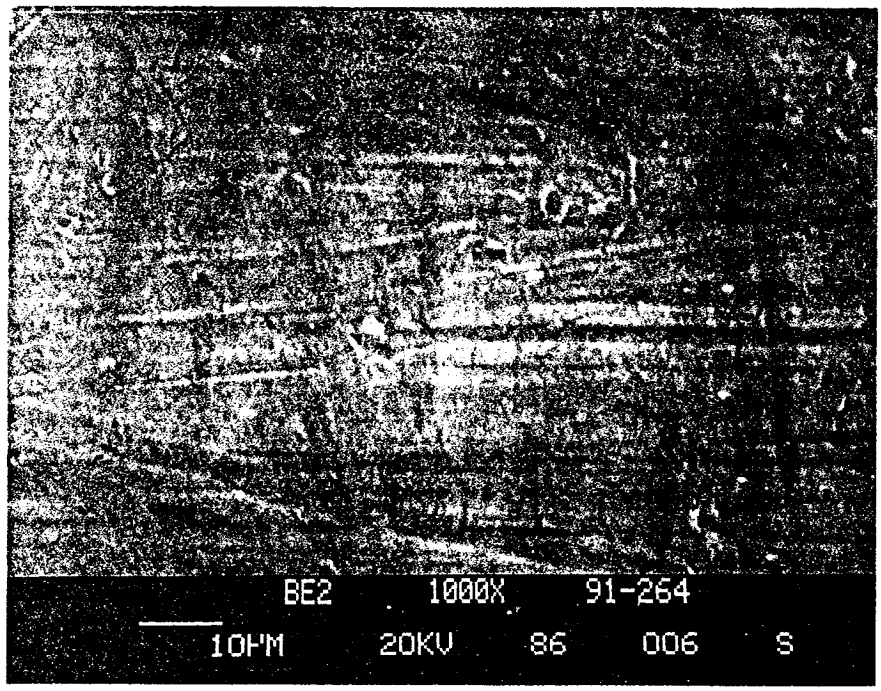

× 1,000

Figure A-42. SEM of the inner ring of bearing No. 352. Machining marks on the upper fillet for comparison with figure A-41.

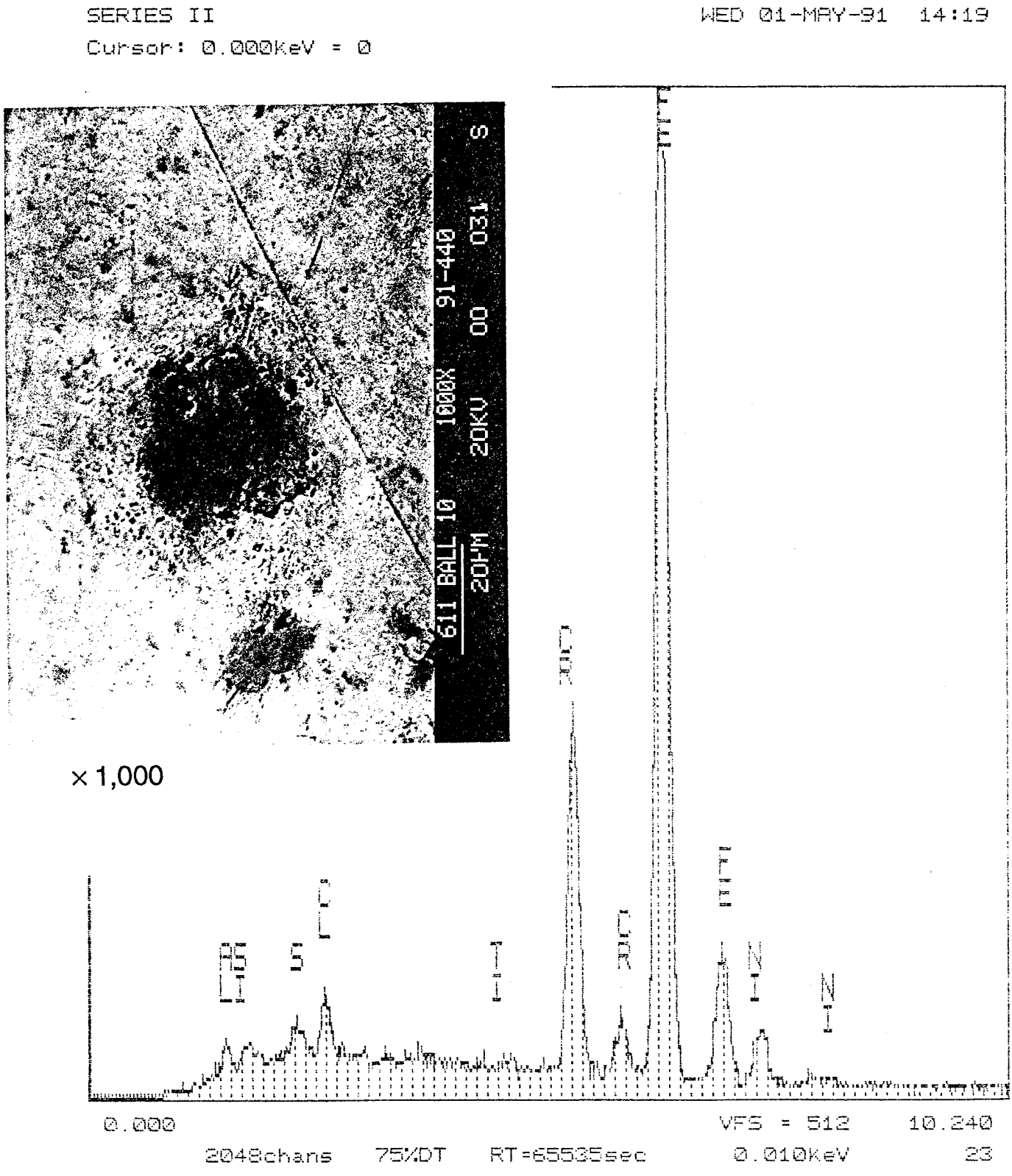

Figure A-43. SEM/EDS of a dark patch on a very lightly worn ball of bearing No. 611. Note presence of Cl (harmful and unexplained), Ni, and Ti (compare figs. A-54 through A-62).

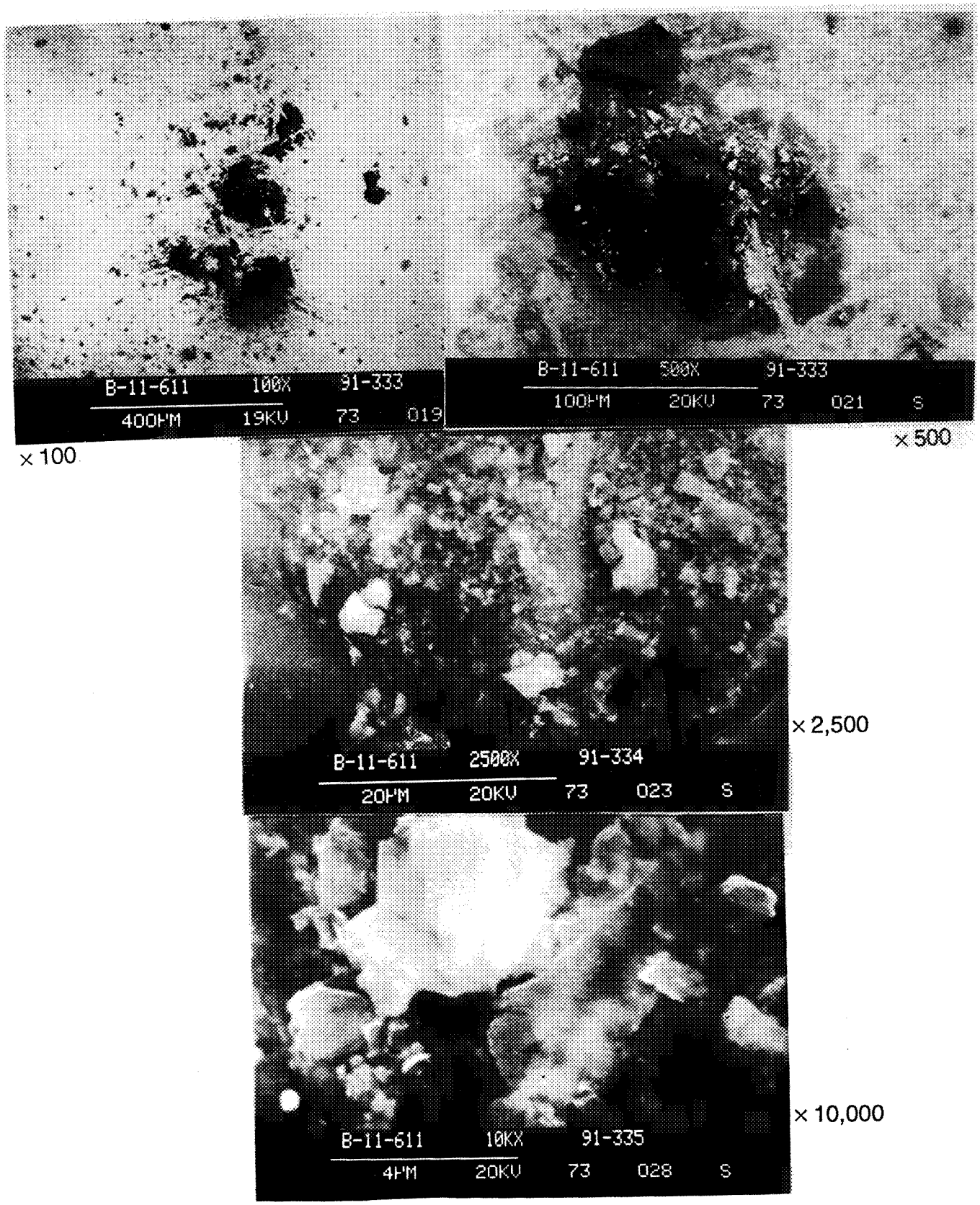

Figure A-44. SEM/EDS of a dark patch on a very lightly worn ball of bearing No. 611. Analysis at a high magnification reveals a laminar structure of the residue, characteristic of molybdenum disulfide, an ingredient of the solid lubricant initially applied to the bearings at the assembly.

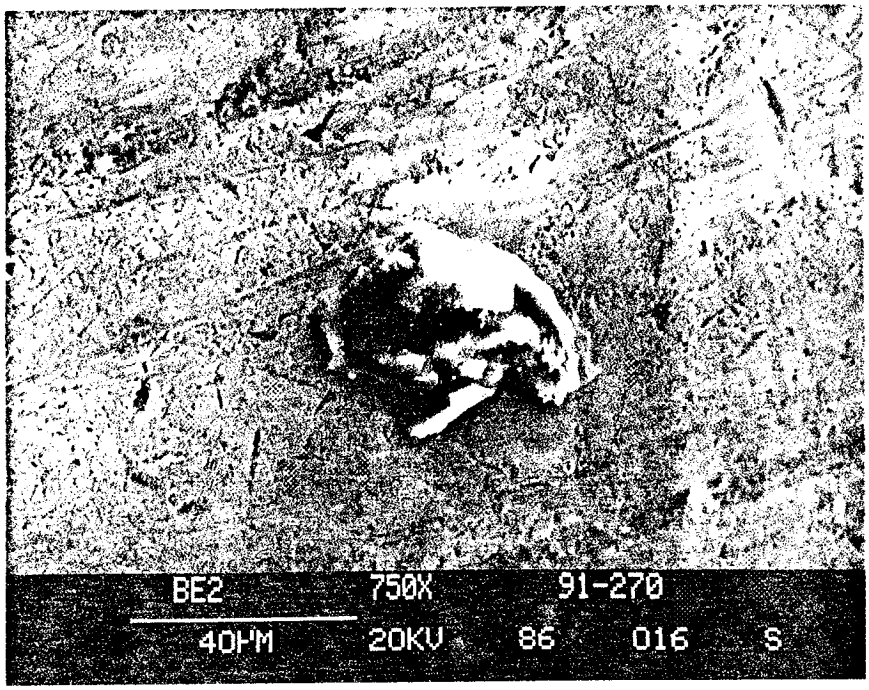

× 750

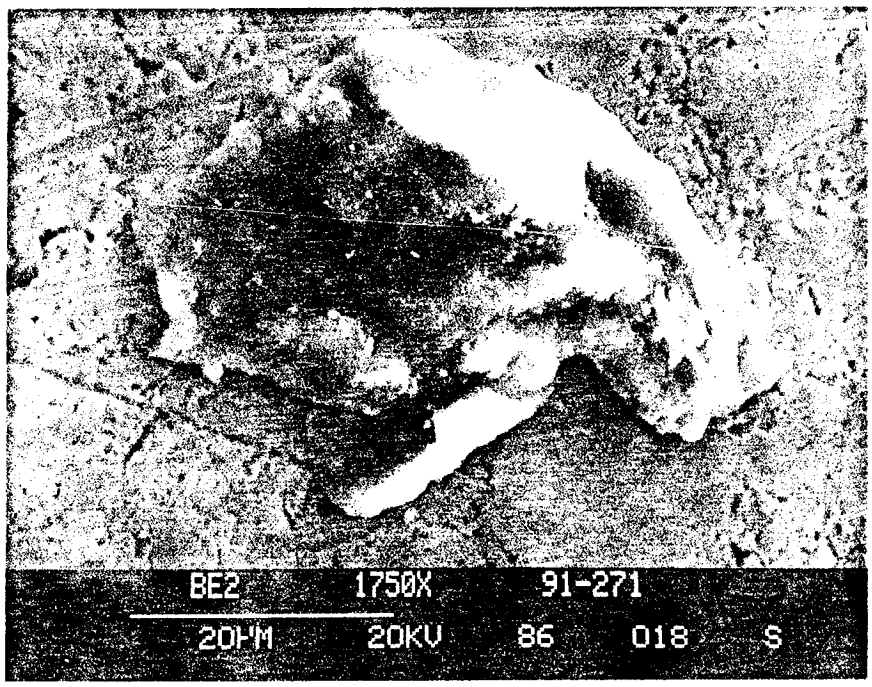

× 1,750

Figure A-45. SEM of a particle found on the inner ring of a very lightly worn bearing No. 611. Its origin is uncertain. Also, note many cuts, scratches, and pits on the ring. Compare figures A-46 and A-47.

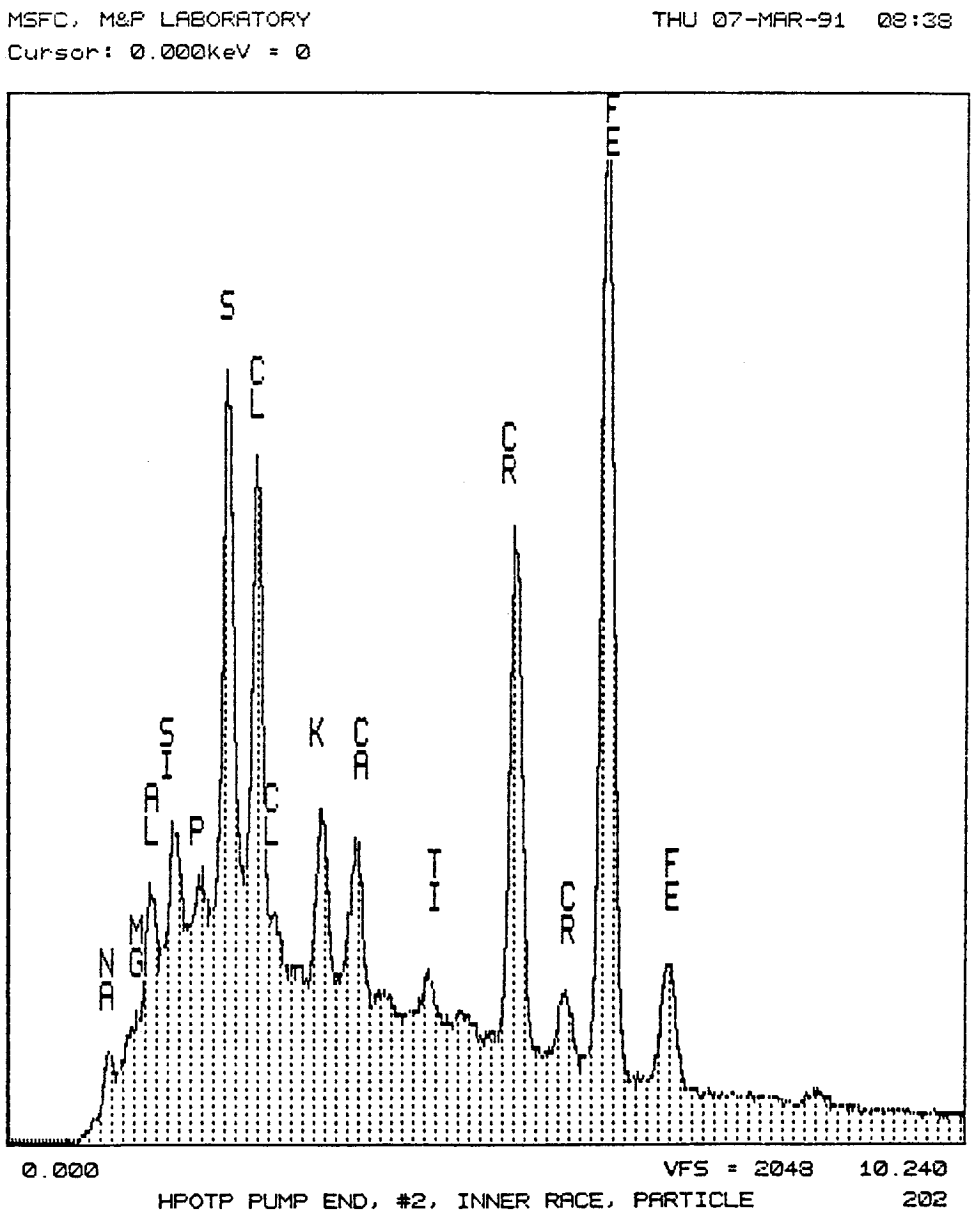

Figure A-46. EDS of a particle found on the inner ring of a very lightly worn bearing No. 611. Note presence of many contaminants which can be seen in figures A-54 through A-62 (inlet filter).

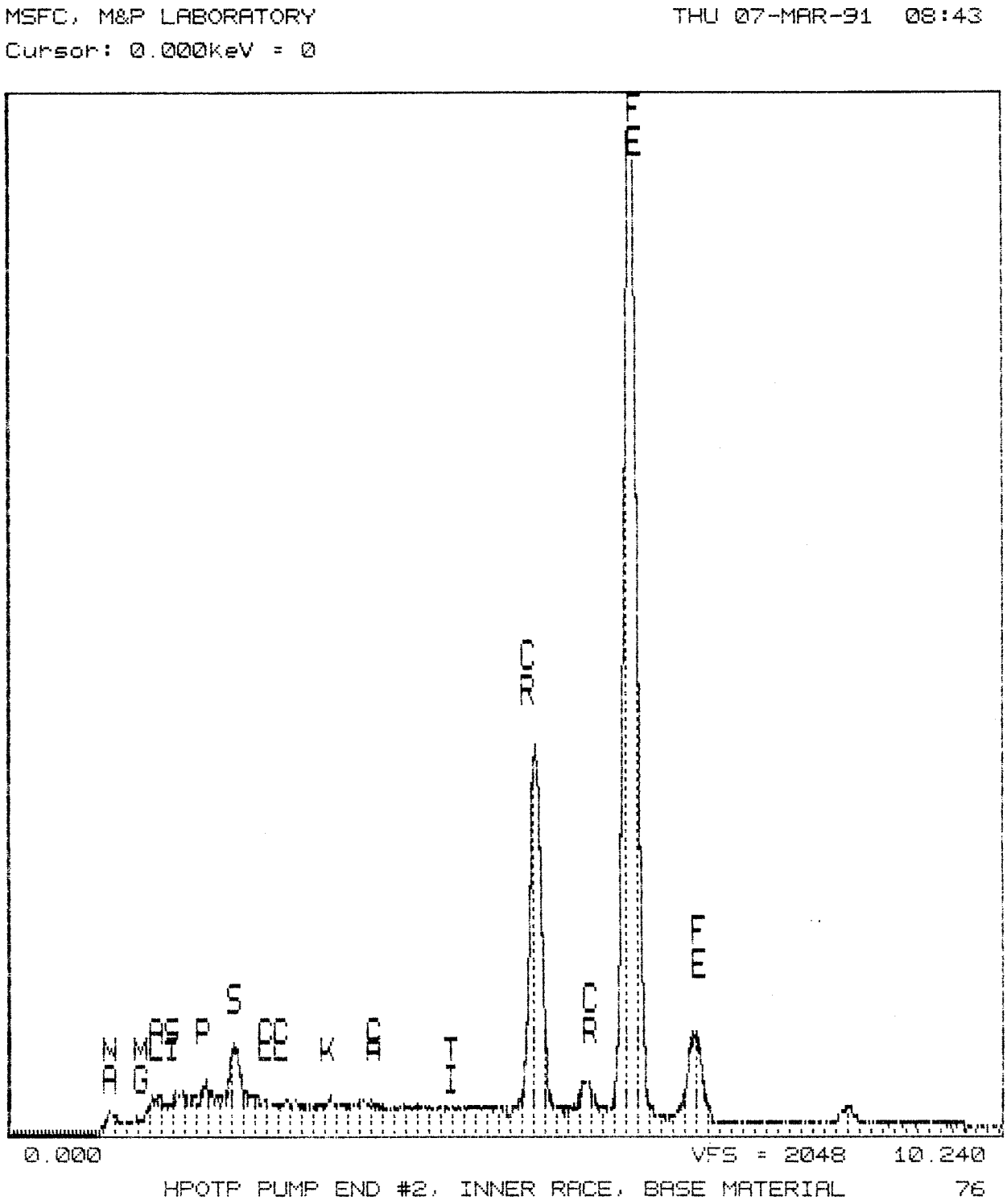

Figure A-47. EDS of the background of the particle shown in figure A-46, bearing No. 611. Note absence of many contaminants found there.

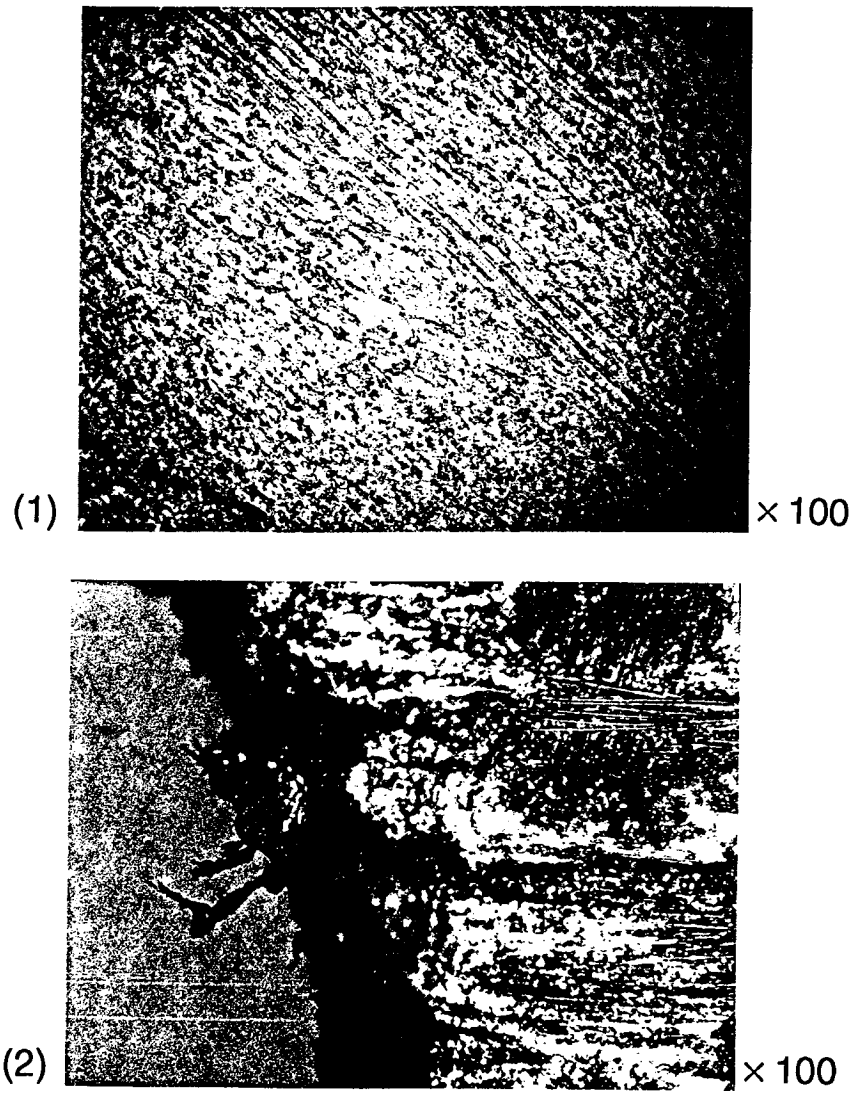

Figure A-48. OM of the heavily worn ball (bearing No. 352): (1) the glass fiber inflicted damage to the surface layer, and (2) ball pocket edge with glass fibers. Note size and spacing of fibers.

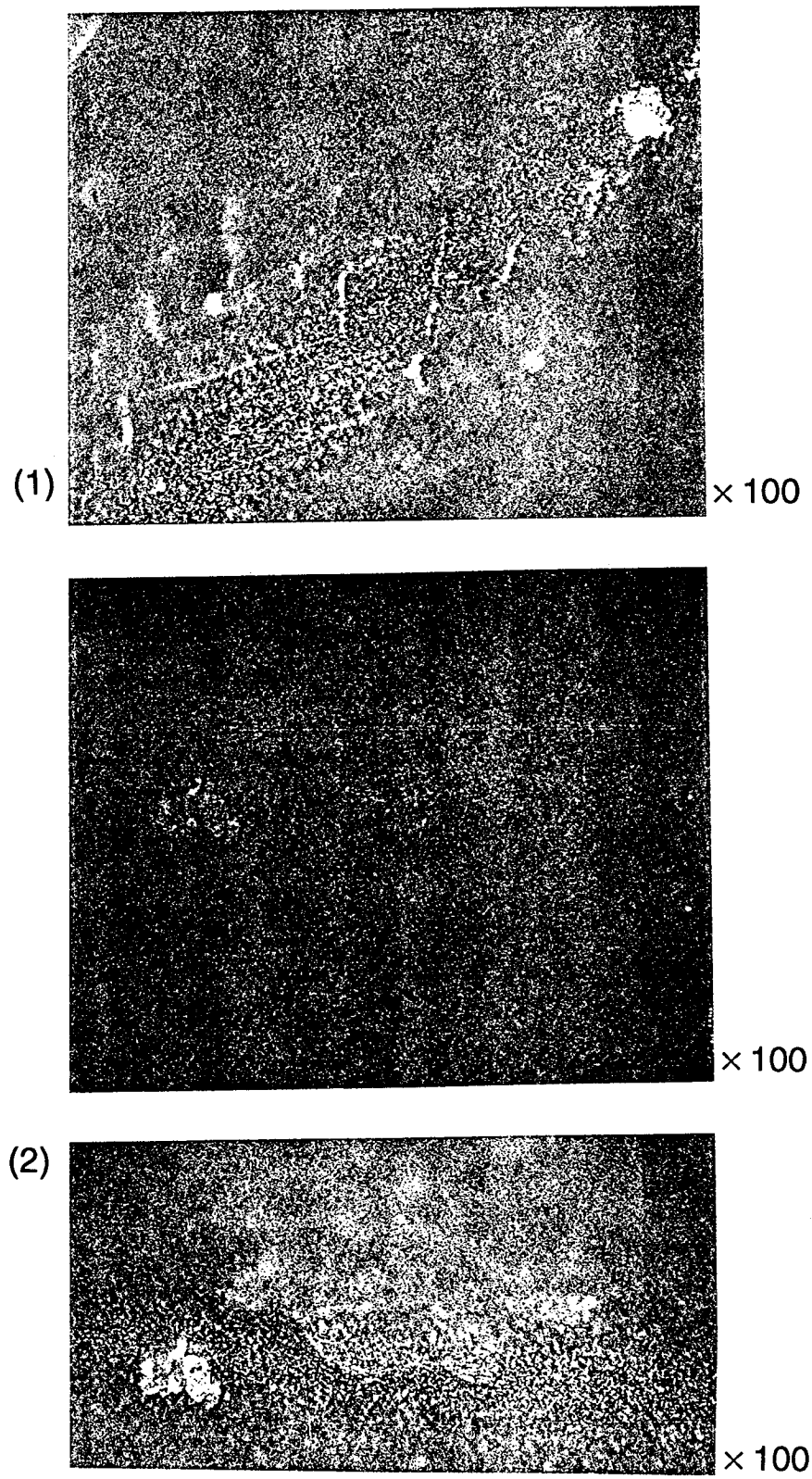

Figure A-49. OM of the inner ring of the heavily worn bearing No. 352: (1) ball skid marks in the high fillet area, (2) freshly exposed new surface after peeling-off, and a flake.

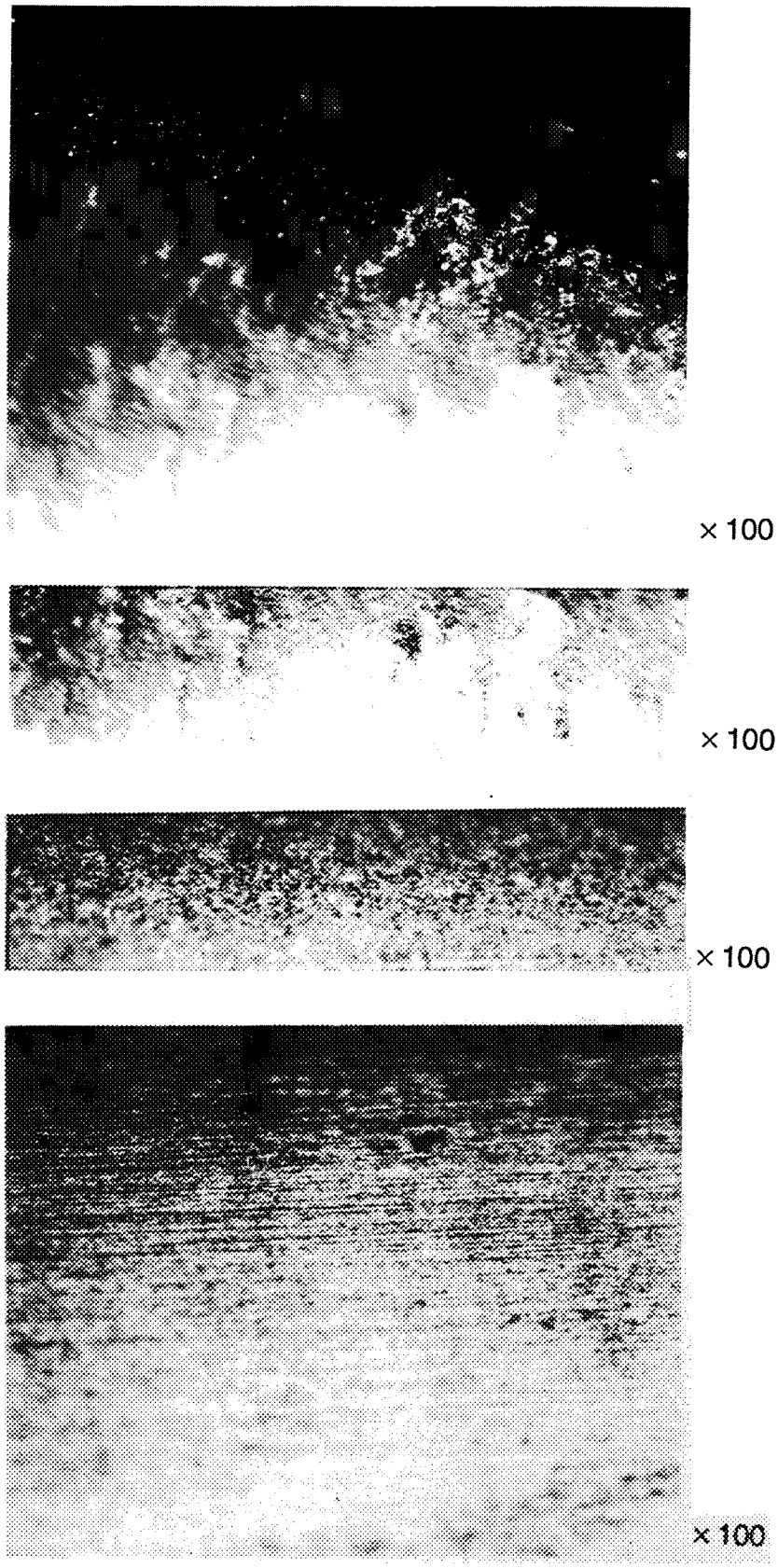

Figure A-50. OM of the inner ring of the heavily worn bearing No. 352, from the top (fillet area) to the bottom (unworn cylindrical surface). Patterns of the adhesive/shear peeling can be seen.

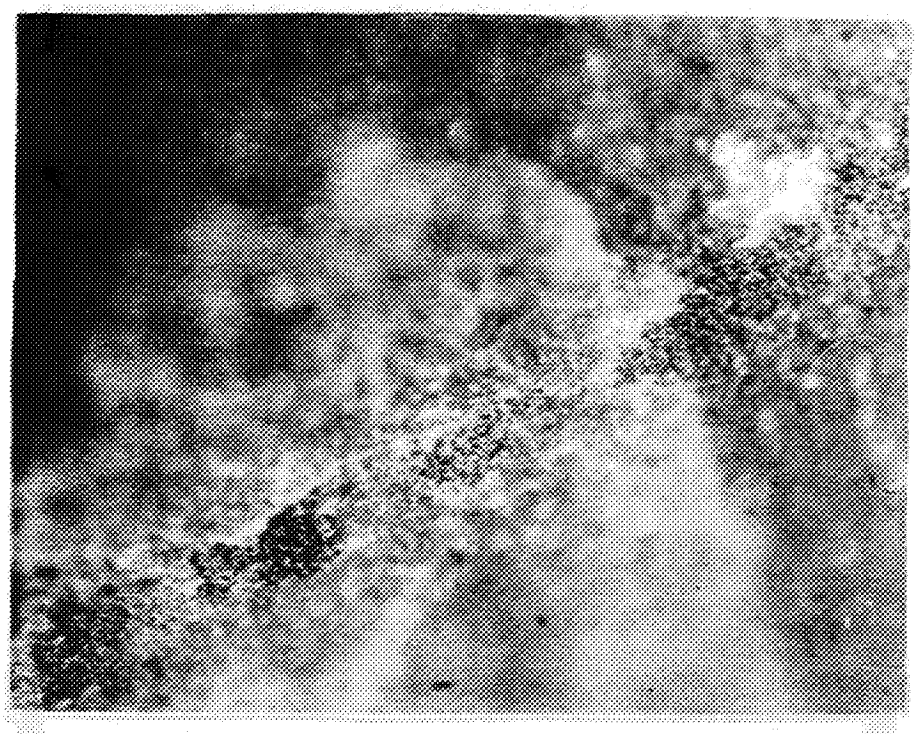

Figure A-51. OM of the inner ring of the heavily worn bearing No. 352: a freshly exposed new surface after peeling-off and a flake. Note that both photos show nearly the same area, and that black or white coloration may be reversed depending on the orientation of a highly reflective surface like this.

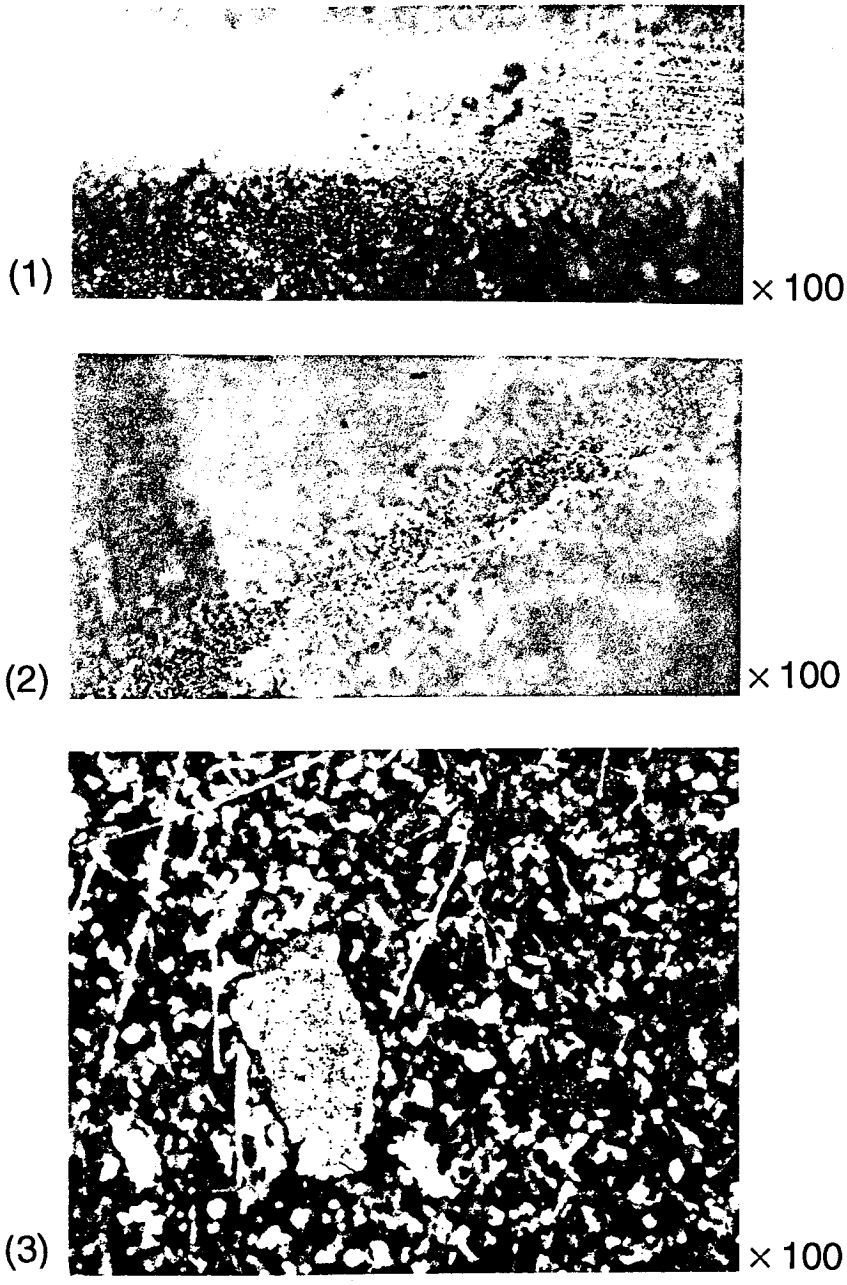

Figure A-52. OM of the inner ring of the lightly worn bearing No. 611, (1) and (2). Note how similar these photos are to figure A-51. (3) A large flake found on the BSMT outlet filter. Note that surface morphology is just like that of (1), (2), or figure A-51.

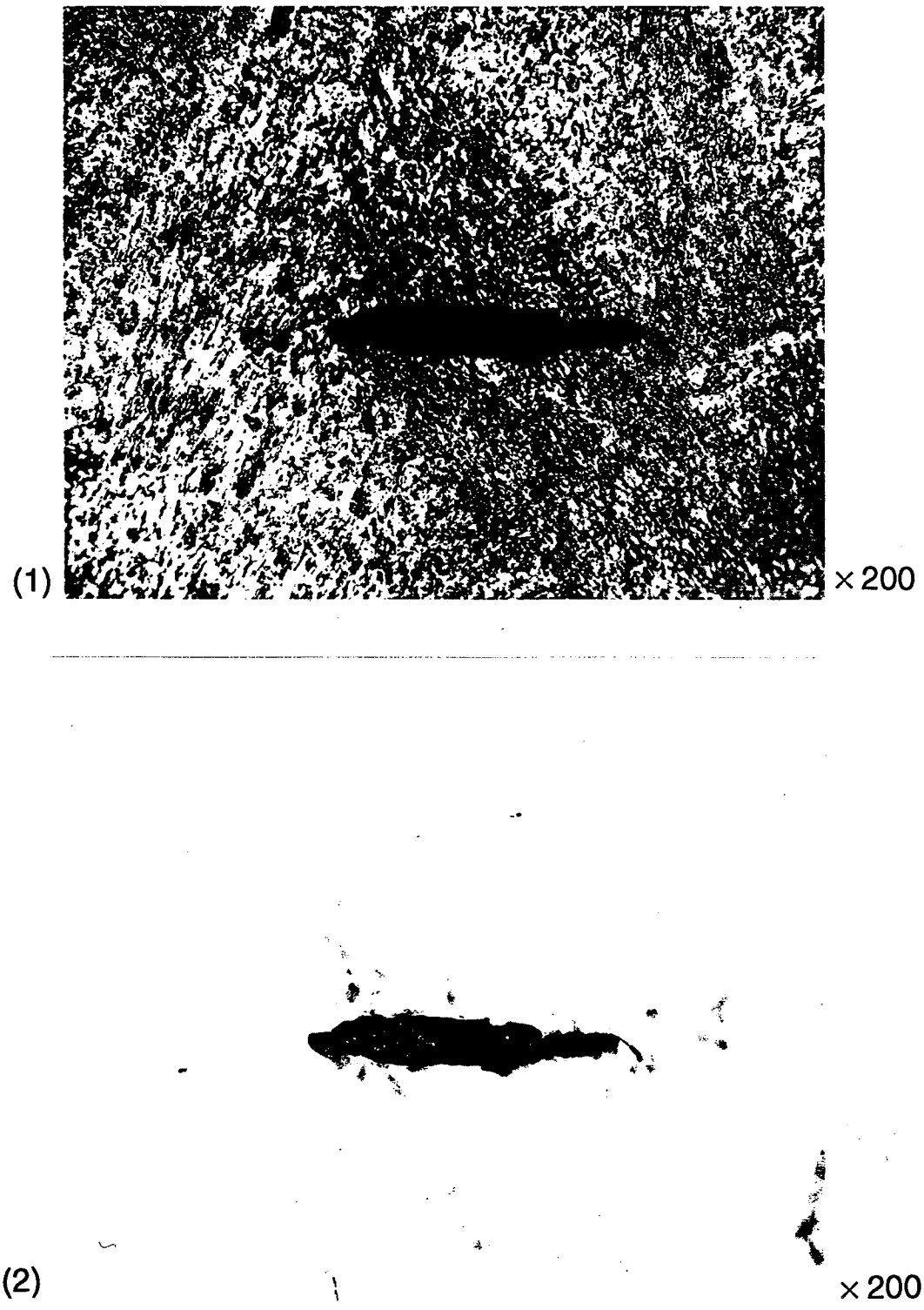

Figure A-53. OM of a lightly worn ball of bearing No. 543. Focus on the background (1) shows adhesive/shear peeling; focus on the wear particle (2) shows a piece of the cage Teflon and a glass fiber.

National Aeronautics and
Space Administration

George C. Marshall Space Flight Center
Marshall Space Flight Center, Alabama 35812
AC(205)544-2121

NASA

Reply to Attn of: EH32 (91-104) March 25, 1991

TO: EH22/R. A. Parr

FROM: EH32/S. V. Caruso

SUBJECT: Analyses of Debris from Bearing Tester

The subject samples have been analyzed as requested (EH32-91-132). A particle count by size was performed and the results are shown in the enclosed contamination analysis report. X-ray fluorescence spectroscopy indicated the results listed below.

(1)

Sample	Elements Detected
Fe 1253-10	Si, Fe, Cr, Ni, Cu, Mo
Fe 1253-40	Si, Fe, Cr, Ni, Cu, Mo
Fe 2643-10	Cr, Fe, Ni, Cu

Please contact Ms. Marceia Clark-Ingram at 544-6229 or Mr. Anthony Berry at 544-5395.

S. V. Caruso
Chief, Analytical and
Physical Chemistry Branch

Enclosure

cc:
EH22/Messrs. Gentz/Henderson
EH31/Mr. McIntosh
EH32/Mr. Berry
EH32/Ms. Clark-Ingram

NASA
Marshall Space Flight Center
Analytical and Physical Chemistry
EH32

Component: Millipore pad Date: 2-25-91

Requested by: Henderson Test Method: Particle Count

(2)

		Particle Count by Micron Size						
LAB #	ID	5-15	16-25	26-50	51-100	101-500	501-1000	>1000
1-2-25-91	FE-1253-10	86,039	100,173	53,371	5,214	511	1,106	74
2-2-25-91	FE-1253-40	147,281	119,146	123,479	91,934	77,514	28	13
3-2-25-91	FE-2643-10	89,515	71,256	76,502	64,101	503	42	6

Remarks: The above particle counts are approximations.

Figure A-54. Analysis of the wear debris found on the BSMT filters (1) and a particle count (2).

National Aeronautics and
Space Administration

NASA

George C. Marshall Space Flight Center
Marshall Space Flight Center, Alabama 35812
AC(205)544-2121

Reply to Attn of: EH32 (91-03) January 14, 1990

TO: EH22/R. A. Parr

FROM: EH32/S. V. Caruso

SUBJECT: Analysis of Debris from Bearing Tester (FE 1253-10)

The subject sample has been analyzed as requested (EH32-91-081). X-ray fluorescence spectroscopy indicated the following results:

Elements Detected
Aluminum
Calcium
Chromium
Copper
Iron
Silicon
Zirconium

Please contact Ms. Marceia Clark-Ingram at 544-6229 or Ms. Diep Trinh at 544-6737 if there are any questions.

S. V. Caruso
Chief, Analytical and
Physical Chemistry Branch

cc:
EH22/Messrs. Gentz/Henderson
EH31/Mr. McIntosh
EH32/Mses. Clark-Ingram/Trinh

Figure A-55. Analysis of the wear debris found on the BSMT inlet filter.

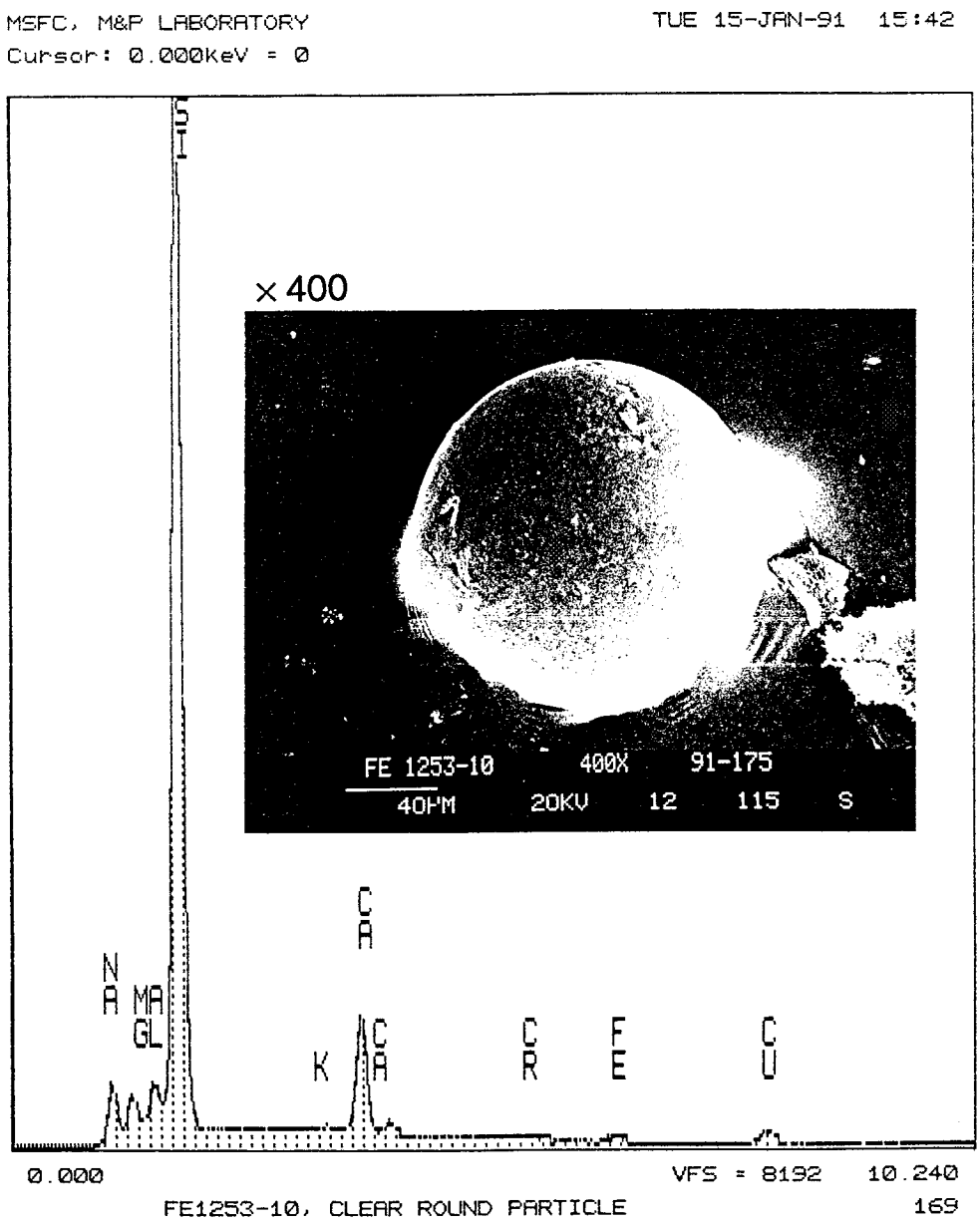

Figure A-56. SEM/EDS of a large Si contaminant particle found on the BSMT inlet filter.

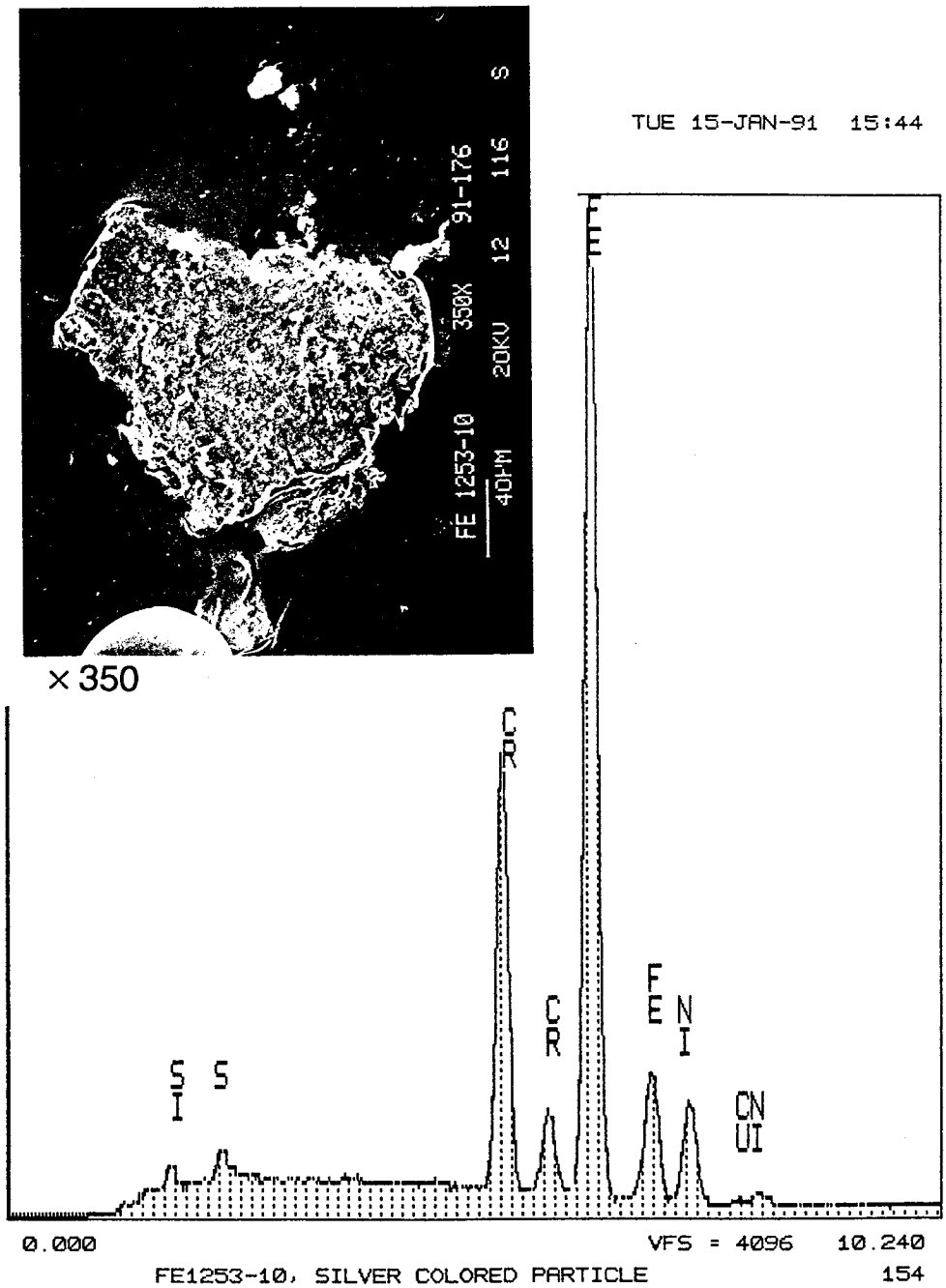

Figure A-57. SEM/EDS of a large 440C contaminant particle found on the BSMT inlet filter. It is unclear how it was deposited there.

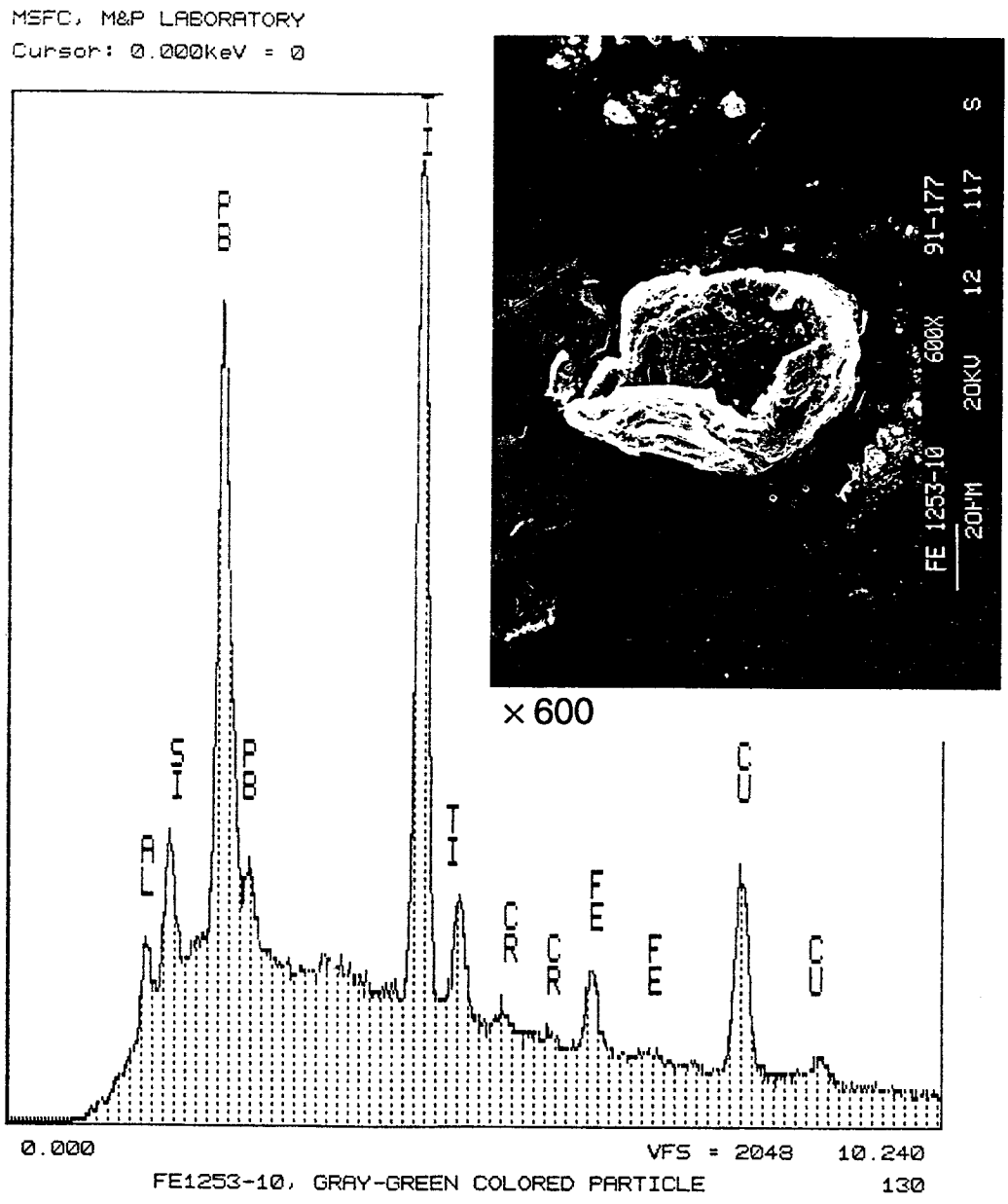

Figure A-58. SEM/EDS of a large Ti-Pb contaminant particle found on the BSMT inlet filter.

C-2

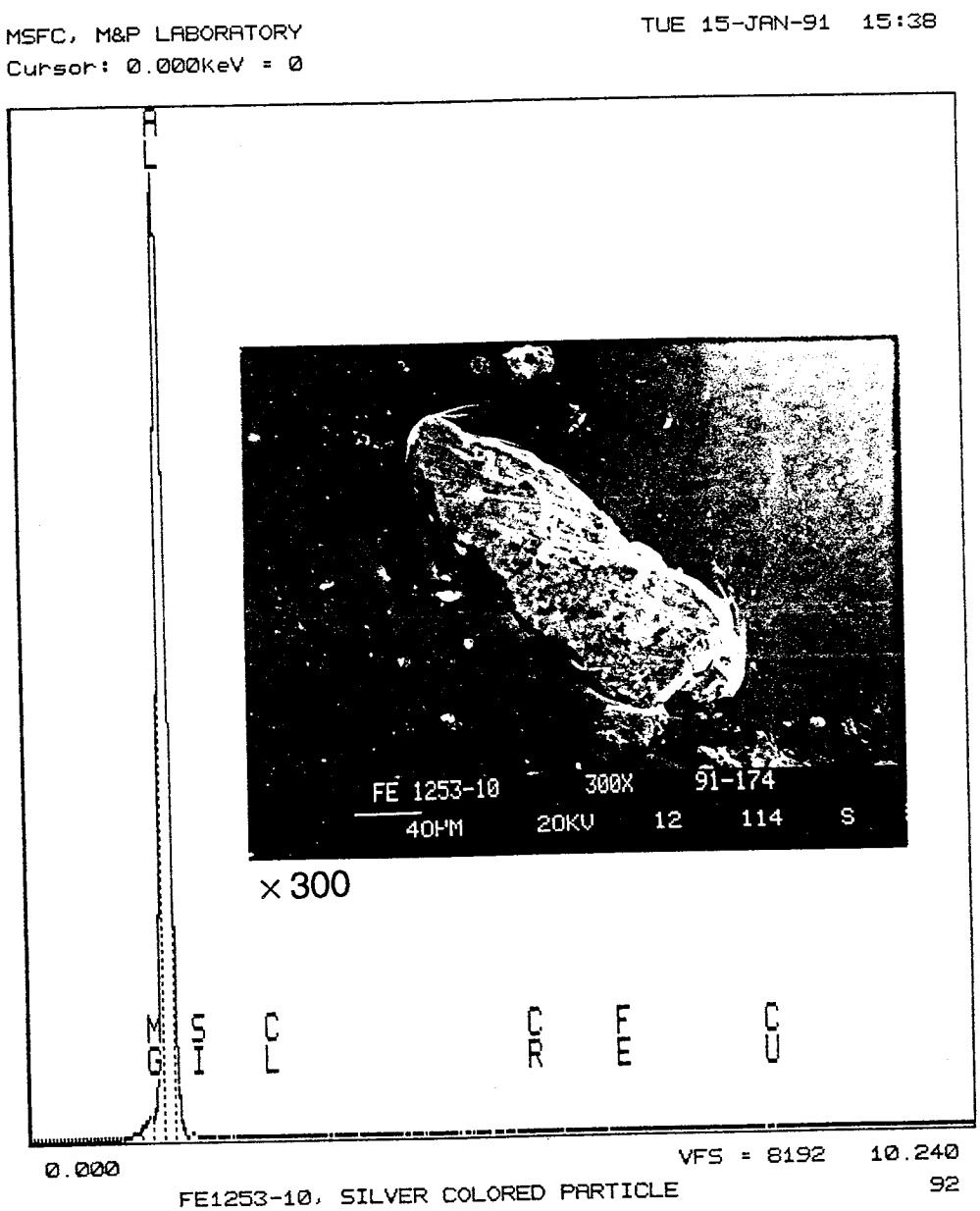

Figure A-59. SEM/EDS of a large Al contaminant particle found on the BSMT inlet filter.

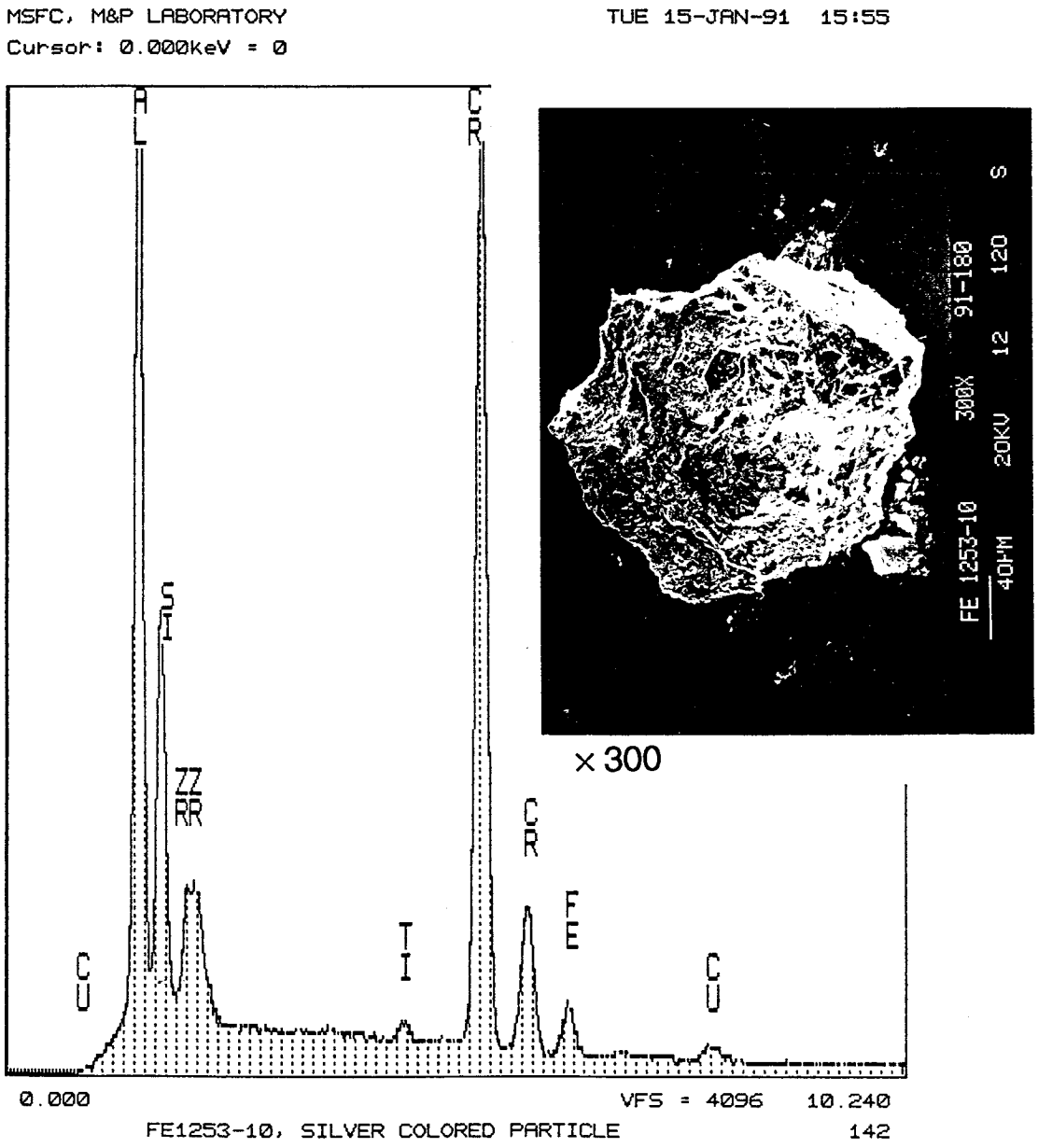

Figure A-60. SEM/EDS of a large Al-Cr-Si-Zr contaminant particle found on the BSMT inlet filter.

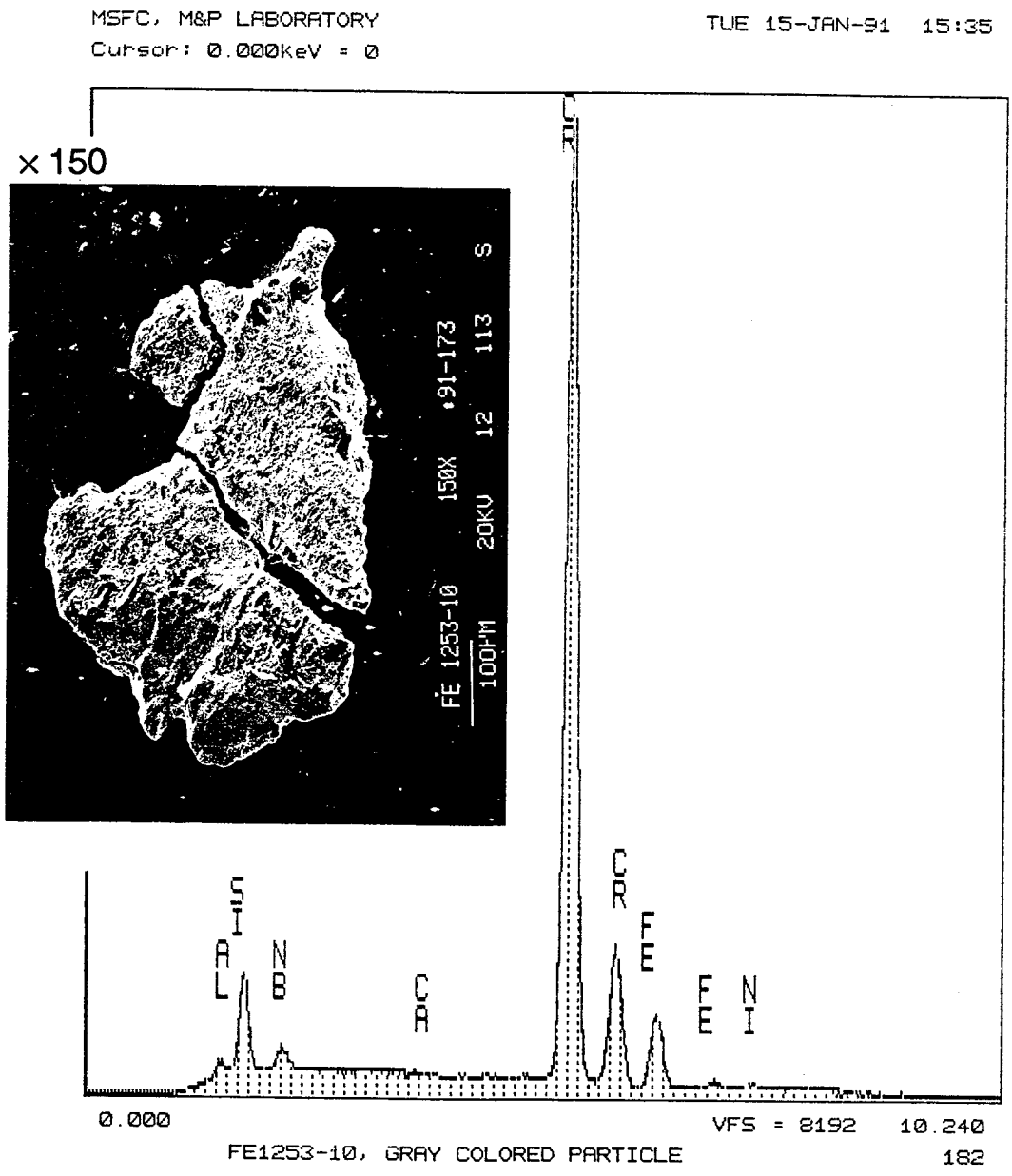

Figure A-61. SEM/EDS of a large Cr contaminant particle found on the BSMT inlet filter.

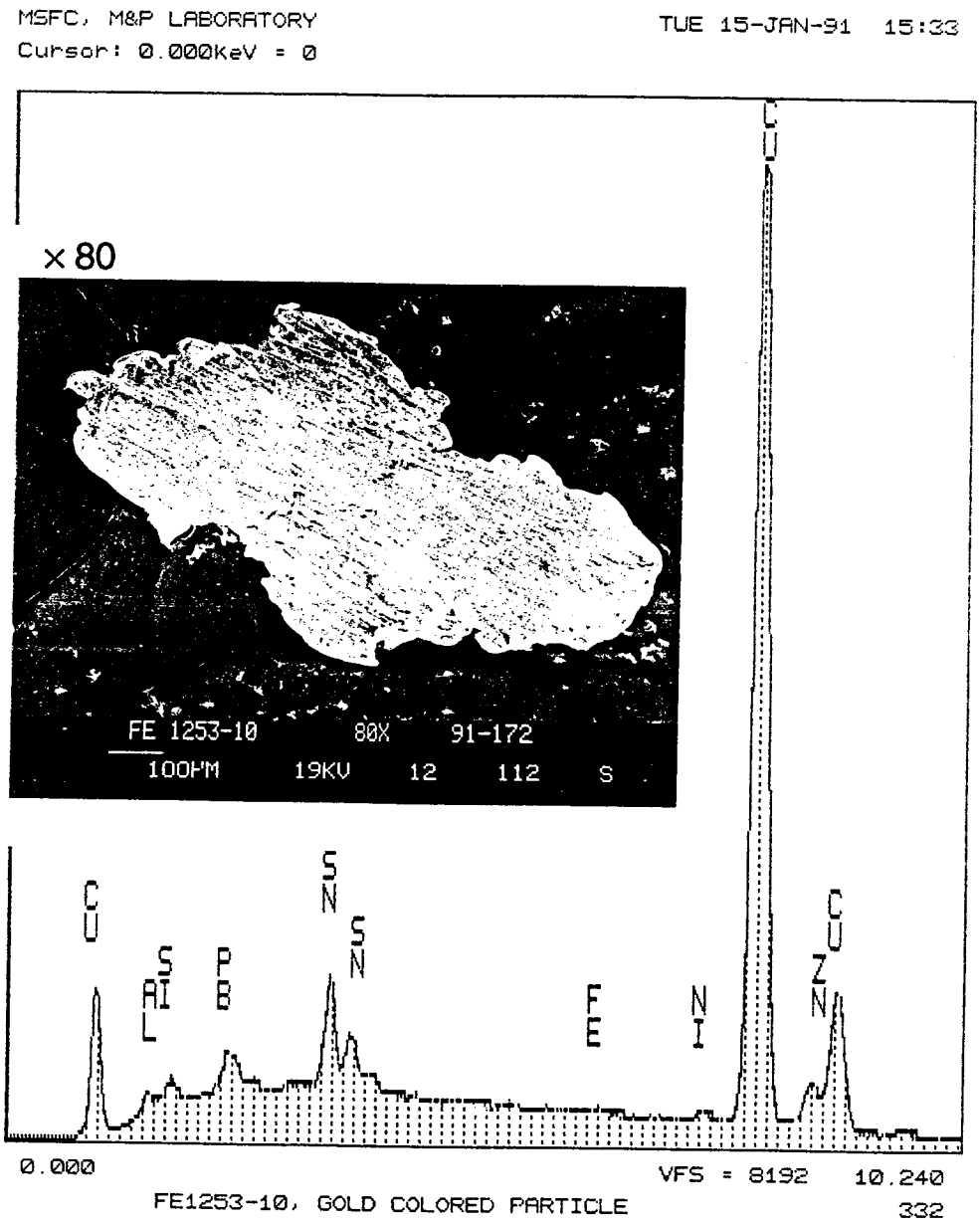

Figure A-62. SEM/EDS of a large Cu-Sn contaminant particle found on the BSMT inlet filter.

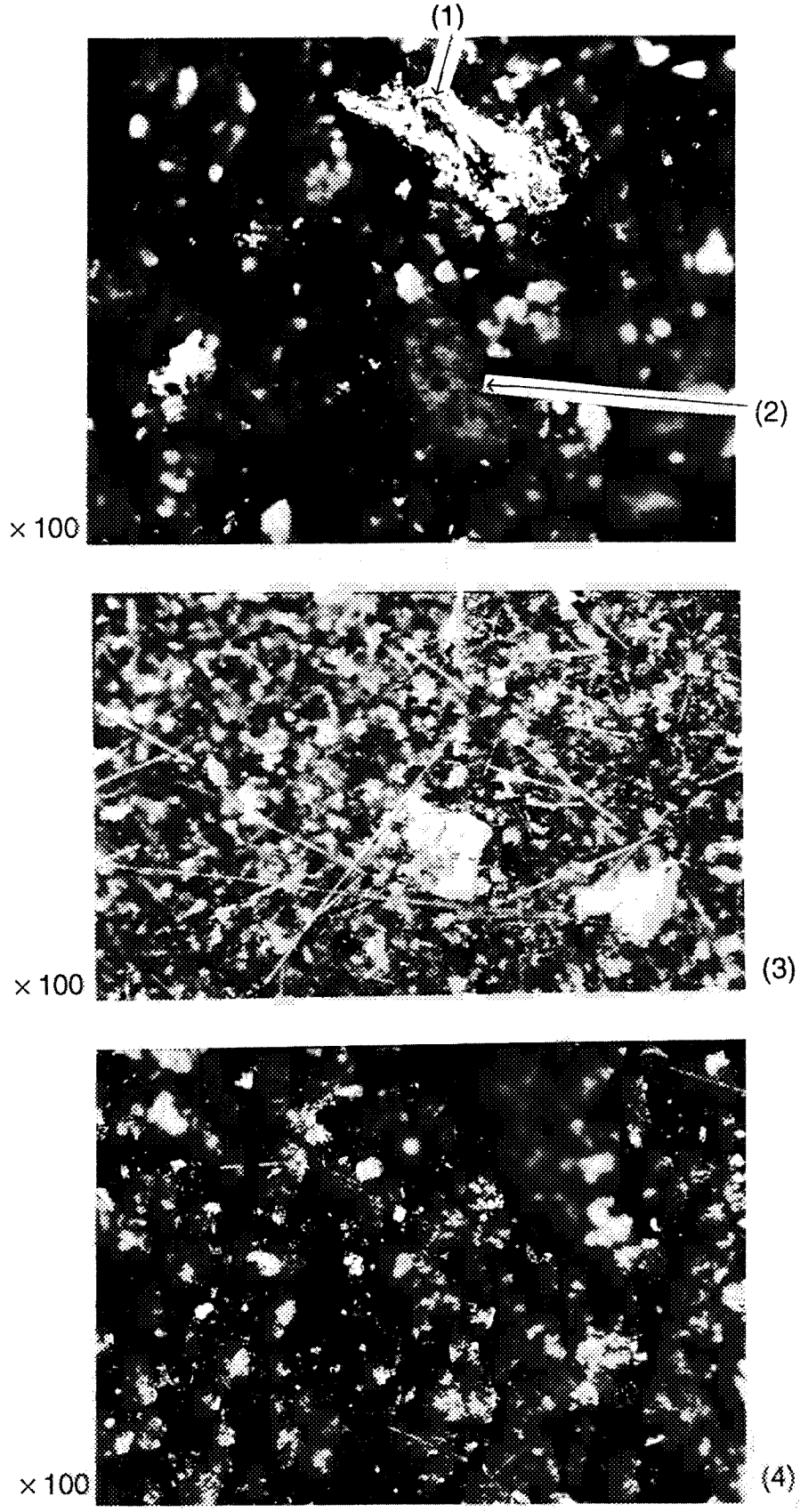

Figure A-63. OM of the wear debris found on the BSMT outlet filter: (1) large metallic flake, (2) large PTFE chunk, (3) glass fiber, and (4) overall.

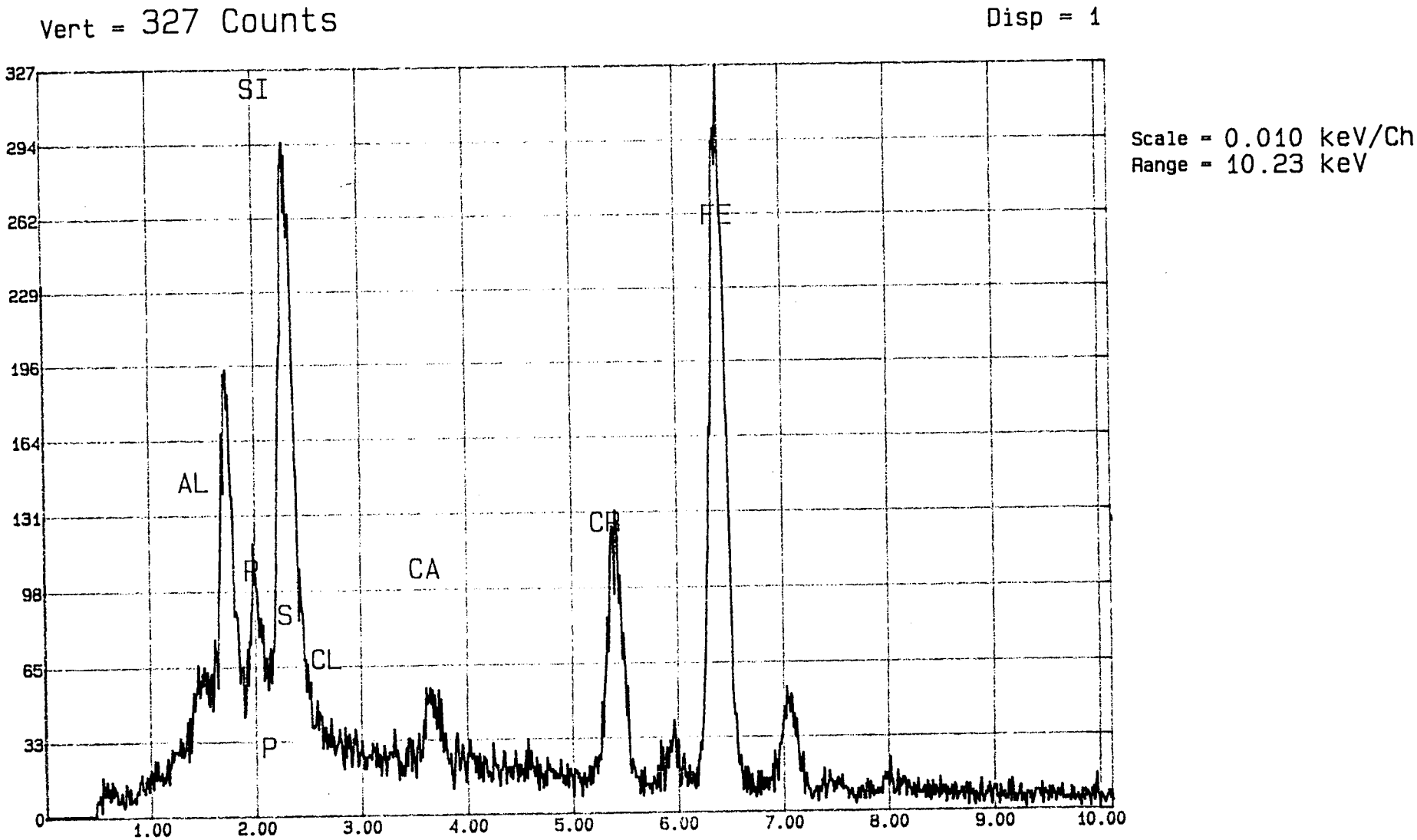

Figure A-64. Microprobe EDS of a dark particle found on the BSMT outlet filter: cage material and base 440C. Base material spectrum may have come from the background because the particle analyzed was small and thin.

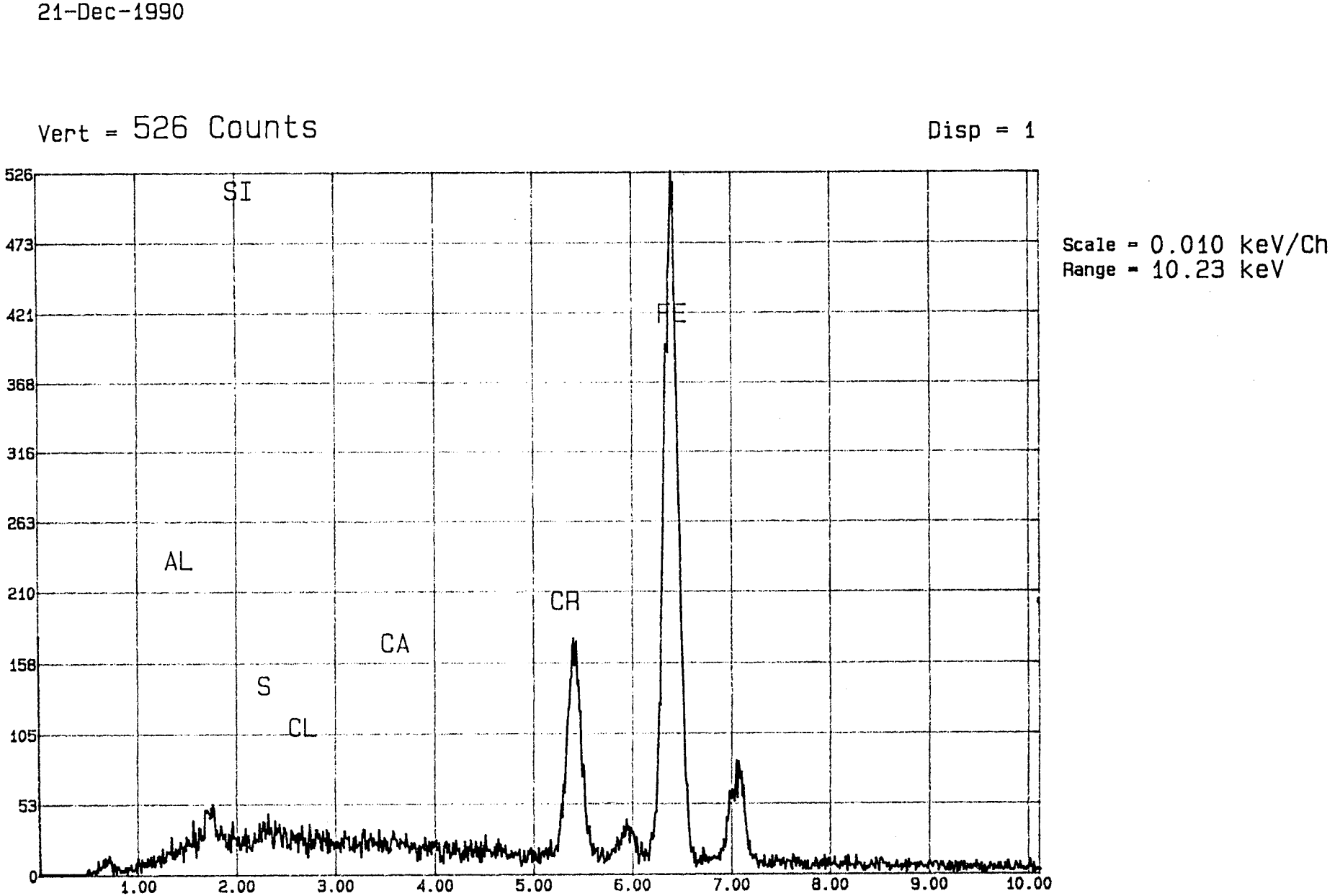

Figure A-65. Microprobe EDS of a light metallic particle found on the BSMT outlet filter: base 440C and some contaminants. The chemistry of this particle is just like that of the base ring (compare fig. A-4) or the base ball material (compare fig. A-13).

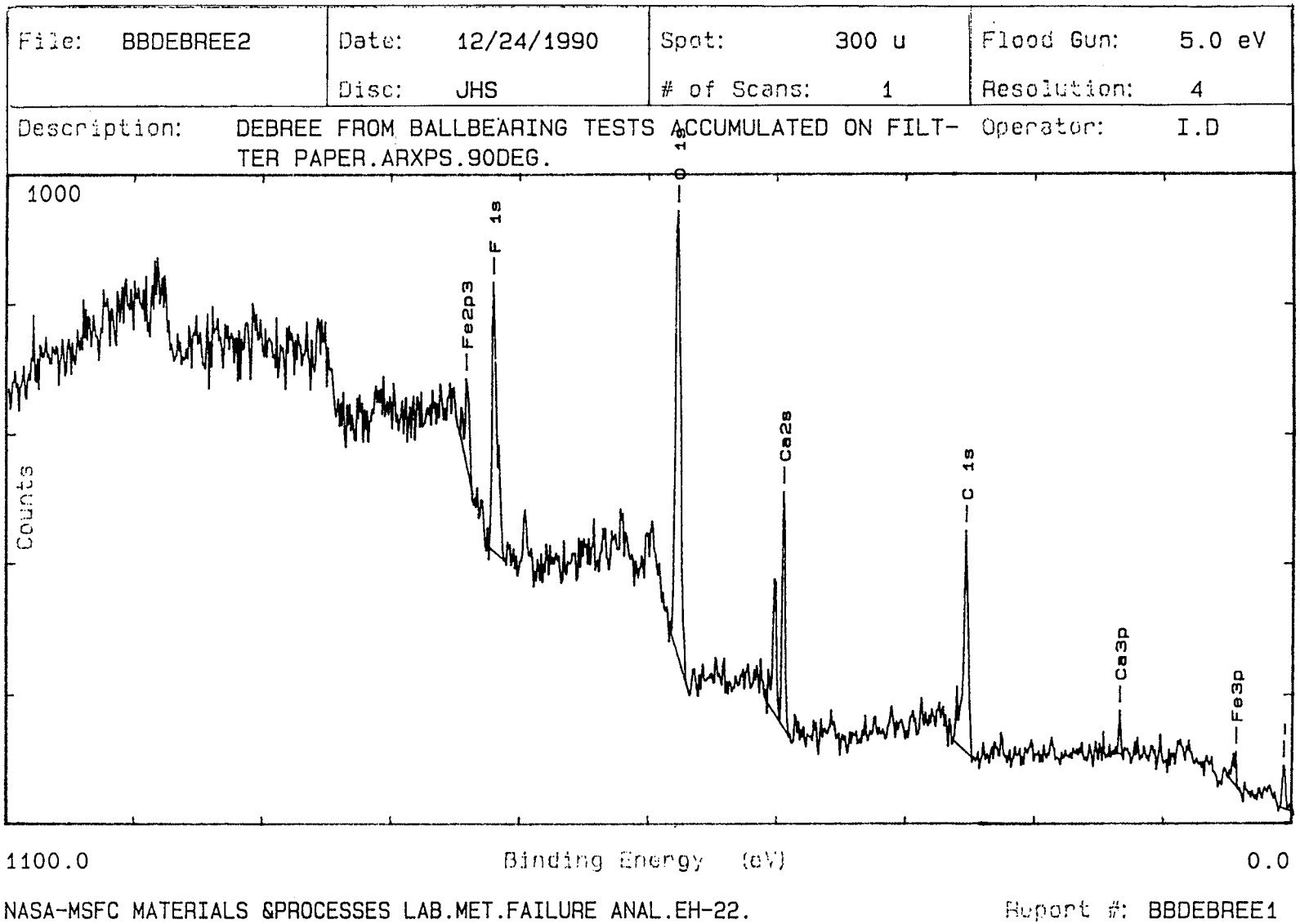

Figure A-66. XPS analysis of the wear debris from the BSMT outlet filter. Note presence of iron oxides, calcium (glass fiber), and Teflon (fluorine).

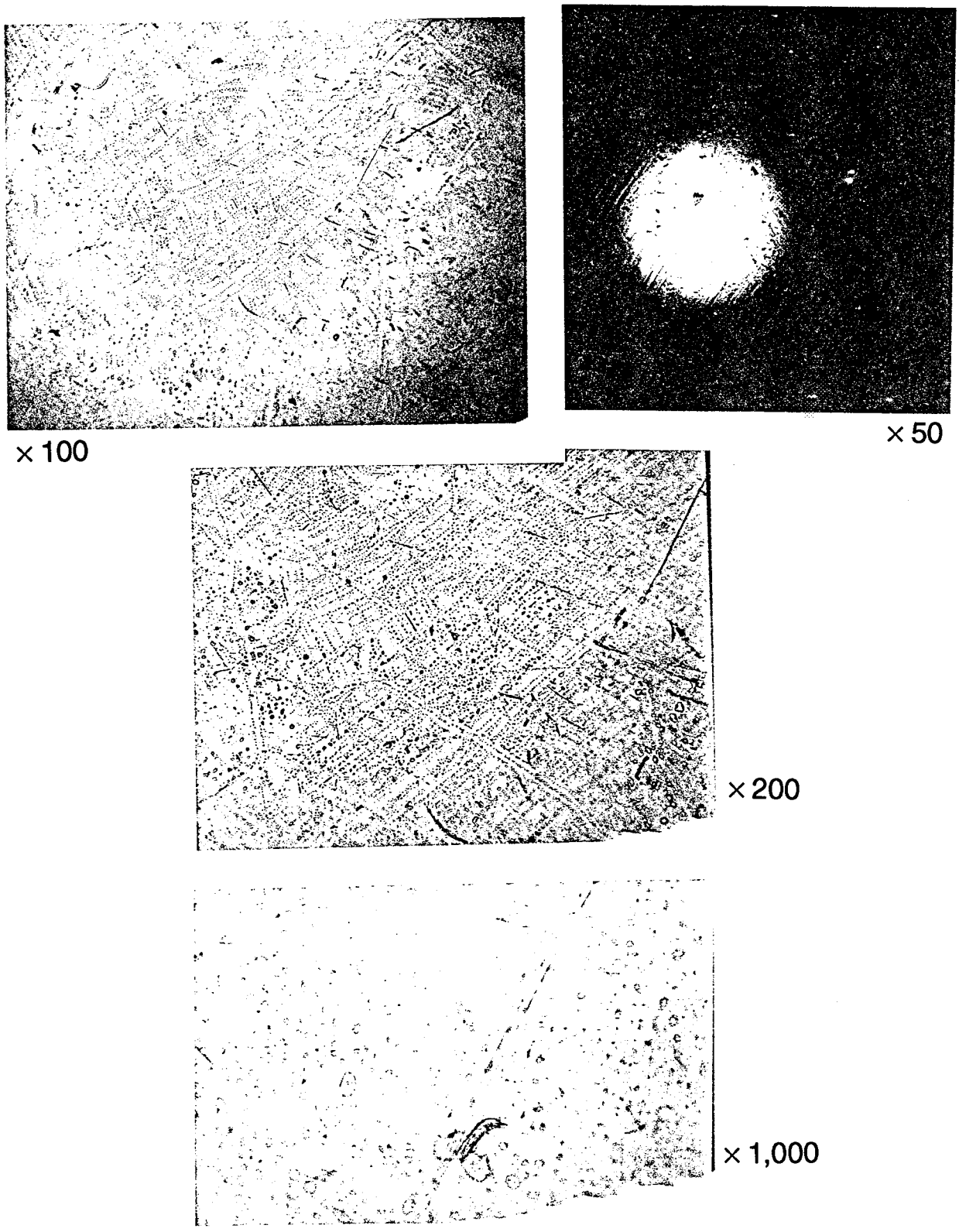

Figure A-67. OM of the surface of a brand new 440C ball. Note adhesive/shear peeling-like appearance of the finish marks.

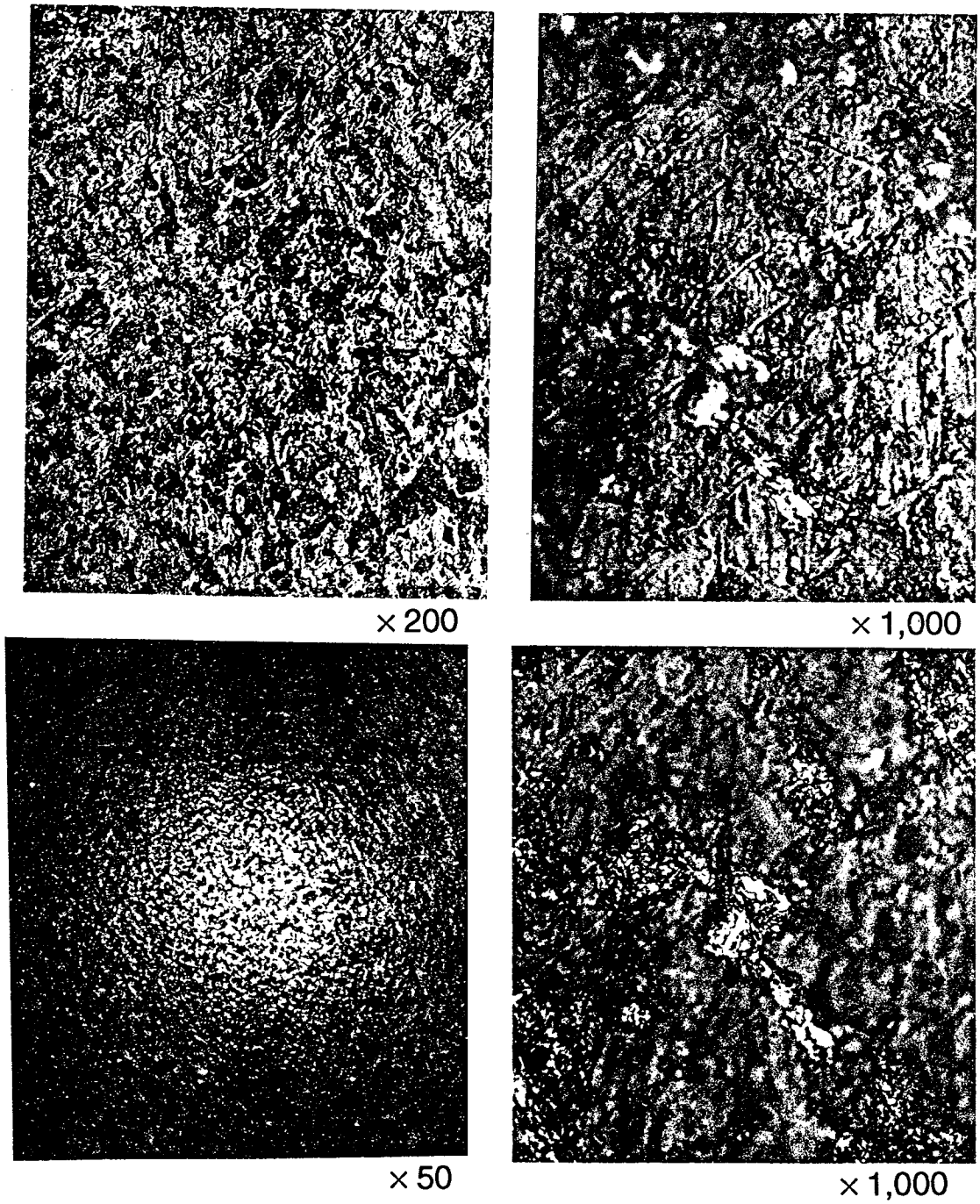

Figure A-68. OM of the heavily worn 440C balls from the BSMT tests in lox: adhesive/shear peeling wear mode is predominant.

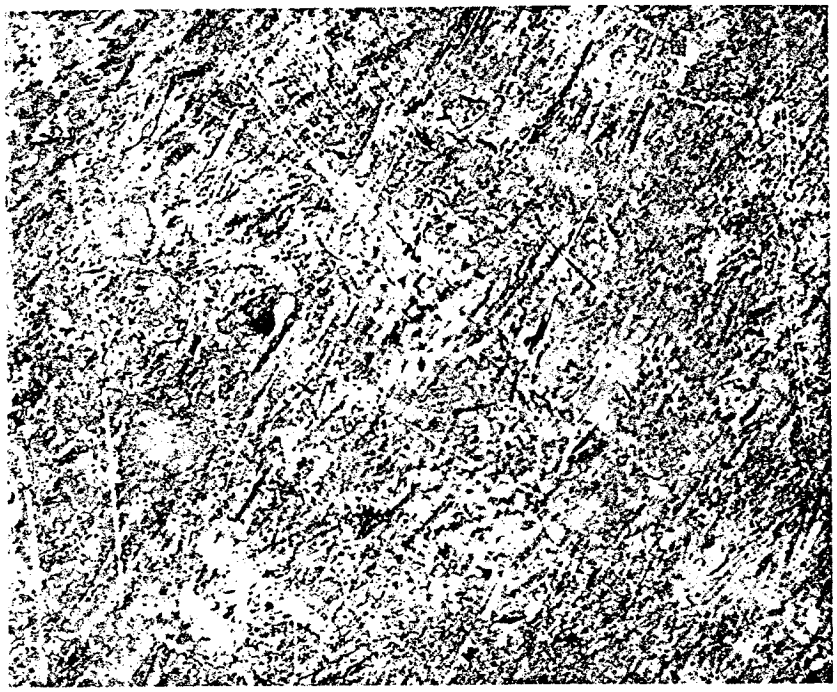

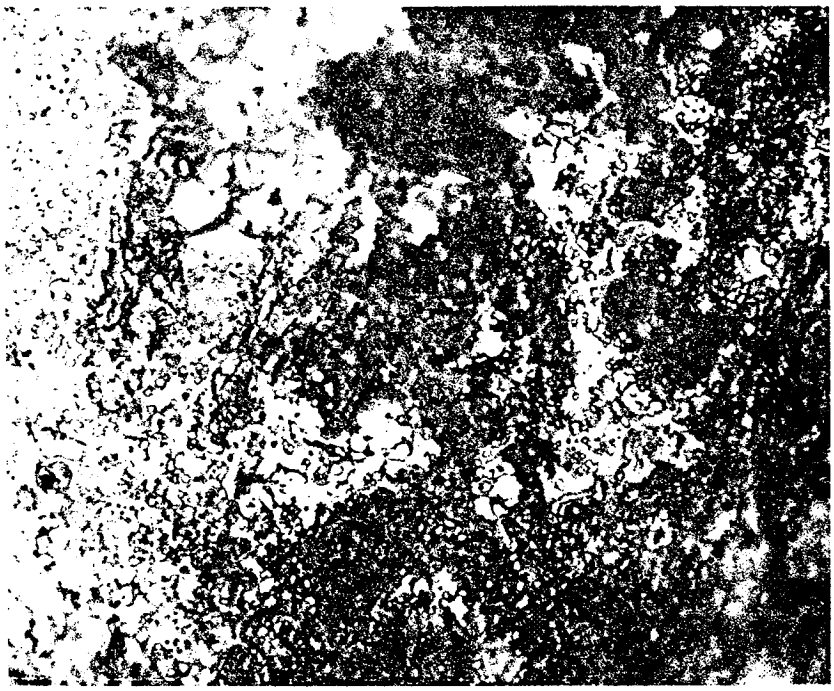

Figure A-69. OM of the heavily worn 440C balls from the past BSMT tests in LN_2: adhesive/shear peeling wear mode is predominant.

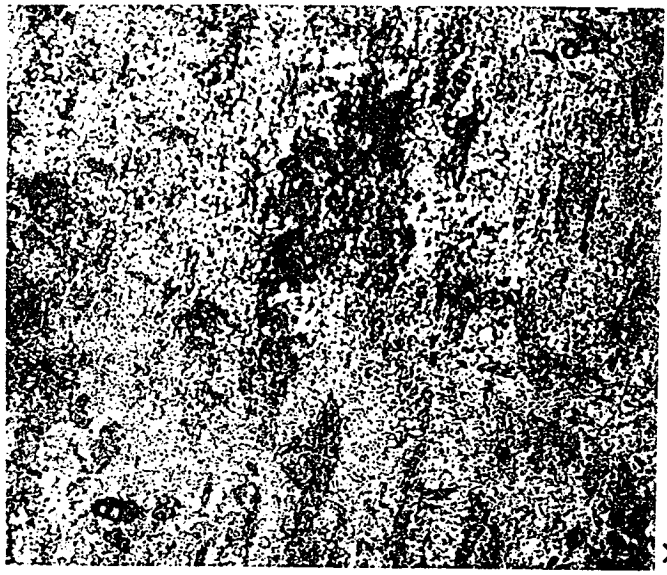

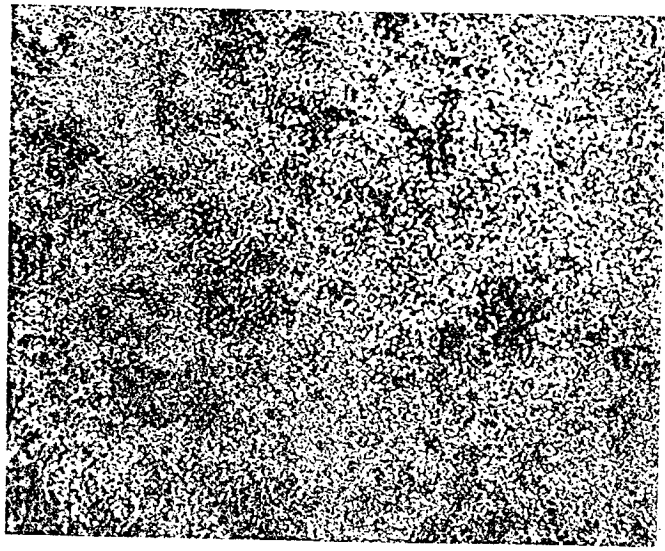

Figure A-70. OM of the heavily worn 440C balls from the past BSMT tests in LN_2: adhesive/shear peeling wear mode is predominant. Observe the variety of patterns.

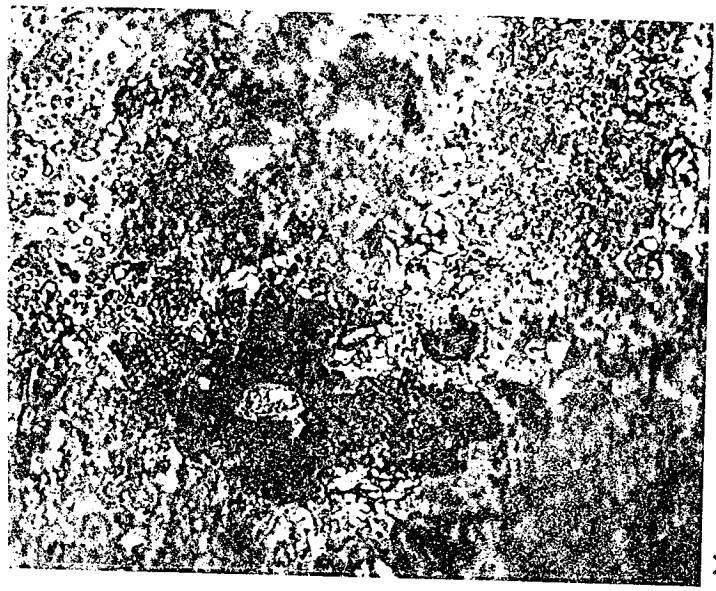

Figure A-71. OM of the heavily worn 440C balls from the past BSMT tests in LN_2: adhesive/shear peeling wear mode is predominant. Note black coloration.

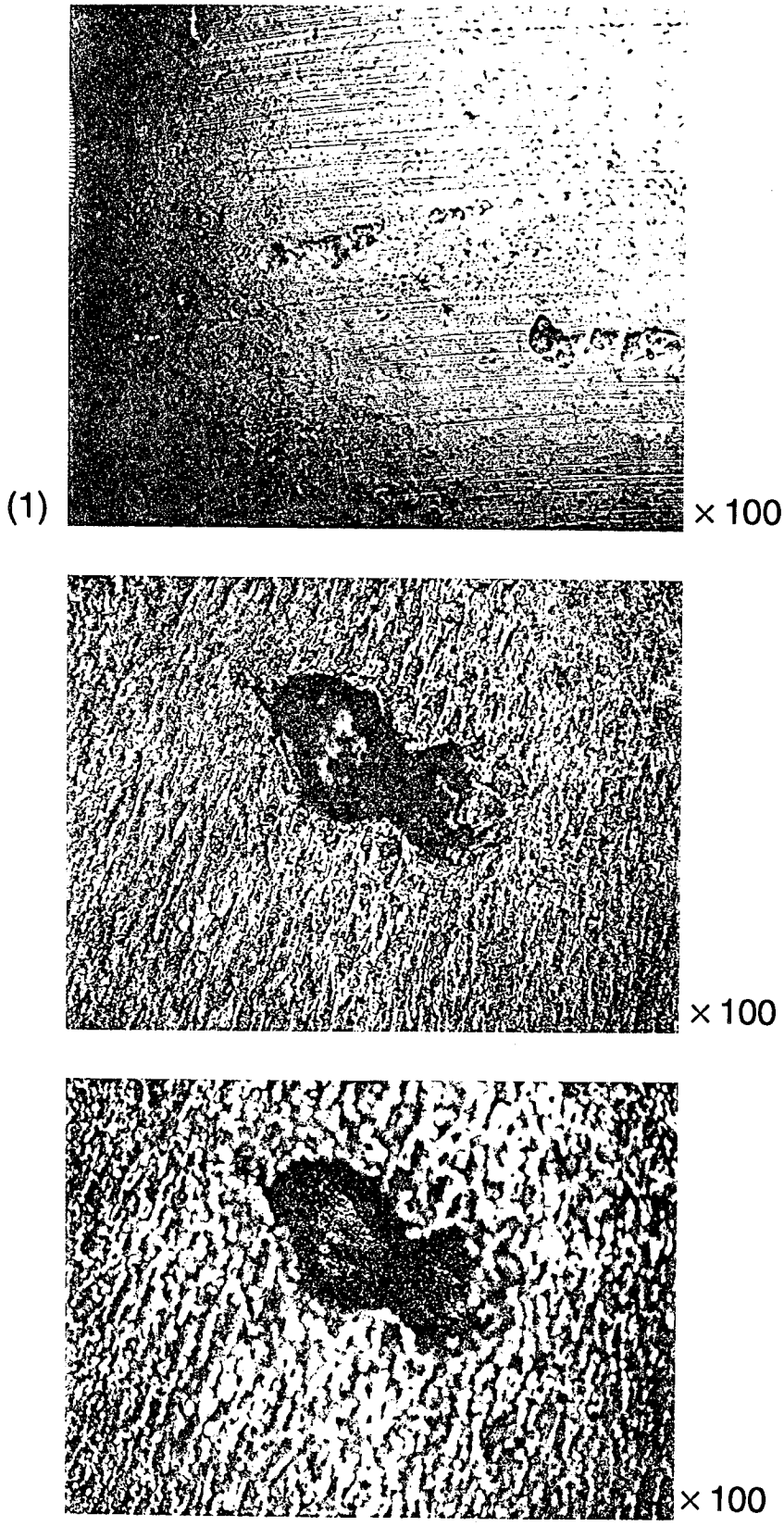

Figure A-70. OM of the heavily worn 440C balls from the past BSMT tests in LN_2: adhesive/shear peeling wear mode is predominant. Note abrasive and polishing action of the cage pocket glass fibers (1).

VOLUME 34 (1991), 2, 241–247
TRIBOLOGY TRANSACTIONS

Analysis of Bearing Incidents in Aircraft Gas Turbine Mainshaft Bearings©

B. L. AVERBACH
Massachusetts Institute of Technology
Cambridge, Massachusetts 02139
and
E. N. BAMBERGER
General Electric Aircraft Engine Business Group
Cincinnati, Ohio 45215

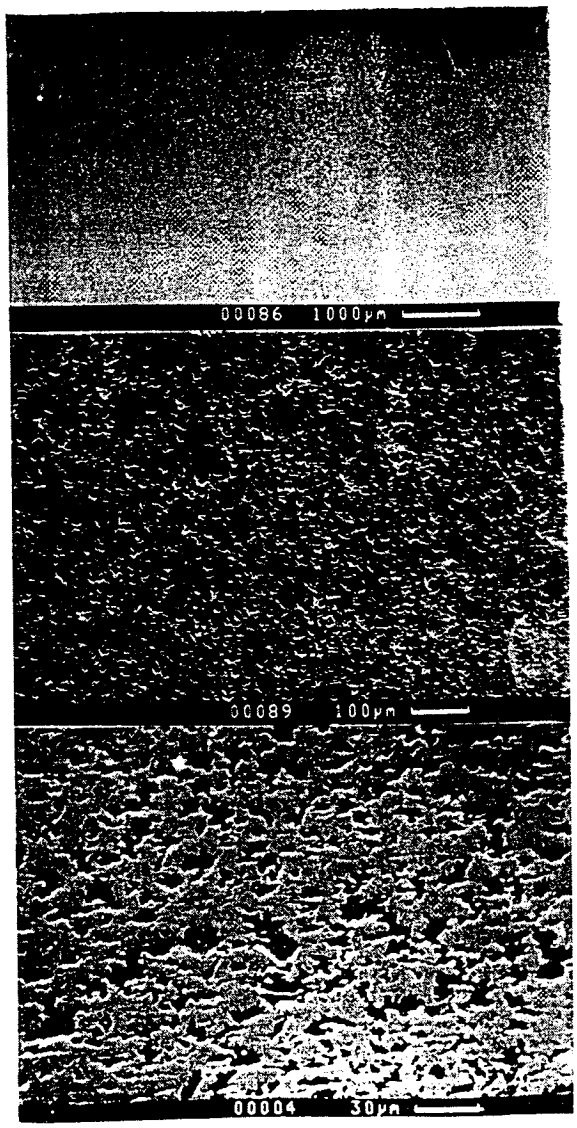

Fig. 2—Surface damage resulting from ball skidding

Figure A-73. Surface damage to bearing rings resulting from ball skidding in poorly lubricated gas turbine bearings from reference 22.

APPROVAL

WEAR MECHANISMS FOUND IN ANGULAR CONTACT BALL BEARINGS OF THE SSME'S LOX TURBOPUMPS

By T.J. Chase

The information in this report has been reviewed for technical content. Review of any information concerning Department of Defense or nuclear energy activities or programs has been made by the MSFC Security Classification Officer. This report, in its entirety, has been determined to be unclassified.

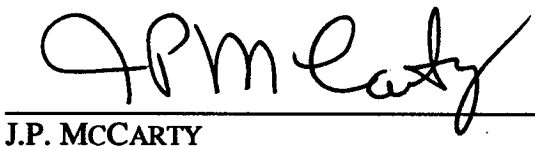

J.P. MCCARTY
Director, Propulsion Laboratory

☆ U.S. GOVERNMENT PRINTING OFFICE 1992—631-060/06172